The Extrinsic Regulation of Hematopoietic Stem Cells in Health and Disease

Matthew N. Decker

Submitted in partial fulfillment of the
requirements for the degree
of Doctor of Philosophy
under the Executive Committee
of the Graduate School of Arts and Sciences

COLUMBIA UNIVERSITY

2018

Abstract

The Extrinsic Regulation of Hematopoietic Stem Cells in Health and Disease

Matthew N. Decker

Hematopoietic stem cells facilitate lifelong production of a diverse repertoire of functional mature blood cells. They are a critical biological reservoir that enable organisms to endure physiological challenges such as inflammation, disease, and age. The functional maintenance of hematopoietic stem cells depends not only on intrinsic cell pathways, but also on extrinsic cues that guide core behaviors like homing and self-renewal. Careful study of these extrinsic regulatory networks can deepen our appreciation of fundamental stem cell biology and motivate therapeutic approaches to treat hematologic disease. Here I show how derangement of the bone marrow regulatory environment perturbs normal hematopoiesis, and demonstrate the dependence of hematopoietic stem cells on a circulating endocrine factor.

Table of Contents

List of Figures and Tables

Acknowledgements

I have been extremely fortunate to do my graduate work under the guidance of Dr. Lei Ding. Lei is a world-class scientist and investigator, but he's also a dedicated and thoughtful mentor. He supported my scientific growth, and as I grew more capable encouraged me to take risks and expand the scope of my work. He's made me a clearer thinker, a better technician, a more independent investigator. I'm incredibly grateful for everything he's done for me, and everything he's prepared me to do.

These past years have flown by because of the amazing labmates who I've been privileged to work with. Juliana, Qingxue, Leticia, Yeojin, Heather, Min-Jung, and Shawn made my every day in the Ding Lab better with their thoughtfulness, their humor, and their excellent taste in lab décor. My only regret about graduating is leaving behind a really special group of people.

My thesis committee has supported me every step of the way; Steve, Steve, and Hans have been part of my PhD journey since my qualifying exam. They've been a constant guiding force, putting their collective wisdom to work not just on the details of experimental design and data interpretation, but towards larger questions about my career path and goals. There's a lot of attrition along the path to a PhD, but my committee helped me leave the program more excited than ever about a career in biomedical research.

I'd be remiss if I didn't thank the amazing core facility directors at Columbia, without whom none of my work would have been possible. I'd especially like to thank Mike Kissner at the CSCI Flow Cytometry Core, who made me actually enjoy spending time on the Aria. Navigating the dual-degree program has required an enormous amount of administrative support,

most of which has come from Zaia Sivo, Jeffrey Brandt, Kate Matthews, and Becky Spurr. The MSTP and CMBS program leadership has been consistently excellent and given me numerous opportunities to present my work at intra- and inter-institutional conferences.

I never would have had the opportunity to complete my PhD without the community of scientific mentors, friends, and family who have shaped me over the years. There are too many of you to name individually, but as I sit here thinking of you all my heart is full. I have been blessed to have you in my life. I am especially grateful to my parents, who gave me the firm footing from which I could explore the world, and my wife Amanda, who makes the world worth exploring.

Chapter 1

Extrinsic regulation of hematopoietic stem cells in homeostasis and disease

Sections of this chapter are published:

Yeojin Lee*, Matthew Decker*, Heather Lee*, and Lei Ding (2017)

Extrinsic regulation of hematopoietic stem cells in in development, homeostasis, and diseases

WIRES Dev Bio 6, e279

*Equal author contributions

INTRODUCTION

Multicellular organisms evolved tissue-specific stem cells to generate, sustain and repair diverse tissue and organ types. Stem cells are maintained in tissues through life-long self-renewal divisions, where one or two stem cells are generated in each round of cell division (He et al., 2009). Stem cells also have multilineage differentiation potential. Thus stem cells are constantly balancing two seemingly opposed functions: maintaining the undifferentiated stem cell state and differentiating into cells of multiple lineages. Work from *Drosophila* has demonstrated that by providing adhesive interactions and biased signaling to stem cells, but not their immediate downstream progenies, stem cell microenvironmental niches provide a perfect solution to this issue (Losick et al., 2011). Understanding how stem cells are regulated by their local niche and by other extrinsic mechanisms is fundamental to the field of stem cell biology.

Hematopoiesis has been a fruitful model for the study of stem cell biology. Multiple cell types constitute the hematopoietic system, including myeloid cells, lymphoid cells, erythroid cells and megakaryocytes. All of these lineages are ultimately generated from multipotent HSCs through a differentiation hierarchy that includes multiple levels of progenitors throughout life (Weissman and Shizuru, 2008). HSCs are also capable of regenerating the hematopoietic system after transplantation. In fact, HSC transplantation is the only cure available for a number of hematologic diseases. Their enormous medical potential aside, HSCs have served as the model tissue stem cell, having defined the rigorous standards of self-renewal and multilineage potential that characterize all tissue stem cells. This definition has provided the framework for understanding stem cell biology in general. Not surprisingly, the proposal of a stem cell niche was first suggested in the hematopoietic system for HSC maintenance (Schofield, 1978).

The high medical value and scarcity of HSCs prompted searches for conditions to culture or expand HSCs *in vitro*. Despite decades of effort, no culture system is able to robustly maintain or expand HSCs. However, these stem cells can clearly thrive within their native environment *in vivo.* Thus, defining the *in vivo* extrinsic regulatory mechanisms is a key step that will allow us to expand and augment the therapeutic utility of HSCs. Hematopoiesis and HSCs change organ sites several times throughout life to meet distinct physiological demands. The dynamic nature of the interaction between HSCs and their environments presents a fascinating yet challenging opportunity to understand HSC regulation. The fluid nature of the hematopoietic tissue and a lack of morphological or positional differences between HSCs and other hematopoietic cells have made the identification of these cells and their *in vivo* environment difficult. Despite these roadblocks, significant advancements have been made regarding the extrinsic regulation of HSCs in recent years. Here, we will summarize our understanding of the extrinsic regulation of HSCs in the context of development, homeostasis and disease. We will also highlight some of the outstanding questions in the field.

OVERVIEW OF TECHNICAL HISTORY

Our knowledge of HSCs is built on experimental evidence made possible by a number of technical advances, including two key innovations: transplantation and flow cytometry. During World War II, it was discovered that people exposed to lethal irradiation could be rescued by transplantation of cells from healthy donor bone marrow. This sparked the quest for cells that can replenish the hematopoietic system (Ford et al., 1956). Work from Till and McCulloch showed that there are cells in the bone marrow that when transplanted can regenerate the blood system and form colonies on the spleens (colony forming unit-spleen or CFU-S) of mice exposed to

lethal doses of irradiation (Till and McCulloch, 1961). It was later discovered that CFU-Ss are not HSCs but hematopoietic progenitors (Jones et al., 1990, 1996). Nonetheless, using cytological methods, Till and McCulloch provided convincing evidence that these colonies contained multiple hematopoietic lineages and were derived from a single hematopoietic progenitor (Becker et al., 1963). These observations have conceptually shaped the field of stem cell biology. The capability to stably reconstitute lethally irradiated recipient mice upon transplantation has become the gold standard in defining HSCs. Throughout the review, HSCs are defined by this criterion. Based on limiting dilution transplantation assays, it was estimated that about 5 cells in every 10^5 C57BL/6 bone marrow cells are HSCs (Abkowitz et al., 2000). But these rare stem cells are so potent that a single transplanted HSC can reconstitute the entire blood system of a lethally irradiated recipient mouse (Kiel et al., 2005; Osawa et al., 1996).

Although HSCs were in the mixture of bone marrow cells used in early *in vivo* experiments, their exact identity remained elusive. No morphological features can distinguish rare HSCs from other hematopoietic cells, which was a major hurdle in the field. The invention of monoclonal antibodies and fluorescence activation cell sorting (FACS) made possible the isolation of HSCs based on the expression of specific cell surface antigens. Cell sorting combined with functional transplantation assays allowed for the development of a series of surface marker profiles that can be used to sort HSCs to high purity, particularly in the bone marrow (Weissman and Shizuru, 2008). The purification of HSCs has facilitated extensive research on intrinsic molecular mechanisms that regulate their self-renewal and differentiation. But how these mechanisms are integrated with the *in vivo* environment had not been clear.

Localizing HSCs *in vivo* is a prerequisite to elucidating their environmental regulation. Much of the focus in the field has been on the adult bone marrow. The complex markers used in

FACS to purify HSCs were not suitable to identifying them on bone marrow tissue sections using microscopy, requiring the use of alternative markers in many early HSC niche studies. Simpler markers with low purity for HSCs (Arai et al., 2004) and tracing assays for transplanted FACS-sorted fluorescent marker-labeled HSCs were initially used to localize HSCs *in situ* (Lo Celso et al., 2009; Xie et al., 2009). But it was not clear whether the localization of these cells reflected the niche of endogenous HSCs under steady state conditions. The development of Signaling Lymphocyte Activation Molecular (SLAM) markers allowed for the identification of HSCs on bone marrow sections *in situ* by simple two-color staining for cells with markers that also strictly defined HSCs by FACS and transplantation (Kiel et al., 2005). More recently developed genetically encoded fluorescent markers have also allowed detailed studies of HSC localization (Chen et al., 2016; Sawai et al., 2016). The advancement of other imaging techniques such as intra-vital live imaging and tissue clearing technology has provided even more comprehensive views of the natural environment of HSCs in the bone marrow (Sipkins et al., 2005; Acar et al., 2015). The imaging of HSC emergence during development has also provided critical information on the niches that maintain HSCs. For example, live imaging of the aorta-gonad-mesonephros (AGM) has provided definitive evidence of hemogenic endothelium (Bertrand et al., 2010; Boisset et al., 2010; Kissa and Herbomel, 2010). Similarly, imaging data regarding the niches in hematopoietic malignancies and other stress conditions are emerging.

Imaging has provided a solid framework for understanding the niche that regulates HSCs. However, functional studies *in vivo* are key to uncovering the mechanisms of HSC extrinsic regulation. Ideally, a defined perturbation of the candidate niche cell type should result in a perturbation of HSCs. Following this logic, several functional approaches have been taken to uncover the nature of bone marrow niche that maintains HSCs. We use the bone marrow as an

example to highlight some functional methods to study HSC extrinsic regulation. Early genetic analysis of *Steel* (with mutated stem cell factor, SCF) and *White* (with mutated cKit receptor) mutants led to the identification of the key role of the SCF-cKit pathway in maintaining HSCs *in vivo* (Broudy, 1997). Additional genetic gain-of-function and loss-of-function studies have been used to elucidate the roles of other cell types and pathways in HSC maintenance (Calvi et al., 2003; Zhang et al., 2003). Many of these studies used whole-body mutant mice where all cells are genetically perturbed. Thus, it is not clear what niche cells are relevant to observed HSC phenotypes. Cell ablation experiments have also been employed to functionally assess the requirement of distinct cell populations in supporting HSCs (Méndez-Ferrer et al., 2010). However, eliminating specific cells by inducing cell death may provoke non-specific HSC phenotypes related to other functions of the candidate niche cells. Ectopic bone marrow formation is another method employed to show the sufficiency of a given cell population in initiating an HSC-supporting environment (Sacchetti et al., 2008; Chan et al., 2009; Song et al., 2010). Purified candidate niche organizing cells are transplanted subcutaneously or under the kidney capsule, sometimes with scaffolds. Over time, bone marrow will be developed and hematopoiesis will be sustained in these ectopic loci. But it is not clear whether these niche-organizing cells or other cells recruited by them are directly supporting HSCs within the ectopic bone marrow. Ultimately, HSC maintenance factors need to be conditionally deleted from candidate niche cells to definitively test the hypothesis that these cells create the niche by elaborating key HSC-supporting factors (Ding et al., 2012; Ding and Morrison, 2013). Some of these functional studies have also been used to define cells and pathways that regulate HSCs extrinsically during development and in hematological disorders. In the following sections, we will discuss extrinsic HSC regulation with the emphasis on evidence from functional studies.

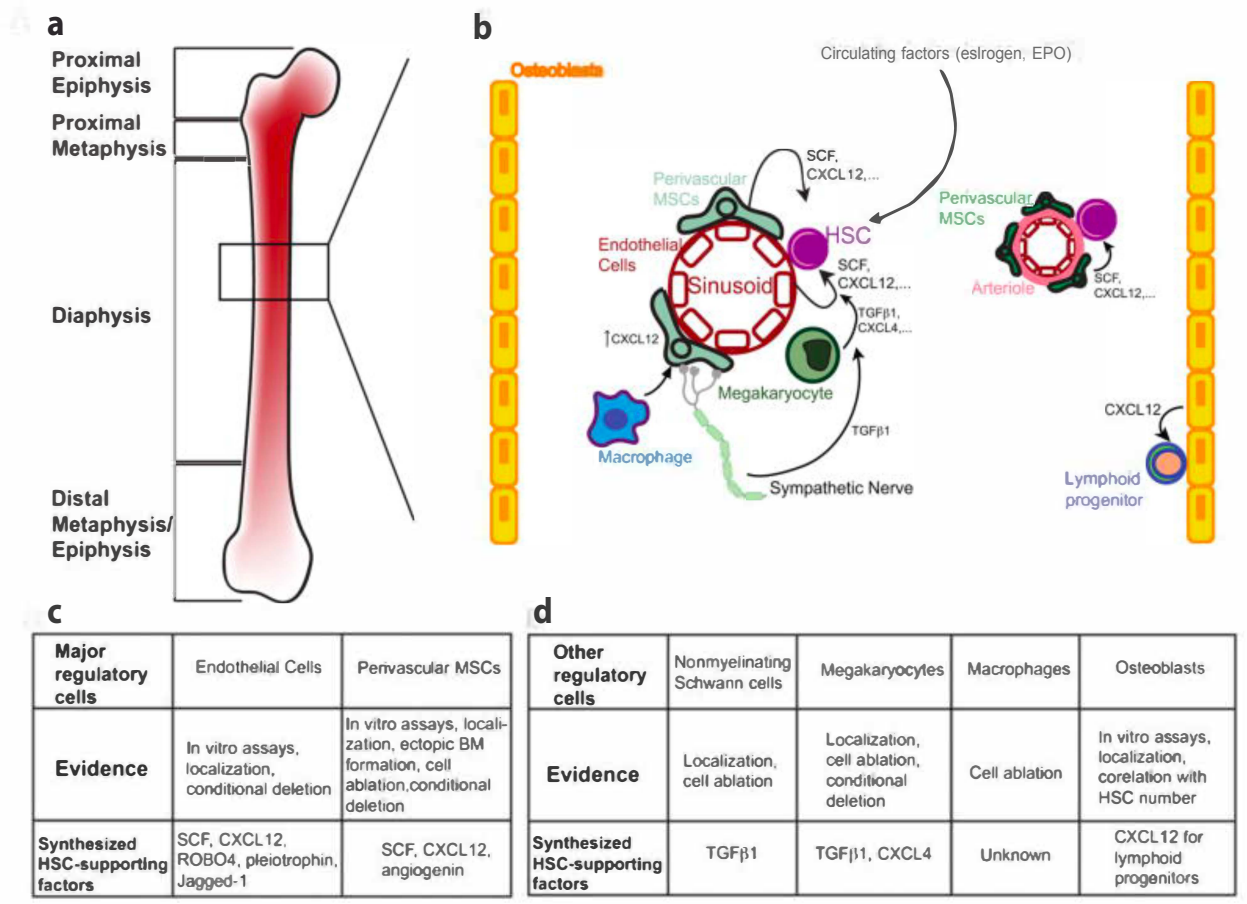

c

Major regulatory cells	Endothelial Cells	Perivascular MSCs
Evidence	In vitro assays, localization, conditional deletion	In vitro assays, localization, ectopic BM formation, cell ablation,conditional deletion
Synthesized HSC-supporting factors	SCF, CXCL12, ROBO4, pleiotrophin, Jagged-1	SCF, CXCL12, angiogenin

d

Other regulatory cells	Nonmyelinating Schwann cells	Megakaryocytes	Macrophages	Osteoblasts
Evidence	Localization, cell ablation	Localization, cell ablation, conditional deletion	Cell ablation	In vitro assays, localization, corelation with HSC number
Synthesized HSC-supporting factors	TGFβ1	TGFβ1, CXCL4	Unknown	CXCL12 for lymphoid progenitors

Figure 1.1 Homeostatic HSC extrinsic regulation

a. Anatomy of a mammalian long bone, the major hematopoietic organ in adults.

b. In the bone marrow, HSCs are regulated by a variety of cell types including endothelial cells, heterogeneous populations of mesenchymal stromal cells, non-myelinating Schwann cells, megakaryocytes, macrophages and osteoblasts. Signals from sympathetic nerves, circulating factors and possibly hypoxia (not pictured) are also important. Key locally synthesized factors for HSC maintenance include SCF, CXCL12, TGF-β1 and CXCL4.

c-d. Major and other HSC regulatory cells in the bone marrow, where major regulatory cells are required to maintain the HSC pool, and other regulatory cells affect the cell cycle, localization and downstream progeny of HSCs through direct and indirect mechanisms.

HOMEOSTATIC EXTRINSIC REGULATION

After development, mammalian HSCs take up residence in the bone marrow niche to sustain homeostatic hematopoiesis. The bone marrow niche is a specialized microenvironment that exquisitely regulates the quiescence, self-renewal, and differentiation of HSC. Studies have shown that bone marrow HSCs preferentially localize near the vasculature, and subsequent loss-of-function experiments have confirmed that both the vascular endothelium and perivascular stroma are crucial sources of HSC regulatory factors. In addition, mature hematopoietic cells and adipo-lineage cells within the bone marrow are able to regulate HSC behavior. Local oxygen levels, the sympathetic nervous system, and both local and circulating cytokines have also been implicated as regulators of HSCs. In total, these extrinsic signals are crucial to maintaining a functional HSC pool and lifelong hematopoiesis (**Figure 1.1**).

The bone marrow niche: location, location, location

Although the concept of an HSC niche was first proposed almost four decades ago (Schofield, 1978), robust characterization of the bone marrow niche was hindered by the lack of markers that could precisely label HSCs *in situ*. One of first studies performed by Lord *et al.* demonstrated that CFU-Ss (later shown to be hematopoietic progenitors, not HSCs) are enriched in endosteum, hinting this region may contain HSC niches (Lord et al., 1975). Initial *in situ* visualization studies indeed showed that transplanted, flow cytometrically purified HSCs homed to the endosteum (Lo Celso et al., 2009; Xie et al., 2009), where osteoblasts were proposed to be a critical component of the niche. Recent work using SLAM or other genetic markers demonstrates that a vast majority of HSCs are directly in contact with the vascular endothelium (Sugiyama et al., 2006; Méndez-Ferrer et al., 2010; Nombela-Arrieta et al., 2013;

Acar et al., 2015; Chen et al., 2016; Sawai et al., 2016), with only a minority of them close to endosteum, pointing to the perivascular microenvironment as the bone marrow HSC niche.

While there is a growing agreement on the central role of the perivascular microenvironment, there is conflicting evidence as to whether HSCs prefer the endosteum. One should be careful to distinguish observations of endogeneous HSCs from those of transplanted HSCs, since the niches may differ in these conditions in several ways. First, it is possible that the niche is perturbed by the myeloablation used in many transplantation experiments, which is known to damage the sinusoidal vasculature (Hooper et al., 2009; Zhou et al., 2014). Second, it has been shown that endosteal cells proliferate rapidly and up-regulate HSC maintenance pathways in response to myeloablation (Dominici et al., 2009; Olson et al., 2013). Finally, it is not clear whether the transplanted HSCs are engaged with their niche or in the process of finding the niche. Thus, it is possible that the endosteal localization frequently seen of transplanted HSCs reflects experimental conditioning rather than homeostatic physiology, although understanding how the niche differs in these states has important clinical implications for transplantation therapies. Discrepancies in the literature thus may in part reflect subtle differences between the 'homeostatic niche' and 'post-transplant niche'. However, the cell types and signaling pathways implicated in HSC maintenance seem to play significant roles in both the homeostatic and post-transplant bone marrow – for example, angiogenin from mesenchymal stromal cells (MSCs) regulates HSC proliferation in homeostasis and promotes hematopoietic regeneration following myeloablative conditioning (Goncalves et al., 2016; Silberstein et al., 2016).

Key cellular components of the bone marrow niche

Functional evidence suggests that a number of cell types contribute critically to the bone marrow niche. As the cellular components of the bone marrow niche have been extensively reviewed elsewhere (Mendelson and Frenette, 2014; Morrison and Scadden, 2014; Hoggatt et al., 2016), we will only summarize some of the key *in vivo* functional evidence here. Early studies showed that osteoblast number was positively correlated with the number of HSCs in two mouse genetic models (Calvi et al., 2003; Zhang et al., 2003), which in part led to the initial proposal of an endosteal bone marrow niche. Osteoblasts have been proposed to regulate HSCs by a variety of mechanisms including granulocyte colony stimulating factor (G-CSF) (Taichman and Emerson, 1994), Notch (Calvi et al., 2003), Wnt (Sugimura et al., 2012), Angiopoietin-1 (ANGPT1) (Arai et al., 2004) and thrombopoietin (TPO) (Yoshihara et al., 2007) signaling and N-cadherin-mediated cell adhesion (Zhang et al., 2003). However, careful functional studies reveal conflicting evidence over the roles of Notch (Maillard et al., 2008), ANGPT1 (Zhou et al., 2015) and N-cadherin (Visnjic et al., 2004; Kiel et al., 2009; Bromberg et al., 2012) and additional data complicates the picture of how osteoblasts regulate HSCs. In several other mouse models where osteoblast number was increased or decreased, HSC number was unchanged (Visnjic et al., 2004; Zhu et al., 2007; Lymperi et al., 2008; Kiel et al., 2009; Calvi et al., 2012). Furthermore, conditional deletion of critical HSC maintenance factors SCF and CXCL12 from osteoblasts has no effect on HSC function (Ding et al., 2012; Ding and Morrison, 2013). However, it has been shown that osteoblasts serve as an important niche component for early lymphoid progenitors by synthesizing CXCL12 (Ding and Morrison, 2013; Greenbaum et al., 2013). It is possible that osteoblasts act through other mechanisms to modify HSC behavior, but their role as a niche cell is not as prominent as initially proposed.

While the evidence about the role of osteoblasts in HSC maintenance is conflicting, there is strong evidence that the vascular endothelium is a crucial cellular component of the niche. Endothelial cells (ECs) drive HSC self-renewal *in vivo* through Notch signaling (Kobayashi et al., 2010; Poulos et al., 2013; Wang et al., 2014; Kusumbe et al., 2016), FGFR signaling (Itkin et al., 2016), gp130 (Yao et al., 2005) and production of SCF (Ding et al., 2012) and CXCL12 (Ding and Morrison, 2013), and HSC homing through release of CXCL12 (Ding and Morrison, 2013) ROBO4 (Smith-Berdan et al., 2011, 2015) and pleiotrophin (Himburg et al., 2010, 2012). The vasculature also plays a critical role in mediating a physiologic response to hematopoietic stress; following myeloablation, regeneration of VEGFR2^{+}sinusoidal ECs is required for effective hematopoietic reconstitution (Hooper et al., 2009; Butler et al., 2010). Moreover, endothelial cell-derived EGF is critical for HSC and hematopoietic regeneration after irradiation (Doan et al., 2013).

Perivascular MSCs that lie in close contact with the bone marrow vasculature have also been identified as major regulators of HSCs. Several markers with overlapping expression patterns have been used to define these perivascular stromal cells, including platelet-derived growth factor receptor α (PDGFRA) (Morikawa et al., 2009; Pinho et al., 2013), leptin receptor (LEPR) (Ding et al., 2012) Prx1-cre (Greenbaum et al., 2013), Osx-cre (Greenbaum et al., 2013), Osx-creER, FAP (Tran et al., 2013), CD146 in humans (Sacchetti et al., 2008), SCF (Ding et al., 2012), CXCL12 (Sugiyama et al., 2006; Ding and Morrison, 2013; Greenbaum et al., 2013), and the *Nestin*-GFP transgene (Méndez-Ferrer et al., 2010). Using some of these markers as tools to manipulate these cells, a number of functional studies have provided strong evidence that the perivascular stromal cells are a critical component of the bone marrow niche. Ablation of *Cxcl12*-expressing or FAP-expressing bone marrow cells led to depletion of HSCs (Omatsu et

al., 2010) and compromised hematopoiesis (Omatsu et al., 2010; Roberts et al., 2013). Conditional deletion of *Scf* from perivascular stromal cells using *Lepr-cre* resulted in HSC depletion (Ding et al., 2012) as did conditional deletion of *Cxcl12* from perivascular stromal cells using *Lepr-cre* or *Prx1-cre* (Ding and Morrison, 2013; Greenbaum et al., 2013). Interestingly, these stromal cells have mesenchymal progenitor activity with the capacity to differentiate into bone and adipocyte lineages *in vitro* and *in vivo* (Lassila et al., 1978; Méndez-Ferrer et al., 2010). Conditional deletion of *Foxc1*, a transcriptional factor involved in mesenchymal cell fate determination, from perivascular stromal cells led to excessive adipogenesis and depletion of HSCs (Omatsu et al., 2014). Recently, angiogenin has been identified as a novel factor from Osx^+ mesenchymal cells for HSC maintenance (Goncalves et al., 2016). Besides these genetic studies, subcutaneously transplanted human $CD146^+$ bone marrow stromal cells have been shown to form ectopic HSC-supporting bone marrow (Sacchetti et al., 2008). Thus, the bone marrow perivascular mesenchymal stromal cells are a critical component of the bone marrow niche.

Other non-hematopoietic cells have also been implicated in HSC maintenance. HSCs from adipocyte-rich bone have decreased function and treatment with adipogenic inhibitors increases the reconstitution potential of HSCs, suggesting that adipocytes may negatively regulate HSCs (Naveiras et al., 2009). Additionally, non-myelinating Schwann cells have been shown to activate latent TGF-β signaling required for HSC maintenance (Yamazaki et al., 2011).

Mature hematopoietic cells have also been connected to HSC regulation. Megakaryocytes physically associate with HSCs, maintain HSC quiescence through secretion of factors such as CXCL4 and TGF-β1, and promote hematopoietic recovery after myeloablation by driving HSC expansion (Bruns et al., 2014; Zhao et al., 2014). Like megakaryocytes, bone marrow

macrophages also modify HSC behavior. Depletion of macrophages leads to increased egress of HSCs from the bone marrow, suggesting that macrophages help retain HSCs in the bone marrow niche through cell homing and adhesion pathways, such as CXCL12-CXCR4 signaling (Winkler et al., 2010; Chow et al., 2011). Macrophages are believed to drive this retention of HSCs indirectly by acting on other niche cells including MSCs (Winkler et al., 2010; Chow et al., 2011). However, a recent study suggested that a subpopulation of macrophages which express Duffy antigen/receptor for chemokines (DARC) directly maintain HSC quiescence via binding of DARC to the HSC cell surface antigen KANGAI1 (KAI1) (Hur et al., 2016). Thus, macrophages can directly and indirectly impact HSCs. In addition, Treg cells have been shown to provide immune privilege in the bone marrow niche (Fujisaki et al., 2011). In summary, these findings highlight the complex and interconnected regulatory interactions of the bone marrow niche.

Hypoxia and the bone marrow niche

The cells of the perivascular bone marrow niche are critical extrinsic regulators of HSCs, but they are not the only factors that influence HSC biology. Numerous studies suggest that oxygen levels in the bone marrow have a major impact on HSC homing and function. In poorly perfused regions of the bone marrow that presumably have lower oxygen tension, the HSC population is enriched, more quiescent, and better able to serially reconstitute irradiated recipient mice (Parmar et al., 2007). Consistent with these findings, HSCs with high levels of reactive oxygen species (ROS), a feature associated with aerobic metabolism, have diminished self-renewal potential (Jang and Sharkis, 2007). Indeed, HSC maintenance seems to require continuous activation of hypoxia-associated transcriptional and metabolic programs (Simsek et

al., 2010; Takubo et al., 2010; Miharada et al., 2011; Casanova-Acebes et al., 2013). Interestingly, harvesting HSCs in a hypoxic environment better preserves transplantable HSCs (Mantel et al., 2015). The importance of these pathways to HSC function has driven many labs to investigate the location of the putative 'hypoxic niche' through indirect (Nombela-Arrieta et al., 2013) and direct (Spencer et al., 2014) measurements of oxygen levels throughout the bone marrow. The most recent and direct evidence shows that the peri-sinusoidal region in the bone marrow is the most hypoxic region of the bone at steady state (Spencer et al., 2014). However, it is possible that the association between HSCs and hypoxia is indirect. The 'hypoxic' profile of HSCs measured by pimonidazole may reflect their metabolic status independent of localization (Nombela-Arrieta et al., 2013). In addition, the hypoxia master regulator HIF-1α may be dispensable in HSCs (Vukovic et al., 2016), although HIF-1α activity drives growth and expansion of vascular endothelium (Kusumbe et al., 2016). Thus, hypoxia may promote the development of the HSC niche, rather than providing direct extrinsic regulation of HSCs.

Heterogeneity of the bone marrow niche

The above data strongly suggest that HSCs reside in a perivascular niche with endothelial cells and mesenchymal stromal cells as critical components. Recent evidence points to potential heterogeneity in the perivascular niche. Perivascular $NG2^{+}LEPR^{-}$Nes-GFP^{bright} mesenchymal cells that predominantly associate with bone marrow arterioles, not sinusoids, have been shown to play a role in HSC maintenance: partial ablation of $NG2^{+}$ cells leads to decreased HSC quiescence and diminished capacity for functional reconstitution (Kunisaki et al., 2013). However, deletion of *Scf* and *Cxcl12* using *NG2-creER* did not significantly affect HSCs (Acar et al., 2015). Further investigation is needed to clarify this discrepancy. Mechanisms other than

SCF and CXCL12 production may account for the HSC phenotype observed in the mice with $NG2^+$ cells ablated. Recently, heterogeneity among endothelial cells in the bone marrow has been suggested to play important roles in regulating distinct HSC behaviors - arterial blood vessels maintain HSCs while sinusoids promote HSC activation and trafficking (Itkin et al., 2016). The functional evidence supporting this conclusion is partly based on evidence that conditional deletion of *Fgfr* from endothelial cells using *Vecadherin-CreER* leads to vasculature leakage and HSC reduction. However, *Vecadherin-creER* recombines in all bone marrow endothelial cells including arteriolar and sinusoidal endothelial cells (Wang et al., 2013). Cre drivers specific to distinct vascular domains are needed to further elucidate the roles of different subsets of the vasculature.

Beyond the bone marrow: systemic regulation of HSCs

The bone marrow microenvironment is the most well-studied component of HSC extrinsic regulation, but extramedullary signals from outside the bone marrow also have a significant impact on HSCs. One prominent example of an extramedullary regulator is the sympathetic nervous system, which has a major influence on the release of HSCs into the blood stream (Lucas et al., 2008; Méndez-Ferrer et al., 2008). Catecholaminergic signaling to both HSCs (Spiegel et al., 2007) and niche cells (Katayama et al., 2006) drives HSC egress from the bone marrow by downregulating the chemokine CXCL12 and upregulating metalloproteinases that degrade the adhesive extracellular matrix. This signaling is linked to the body's circadian rhythm, which also drives clearance of aged neutrophils from the bone marrow niche (Casanova-Acebes et al., 2013).

There is growing evidence that systemically circulating factors also influence the biology of HSCs. New studies have shown that physiological circulating estrogen (Nakada et al., 2014) and induced upregulation of endogenous erthyropoietin (EPO) (Grover et al., 2014) can directly promote HSC proliferation or instruct HSC differentiation to specific cell fates. These molecular signals originate outside the bone marrow but are still able to regulate the fate and behavior of HSCs, raising the possibility that other endogenous hematopoietic cytokines synthesized outside the bone marrow may directly maintain the HSC pool.

DISRUPTION OF EXTRINSIC REGULATION

The bone marrow homeostatic niche must balance activating HSCs to replace lost progenitors while maintaining quiescent HSCs for future needs. This finite equilibrium can be disturbed in aging or other hematopoietic disorders. Aging of the hematopoietic system is associated with a decline of HSC function and hematopoiesis. This may be related to the demands of the an aging individual - to minimize oncogenic transformation at the cost of self-renewal activity (Signer and Morrison, 2013). It is evident that the extrinsic regulatory mechanisms play a role in HSC aging. Just as the HSC extrinsic regulation is important in homeostasis and aging, its dysregulation also plays a key role in coping with or even initiating pathological hematopoiesis. Below, we will discuss illustrative examples of the extrinsic regulation of HSCs in inflammation, malignancies, and aging.

Inflammation

Extrinsic regulatory mechanisms can protect against infection and injury by modulating HSCs. During infection, the hematopoietic system must generate a sufficient immune response that often requires more mature hematopoietic cells from HSCs. Inflammatory signaling from Toll-like receptors (TLRs) and cytokines such as interferon-γ (IFNγ), interferon-α (IFNα), and tumor necrosis factor-α (TNFα) can activate HSCs (Riether et al., 2015). These signals can be sensed directly by HSCs, but the bone marrow hematopoietic environment also plays a key role in mediating some of these immune responses (Essers et al., 2009). For example, it has been shown that bacterial cell wall products from *E.coli* infection activate TLR and nucleotide-binding oligomerization domain-containing receptors (NOD) signaling, which induces G-CSF expression and decreases CXCL12 expression from niche endothelial cells, which in turn mobilizes HSCs to the spleen (Burberry et al., 2014). Similarly, IFNγ has been linked to increased HSC proliferation and mobilization to the spleen (Baldridge et al., 2010). This effect can be mediated by MSCs expressing IL6 in response to IFNγ, which results in increased myeloid differentiation in response to infection (Schürch et al., 2014).

Hematologic malignancies

Abnormalities in the niche are associated with hematologic malignancies. Leukemia-initiating cells (LICs) hijack the HSC mechanisms to persist and fuel the growth of leukemia. For an LIC to emerge and thrive, it must lose the restraints of HSC regulatory mechanisms keeping its growth and function in check. Some of those mechanisms are intrinsic to the LICs, but many are dependent on the niche. Whatever the inciting cause, as leukemia develops, there is ongoing

crosstalk between the niche and LICs that eventually leads to further dysregulation and loss of normal hematopoiesis.

A growing number of papers have demonstrated that the niche can be the inciting factor in developing malignancy. Myeloproliferative neoplasms (MPN) or myeloproliferation can be induced by deletion of *IkBa* (an inhibitor of NFkB), *Mindbomb-1* (a notch ligand regulator) or retinoic acid receptor-γ in the bone marrow microenvironment (Rupec et al., 2005; Walkley et al., 2007a; Kim et al., 2008). Furthermore, conditional deletion of *Rbpj* (a notch pathway component) from endothelial cells also promotes myeloproliferation (Wang et al., 2014). Moreover, conditional deletion of *retinoblastoma* protein (*Rb*) from both hematopoietic cells and stromal cells, causes a myeloproliferative-like disorder, but not when only deleted from myeloid progenitors or stromal cells (Walkley et al., 2007b). In a similar fashion, conditional deletion of *Dicer1* from osteoprogenitors but not more mature osteoblasts causes transplantable myelodysplasia and secondary leukemia (Raaijmakers et al., 2010). Finally, Kode *et al.*induced acute myelogenous leukemia (AML)–like disease by constitutively activating β-catenin in osteoblasts (Kode et al., 2014). These studies directly demonstrate the causal role of the niche in hematopoietic malignancies.

The interaction of leukemia cells and their niche is reciprocal. Several studies have shown that the introduction of leukemia can alter the niche, and often in ways that support the progression of leukemia and suppress normal hematopoiesis. Live imaging of mouse bone marrow transplanted with human leukemia cells showed that leukemic cells alter the stromal niche (Colmone et al., 2008). These abnormal niches sequester normal HSPCs and impair normal hematopoiesis. Chronic myelogenous leukemia (CML) cells have been shown to alter key niche factors – such as decreasing CXCL12 and SCF and increasing G-CSF – that prevent HSCs from

occupying their normal niche and instead promote leukemic cell development (Zhang et al., 2012; Schepers et al., 2013). Similarly, the MPN bone marrow niche undergoes an alteration of niche signals and loss of bone marrow Schwann cells and nestin^{+} MSCs (Arranz et al., 2014). Rescuing some of the lost sympathetic tone with a selective β3 adrenergic agonist reduced the severity of disease. Besides leukemia, the niche can also be an active participant in disease progression in other hematopoietic disorders. It has been shown that myelodysplastic syndrome (MDS)-initiating hematopoietic cells have the ability to induce neighboring MSCs to propagate a diseased microenvironment and facilitate the development of MDS (Medyouf et al., 2014). These results demonstrate that abnormal hematopoietic cells may benefit from the changes they induce in the niche.

Recent understanding of how the bone marrow niche contributes to malignancy has led to the development of niche-targeted therapies with promising initial results. For example, AML cells exploit the CXCL12/CXCR4 axis for proliferation and survival, and high expression of CXCR4 on LICs correlates with worse prognosis. Inhibitors of CXCR4, most notably plerixafor, in combination with traditional chemotherapy agents have improved outcomes in AML murine models and clinical trials (Rashidi and DiPersio, 2016). While niche-targeted agents have yet to become a part of standard treatments, research in this area is likely to grow.

Aging

The effects of aging on HSC function have been well described. Old HSCs have a decreased regenerative potential, are biased towards the myeloid lineage, and are more easily mobilized in response to cytokine cues (Geiger et al., 2013). Some of these phenotypes are

linked to intrinsic changes within the HSC, but others have been proposed to be the result of an aging microenvironment. The effects of aging specifically on the bone marrow HSC niche has only begun to be explored. Transplantation of HSCs from young mice to old recipient mice (or vice versa) shows that at least part of the aging HSC phenotypes can be attributed to an aging environment. Young bone marrow HSCs home inefficiently to old bone marrow compared with young bone marrow, showing that there is a relevant difference in interactions between HSCs and the old environment that affects HSC engraftment (Liang et al., 2005). Details on which signaling interactions differ and how engraftment is altered have yet to emerge. Similarly, old HSCs are less myeloid-biased when transplanted into young mice, suggesting that the age of the environment plays a key role in HSC differentiation lineage bias, which could be explained by an increase in the inflammatory cytokine RANTES (Ergen et al., 2012). Systemic age-related changes might also influence HSCs. Parabiosis experiments between old and young mice have demonstrated blood-borne factors that vary with age can influence muscle satellite stem cell and neural stem/progenitor cells function (Conboy et al., 2005; Villeda et al., 2011). These studies suggest the possibility of systemic mechanisms for stem cell aging in general, but direct evidence for age-related systemic changes in HSC regulation is still needed. The question still remains of exactly how other age-related changes in HSCs are regulated by an old environment, both locally and systemically.

Chapter 2

Leptin-receptor expressing bone marrow stromal cells are myofibroblasts in primary myelofibrosis

The work described in this chapter is published:

Matthew Decker*, Leticia Martinez-Morentin*, Guannan Wang*, Yeojin Lee, Qingxue Liu, Juliana Leslie, and Lei Ding (2017)

Leptin-receptor expressing bone marrow stromal cells are myofibroblasts in primary myelofibrosis

Nature Cell Biology, Vol 19, Issue 6, p677-688

*Equal author contributions

M.D., L.M., G.W., Y.L., and L.D. performed all the experiments with the help of Q.L. and J.L. M.D., L.M., G.W., and L.D. designed the experiments, interpreted the results, and wrote the manuscript

SUMMARY

Bone marrow fibrosis is a critical component of primary myelofibrosis (PMF). But the origin of myofibroblasts that drive fibrosis is unknown. Using genetic fate mapping we found that bone marrow Leptin receptor (*Lepr*) – expressing mesenchymal stromal lineage cells expanded extensively and were the fibrogenic cells in PMF. These stromal cells down-regulated the expression of key hematopoietic stem cell (HSC)- supporting factors and up-regulated genes associated with fibrosis and osteogenesis, indicating fibrogenic conversion. Administration of imatinib or conditional deletion of platelet-derived growth factor receptor a (*Pdgfra*) from *Lepr*$^{+}$ stromal cells suppressed their expansion and ameliorated bone marrow fibrosis. Conversely, activation of the PDGFRa pathway in bone marrow *Lepr*$^{+}$ cells led to expansion of these cells and extramedullary hematopoiesis, features of PMF. Our data identify *Lepr*$^{+}$stromal lineage cells as the origin of myofibroblasts in PMF and suggest that targeting PDGFRa signaling could be an effective way to treat bone marrow fibrosis.

INTRODUCTION

Hematopoietic stem cells (HSCs) are maintained by their microenvironmental niches. Recently, we identified bone marrow *Lepr*$^{+}$ mesenchymal stromal cells as a critical component of the niche that elaborates multiple factors, including stem cell factor (SCF) and CXCL12 (Ding et al., 2012; Ding and Morrison, 2013). These stromal cells include skeletal stem cells that are the main source of bone in the adult bone marrow (Zhou et al., 2014). Although our understanding of the mesenchymal stromal cells under steady state has advanced quickly, how these cells are altered by and contribute to hematological diseases has not been well characterized (Schepers et al., 2015).

Primary myelofibrosis (PMF) is a subtype of myeloproliferative neoplasms (MPNs) with clinical characteristics, including anemia, bone marrow fibrosis and extramedullary hematopoiesis (Abdel-Wahab and Levine, 2009). Most PMF patients are elderly. PMF originates clonally from abnormal hematopoietic stem/progenitor cells. Allogeneic HSC transplantation is the only possible cure. However, this approach is too toxic for elderly people, precluding its application to most PMF patients. The hematopoietic-intrinsic molecular mechanisms that lead to PMF have been studied extensively (Tefferi, 2016). Several driver mutations have been identified, including JAK2V617F and MPLW515L mutations that lead to constitutive activation of JAK2 kinase and the upstream receptor MPL, respectively (Tefferi, 2016). Calreticulin mutations that activate the MPL receptor (Araki et al., 2016; Chachoua et al., 2016; Marty et al., 2016) have recently been discovered in most JAK2/MPL mutation-negative patients (Klampfl et al., 2013; Nangalia et al., 2013). Thus, activation of the MPL-JAK-STAT pathway in haematopoietic cells is a general feature of MPNs, regardless of the specific molecular mechanisms. Consistent with this, a comprehensive genomic analysis has identified gene signature of JAK-STAT activation in all MPN patients, independent of mutations (Rampal et al., 2014). Currently, JAK inhibitors have been actively explored as a means to treat PMF. While these inhibitors control symptoms, they do not resolve the disease, particularly the bone marrow fibrosis (Tefferi, 2016). Thus, a deeper understanding of the fibrotic component of PMF pathogenesis is required to devise more effective therapies.

The cellular mechanisms underlying bone marrow fibrosis are still being elucidated. An earlier study of X chromosome-linked markers in a female PMF patient revealed that hematopoietic cell overproliferation was clonal while the bone marrow fibrosis was not (Jacobson et al., 1978). Mouse models with MPN-associated mutations have demonstrated that

MPNs originate from abnormal hematopoietic clone (Lundberg et al., 2014). But how overproliferating hematopoietic cells lead to bone marrow fibrosis and extramedullary hematopoiesis is not clear. Megakaryocyte deregulation and hyperplasia is a defining cellular feature of PMF (Tefferi, 2016; Papadantonakis et al., 2012). Overexpression of the major megakaryopoietic cytokine, thrombopoietin (TPO), leads to megakaryocyte hyperplasia and PMF in mice (Villeval et al., 1997; Yan et al., 1995). Gata1^{low} mice with a block in megakaryocyte maturation (Shivdasani et al., 1997) developed myelofibrosis, suggesting a disease model where dysregulated megakaryocytes secrete excessive cytokines, including transforming growth factor-beta 1 (TGFβ1) and platelet-derived growth factor (PDGF) that drive bone marrow fibrosis (Vannucchi et al., 2002). Indeed, targeting deregulated megakaryocytes by inhibiting the AURKA pathway eliminated bone marrow fibrosis (Wen et al., 2015). However, the bone marrow stromal cells that respond to the cytokines elaborated by hyperplastic megakaryocytes and that directly deposit reticulin and collagen fibers have not been identified.

PDGFs are potent cytokines that promote mesenchymal cell proliferation and are implicated in many fibrotic diseases, including pulmonary and liver fibrosis (Bonner, 2004). Activation of PDGFRa signaling is sufficient to drive fibrosis in diverse organs (Olson and Soriano, 2009; Iwayama et al., 2015). PMF patients have significantly higher concentrations of PDGFs in circulation, likely due to increased release (Gersuk et al., 1989). However, whether PDGFR pathways play a role in bone marrow fibrosis has not been directly addressed.

It has been speculated that cells of the fibroblastic lineage are the origin of myofibroblasts in PMF (Abdel-Wahab and Levine, 2009; Tefferi, 2005). A number of markers have been used to identify mouse bone marrow fibroblastic stromal cells, also referred to as colony-forming unit-fibroblast (CFU-F), including Nestin-GFP, CD51, PDGFRa, PDGFRb and

NG2 (Morikawa et al., 2009; Méndez-Ferrer et al., 2010; Komada et al., 2012; Kunisaki et al., 2013; Pinho et al., 2013). Using some of these markers, several studies characterized the mesenchymal stromal cells in MPN mouse models. In a chronic myeloid leukemia (CML) model, Schepers *et al* reported an expansion of $Lin^{-}CD45^{-}CD31^{-}CD51^{+}Sca1^{-}$ osteoblastic lineage cells and increase collagen deposition. However, it was not clear whether these cells were the origin of bone marrow fibrosis (Schepers et al., 2013). In a $Jak2^{V617F}$ MPN model, Arranz *et al* performed lineage-tracing using *Nestin*-creER to assess the contribution of $Nestin^{+}$ stromal cells. No obvious contribution of these cells to bone marrow fibrosis was noted (Arranz et al., 2014). As a result, the stromal cells that directly contribute to bone marrow fibrosis are unknown. Given the central role of PDGFR signaling in myofibroblasts and fibrosis, we searched for bone marrow stromal cells that express PDGFRs. Previously, we reported that *Lepr*$^{+}$ stromal cells are uniformly positive for PDGFRa and PDGFRb (Ding et al., 2012; Zhou et al., 2014). Conversely, virtually all $PDGFR^{+}$ stromal cells in the bone marrow are *Lepr*$^{+}$ (Zhou et al., 2014). This raises the question of whether the $Lepr^{+}PDGFR^{+}$ stromal cells are the origin of myofibroblasts in PMF.

We set out to identify the stromal cells that generate reticulin and collagen fiber in myelofibrosis using lineage tracing. We found that *Lepr*$^{+}$ mesenchymal stromal cells were the source of myofibroblasts and underwent expansion in PMF. These cells down-regulated key HSC maintenance factors and up-regulated fibrogenic and osteogenic genes. Conditional deletion of *Pdgfra* from *Lepr*$^{+}$ mesenchymal stromal cells or administrating imatinib suppressed their expansion and largely abolished bone marrow fibrosis. Conversely, activation of PDGFRa pathway in *Lepr*$^{+}$ mesenchymal stromal cells led to their expansion and extramedullary hematopoiesis. Our results identify the activation of the PDGFRa pathway in *Lepr*$^{+}$ cells as an

important contributor to myelofibrosis and provide a proof of principle that inhibiting the PDGFRa pathway in mesenchymal stromal cells is an attractive strategy to treat bone marrow fibrosis.

RESULTS

Development of primary myelofibrosis in *Tpo*-overexpressing mice

We adapted a retroviral mouse PMF model by transplanting *Tpo*-overexpressing (TOE) retrovirally-infected bone marrow cells into irradiated mice. Consistent with prior reports (Yan et al., 1995; Villeval et al., 1997), these mice developed high levels of serum TPO (**Figure 2.1a**), thrombocythemia (**Figure 2.1b**), and a trend towards leukocytosis (**Figure 2.1c**) within three months after the transplantation. The bone marrow from the TOE mice was pale, particularly in mice with advanced PMF (**Figure 2.1d**). Enlarged spleens with extramedullary hematopoiesis were evident accompanied by a 3-fold increase in spleen weight (**Figure 2.1e-f**). Bone marrow myeloid cells significantly expanded in TOE mice (58±13% cells were myeloid cells in TOE vs 40±8% in controls) (**Figure 2.1g**). These mice displayed megakaryocyte hyperplasia in the bone marrow (**Figure 2.1h**) and profound fibrosis in the spleen and bone marrow (**Figure 2.1i-j**). Large amounts of collagen fibers and osteosclerosis associated with fibrosis made dissociation of bone marrow cells from TOE mice into single cell suspension difficult. These observations indicate that the TOE model developed features of PMF as previously reported (Yan et al., 1995; Villeval et al., 1997).

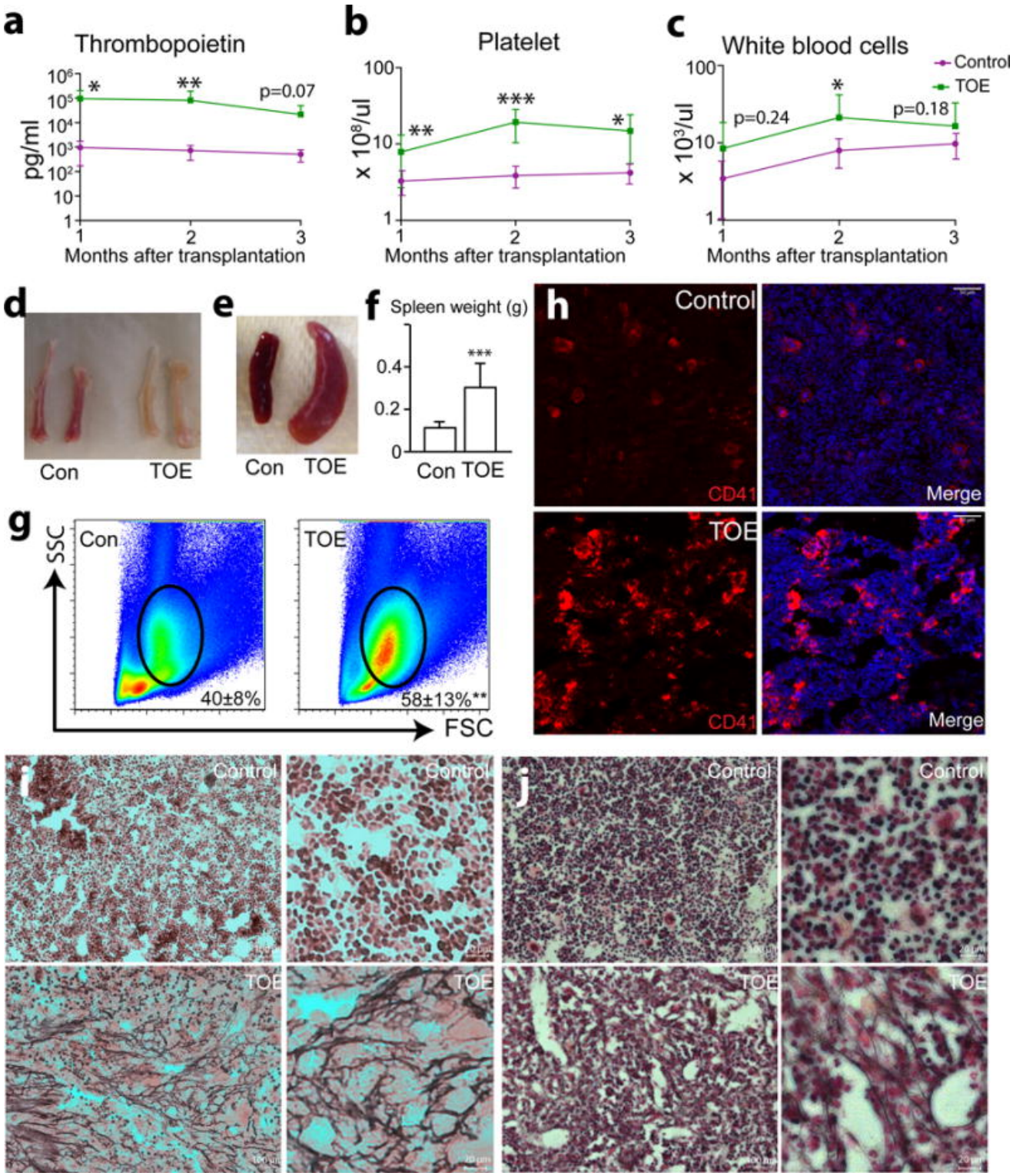

Figure 2.1 TOE mice develop clinical features of PMF

Figure 2.1 TOE mice develop clinical features of PMF

a. Plasma TPO levels determined by ELISA 1 to 3 months after the bone marrow transplantation showing elevated TPO level in TOE mice compared with controls (mice transplanted with control vector virus-infected bone marrow cells) (n=16, 15 and 7 mice for control, n=15, 13 and 7 mice for TOE, at month 1-3 after transplantation, respectively).

b-c. Peripheral blood count analysis of TOE and control mice 1 to 3 months after bone marrow transplantation (n=16, 15 and 7 mice for control, n=15, 13 and 7 mice for TOE, at month 1-3 after transplantation, respectively for **b**) (n=16, 15 and 12 mice for control, n=15, 13 and 10 mice for TOE, at month 1-3 after transplantation, respectively for **c**).

d. Long bones from TOE mice were pale compared with vector controls.

e. TOE mice showed enlarged spleens.

f. Quantification of the spleen weight (n=13 mice for control and TOE, each).

g. TOE mice bone marrow showed a significant increase of myeloid cell frequency (n=8 mice for control, n=7 mice for TOE).

h. Images of bone marrow sections showing that megakaryocyte lineage cells were overproliferated in the bone marrow of TOE mice. Megakaryocytes were marked by CD41 antibody staining (in red). Nuclei were stained with DAPI (in blue).

i-j. Reticulin staining showing extensive fibrosis in the spleen (**i**) and bone marrow (**j**) from TOE mice. Right panels of **i** and **j** are higher magnification images. TOE, Tpo-overexpressing. Con, control vector virus. *$p<0.05$, ** $p<0.01$, *** $p<0.001$. Images are representative of at least 3 biological replicates.

HSCs undergo proliferation and mobilization in TOE mice

We examined HSC and progenitor compartments in TOE mice 2–4 months after the bone marrow transplantation. There was a 5-fold increase of the frequency of $Lin^{-}Sca1^{+}cKit^{+}CD150^{+}CD48^{-}$ HSCs in the bone marrow of TOE mice compared with mice transplanted with control virus-infected bone marrow cells (**Figure 2.2a-b**). Bone marrow cellularity was significantly reduced in TOE mice (**Figure 2.2c**). An overall quantification revealed increased HSC number in TOE bone marrow (**Figure 2.2d**). There were variations among the TOE mice in term of hematopoietic phenotypes presumably due to variable amount of TPO (thus variable fibrosis induction strength) in individual mice. When the mice were grouped into intermediate and advanced stages based on their hematopoietic parameters (e.g. color of the bone marrow and ease of bone marrow dissociation), we observed an initial significant increase of bone marrow HSC number in intermediate followed by a reduction of HSCs in advanced PMF mice (**Figure 2.2e**) consistent with clinical data on different stages of PMF patients (Reilly et al., 2012). This is associated with a gradual depletion of bone marrow cellularity (**Figure 2.2f**). HSCs from TOE mice incorporated more BrdU in 5-day pulse experiments (**Figure 2.2g**) suggesting they proliferated more.

There was a 1.6-fold more of mechanically dissociable cells in the spleens from TOE mice (**Figure 2.2h**). This was probably an underestimate because dissociation of TOE spleens was difficult due to extensive fibrosis. HSC frequency and number increased significantly in the TOE spleens (**Figure 2.2i-j**). HSCs shifted from the bone marrow to the spleen in advanced PMF mice (**Figure 2.1k**). These data suggest a pathogenic process of PMF: HSCs initially overproliferate and start mobilizing to the spleen; as the disease progresses, the bone marrow becomes fibrotic and hypocellular, and many HSCs shift to the spleen.

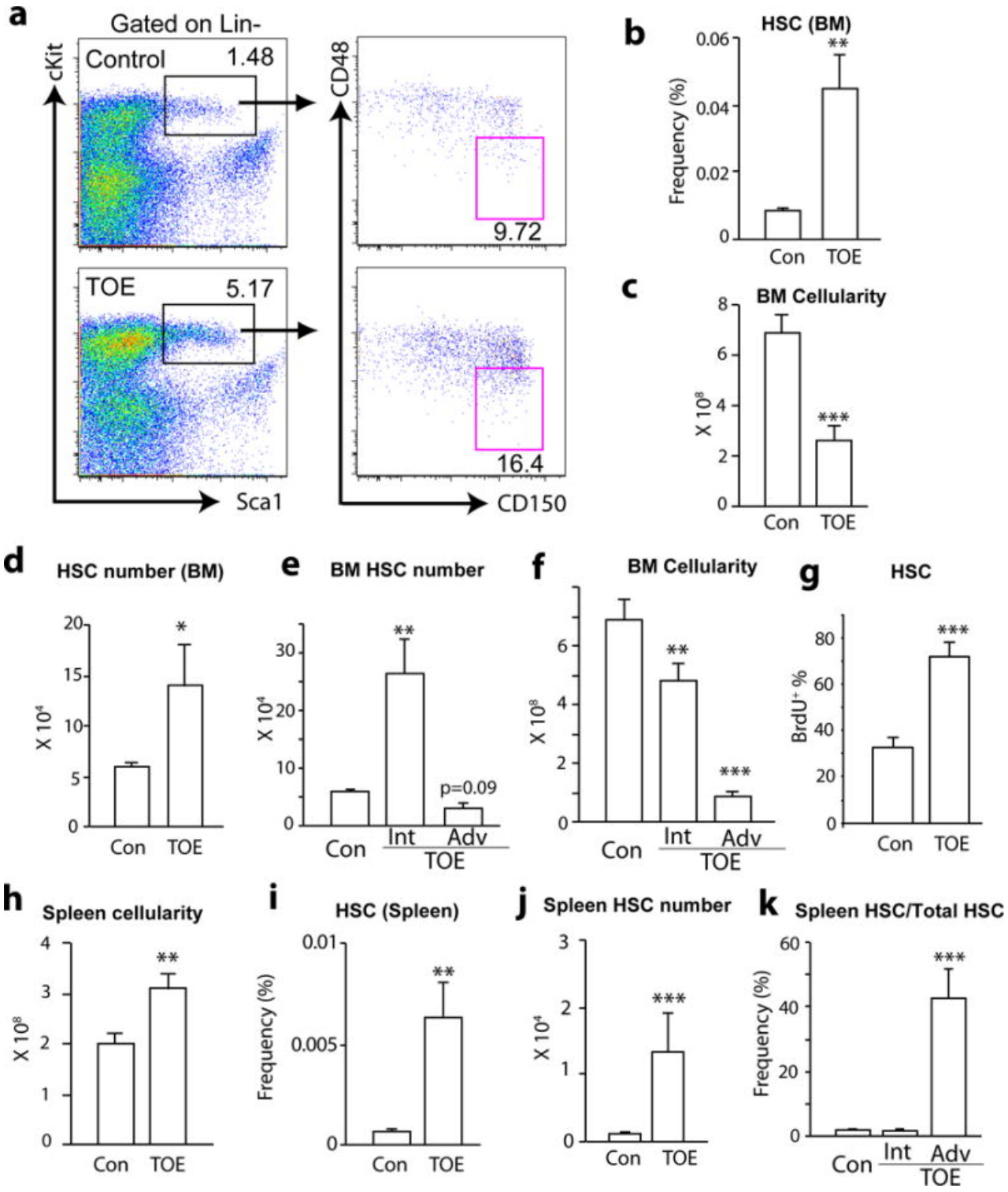

Figure 2.2 HSCs overproliferate and mobilize to the spleen in TOE mice

Figure 2.2 HSCs overproliferate and mobilize to the spleen in TOE mice

a. Representative flow cytometric plot showing the increased $Lin^{-}Sca1^{+}cKit^{+}CD150^{+}$ $CD48^{-}$ HSC frequency in TOE mice.

b. Bone marrow HSC frequency was significantly increase in TOE mice (n=21 mice for control and n=22 mice for TOE).

c. TOE mice had a significant reduction of bone marrow cellularity (n=21 mice for control and n=18 mice for TOE).

d. TOE mice had an increased HSC number in the bone marrow (n=20 mice for control and n=18 mice for TOE).

e. There was a significant increase of bone marrow HSC number in intermediate PMF followed by a reduction of bone marrow HSCs in advanced PMF (n=20 mice for control, n=9 mice for intermediate PMF, n=10 mice for advanced PMF).

f. As the PMF developed, there was a gradually more severe reduction of bone marrow cellularity in TOE mice (n=20 mice for control, n=9 mice for intermediate PMF, n=10 mice for advanced PMF).

g. Bone marrow HSCs from TOE mice incorporated significantly more BrdU in 5-day pulse experiments (n=4 mice for control and n=8 mice for TOE).

h. Spleen cellularity from TOE was significantly increased (n=15 mice for control and n=12 mice for TOE).

i-j. HSC frequency and number from spleens of TOE mice were significantly increased (n=22 mice for control and n=23 mice for TOE in (**i**), n=13 mice for control and n=11 mice for TOE in (**j**)).

k. Quantification of spleen and bone marrow HSC number showed a significant mobilization to the spleen in advanced stage of PMF (n=12 mice for control, n=6 mice for intermediate PMF and n=7 mice for advanced PMF). TOE, Tpo-overexpressing. Con, control vector virus. Int, intermediate stage. Adv, advanced stage. *$p<0.05$, ** $p<0.01$, *** $p<0.001$.

Lepr$^+$ mesenchymal stromal cells undergo fibrotic expansion

The above data suggest that bone marrow fibrosis contributes to bone marrow hematopoietic failure. However, the identity of cells that deposit collagen fibers and render bone marrow fibrotic is elusive. Bone marrow *Lepr*$^+$ mesenchymal stromal cells, which uniformly express PDGFRa and PDGFRb (Ding et al., 2012; Zhou et al., 2014) arise perinatally and are major contributor to bone formed in adults but not during development (Zhou et al., 2014). They give rise to nearly all CFU-Fs in adult bone marrow and can differentiate into bone, cartilage and adipocytes *in vitro* and *in vivo* (Zhou et al., 2014). These observations prompted us to test whether *Lepr*$^+$ stromal cells are responsible for bone marrow fibrosis *in vivo*. The frequency of enzymatically dissociated CD45/Ter119$^-$PDGFRa$^+$ stromal cells significantly increased in TOE mice (**Figure 2.3a** and **Figure 2.4a**). *Lepr-cre* knockin allele recombines specifically in PDGFRa$^+$ bone marrow mesenchymal stromal cells (Ding et al., 2012; Zhou et al., 2014). We fate-mapped *Lepr*$^+$ lineage cells using *Lepr-cre; tdTomato* mice in which PMF was induced by transplanting TOE retrovirus-infected bone marrow cells (**Figure 2.3b**). Consistent with the increased stromal cell frequency, tdTomato$^+$ cells expanded dramatically in TOE mice compared with mice transplanted with bone marrow cells infected with control virus (**Figure 2.3c-f** and **Figure 2.4b**). These tdTomato$^+$ stromal lineage cells elaborated extensive cellular processes resembling myofibroblasts (**Figure2.3e-f** and **Figure 2.4c-d**), suggesting that these cells assumed a fibrotic cell fate.

To directly assess whether the *Lepr*$^+$ stromal cells are the myofibroblastic cells, we used *Collagen1a1*-GFP (Col-GFP) reporter mice (Yata et al., 2003) which labels Collagen1a1-expressing myofibroblastic cells in multiple organs (Iwayama et al., 2015; Lin et al., 2008; Mederacke et al., 2013). We generated *Lepr-cre; tdTomato; Col-gfp* mice to examine whether

tdTomato$^+$ cells are Col-GFP$^+$ in the PMF bone marrow. In *Lepr-cre; tdTomato; Col-gfp* mice without PMF induction, sparse tdTomato$^+$ cells and Col-GFP$^+$ cells overlapped (**Figure 2.3g-i**), suggesting that *Lepr*$^+$ stromal cells expressed collagen and had some fibrogenic capacity even under steady state. We then induced PMF by transplanting TOE virus-infected bone marrow cells into these mice. At three to four months after the transplantation, mice were analyzed. Consistent with our earlier observation, tdTomato$^+$ stromal lineage cells underwent a significant expansion in TOE bone marrow (**Figure 2.3j-o**). Virtually all of the tdTomato$^+$ cells were Col-GFP$^+$ (**Figure 2.3j-o** and **Figure 2.4e**). Conversely, virtually all Col-GFP$^+$ cells were tdTomato$^+$ (**Figure 2.3j-o** and **Figure 2.4f**). These data demonstrate that *Lepr*$^+$ lineage cells are the major if not exclusive source of myofibroblasts responsible for fibrosis in the PMF bone marrow.

Mesenchymal stromal cells down-regulate key niche factors for HSCs

Lepr$^+$ mesenchymal stromal cells plays a critical role in bone marrow HSC maintenance by generating key niche factors, CXCL12 and SCF (Ding et al., 2012; Ding and Morrison, 2013; Oguro et al., 2013). Bone marrow *Lepr*$^+$ cells, *Cxcl12*^{high} cells and *Scf*^{high}cells are essentially the same mesenchymal population (Ding et al., 2012; Ding and Morrison, 2013; Zhou et al., 2014). Fibrogenic conversion of these cells may alter their capacity to support HSCs. We examined the niche function of these cells in PMF by evaluating the expression of key niche-derived HSC maintenance factors. We directly assessed CXCL12 expression in the bone marrow from *Cxcl12*$^{DsRed/+}$ knockin mice (Ding and Morrison, 2013) with PMF induction. *Cxcl12*$^{DsRed/+}$ mice reconstituted with empty vector virus-infected bone marrow cells were used as controls. The expression level of *Cxcl12*-DsRed was reduced in TOE mice

compared with controls, although the frequency of these cells did not seem to change as revealed by confocal microscopy (**Figure 2.5a-d**) and by flow cytometry (**Figure2.5e**). Quantification of the intensity of *Cxcl12*-DsRed and quantitative real-time PCR (qRT-PCR) analysis showed that there was significant reduction of DsRed expression level and *Cxcl12* transcripts by mesenchymal stromal cells (**Figure 2.5f-h**). Since CXCL12 is a major HSC retention signal (Ding and Morrison, 2013; Greenbaum et al., 2013) its down-regulation provides a potential mechanistic explanation for HSC mobilization out of the bone marrow in PMF.

Taking advantage of an $Scf^{gfp/+}$ knockin reporter [1], we assessed the expression of *Scf*-GFP^+ in the PMF bone marrow. There was a down-regulation of *Scf*-GFP expression level in the PMF bone marrow revealed by confocal microscopy (**Figure 2.5i-l**). By flow cytometry, the frequency of $CD45/Ter119^-$*Scf*-GFP^+ stromal cells did not differ significantly between TOE and control bone marrow (**Figure 2.5m**). The *Scf*-GFP expression level at single-cell resolution was significantly reduced in PMF bone marrow as assessed by flow cytometry (**Figure 2.5n-o**). qRT-PCR analysis also showed a significant reduction of *Scf* transcripts (**Figure 2.5p**). Overall, the above data suggest that adaptation of a fibrotic cell fate by mesenchymal stromal cells leads to lower expression of key HSC niche factors and thus compromised bone marrow niche.

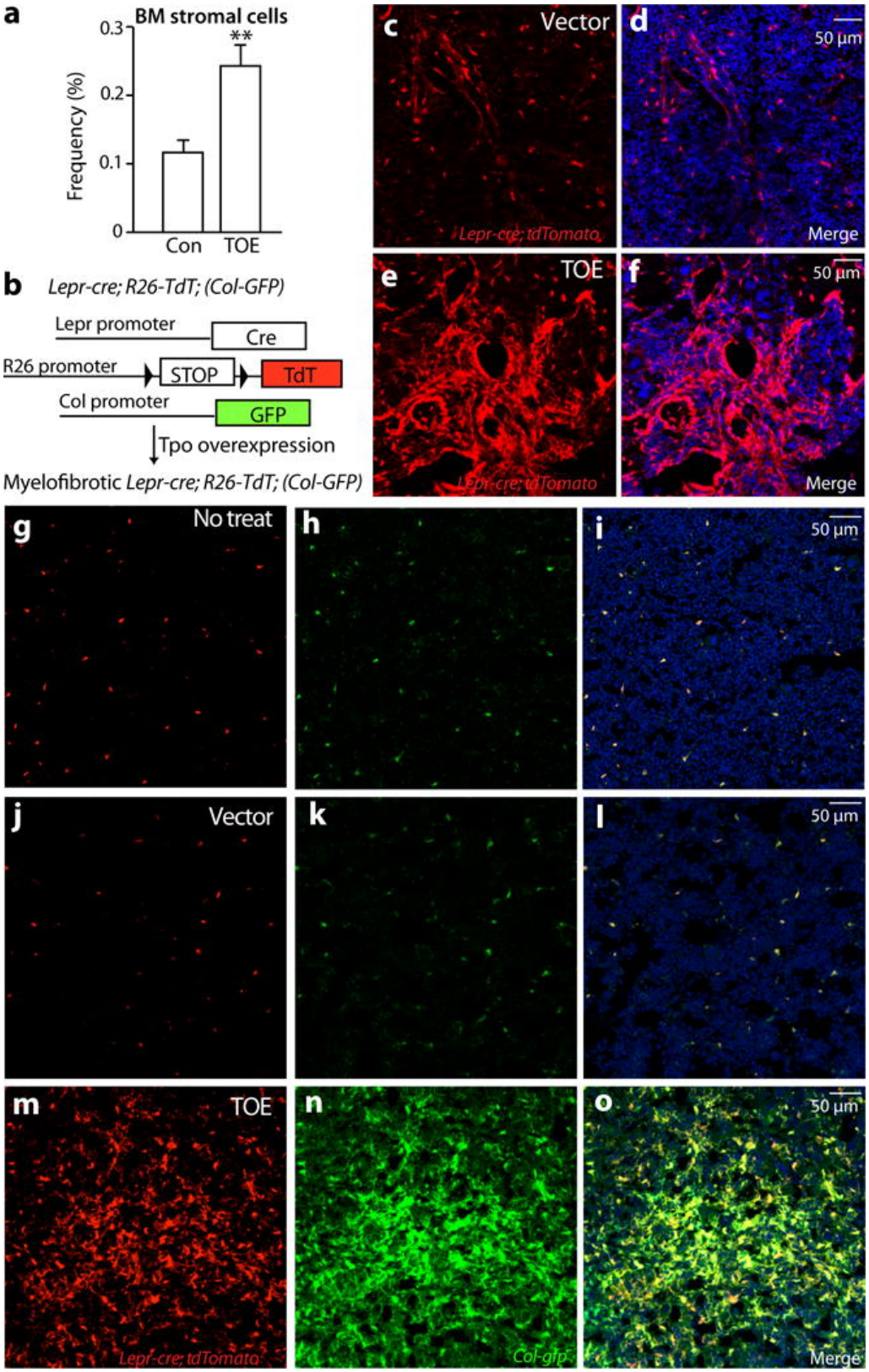

Figure 2.3 Bone marrow mesenchymal stromal cells undergo expansion and fibrotic conversion in PMF

Figure 2.3 Bone marrow mesenchymal stromal cells undergo expansion and fibrotic conversion in PMF

a. Flow cytometric analysis of enzymatically dissociated bone marrow cells showing a significant increase of mesenchymal stromal cells (n=17 mice for control and n=18 mice for TOE).

b. A scheme depicting the *in vivo* lineage tracing experiments.

c–f. *Lepr-cre; loxptdTomato* mice were transplanted with Tpo-overexpressing virus-infected bone marrow cells (TOE) or control virus infected bone marrow cells (control). Two to three months after the transplantation, the fate of *Lepr-cre*-expressing lineage cells was followed by assessing the tdTomato$^+$ cells. Confocal images showing a substantial expansion of *Lepr-cre* expressing lineage cells in TOE mice.

g–i. Confocal images showing *Lepr-cre*-expressing tdTomato$^+$ mesenchymal stromal cells were Col-GFP$^+$ in *Lepr-cre; loxptdTomato; Col-gfp* mice under steady state.

j–o. Bone marrow mesenchymal stromal cells from TOE PMF *Lepr-cre; loxptdTomato; Col-gfp* mice underwent expansion and were Col-GFP$^+$. Vector controls were *Lepr-cre; loxptdTomato; Col-gfp* mice transplanted with control virus-infected bone marrow cells. TOE, Tpo-overexpressing. Con, control vector virus. *$p<0.05$. Images are representative of at least 3 biological replicates.

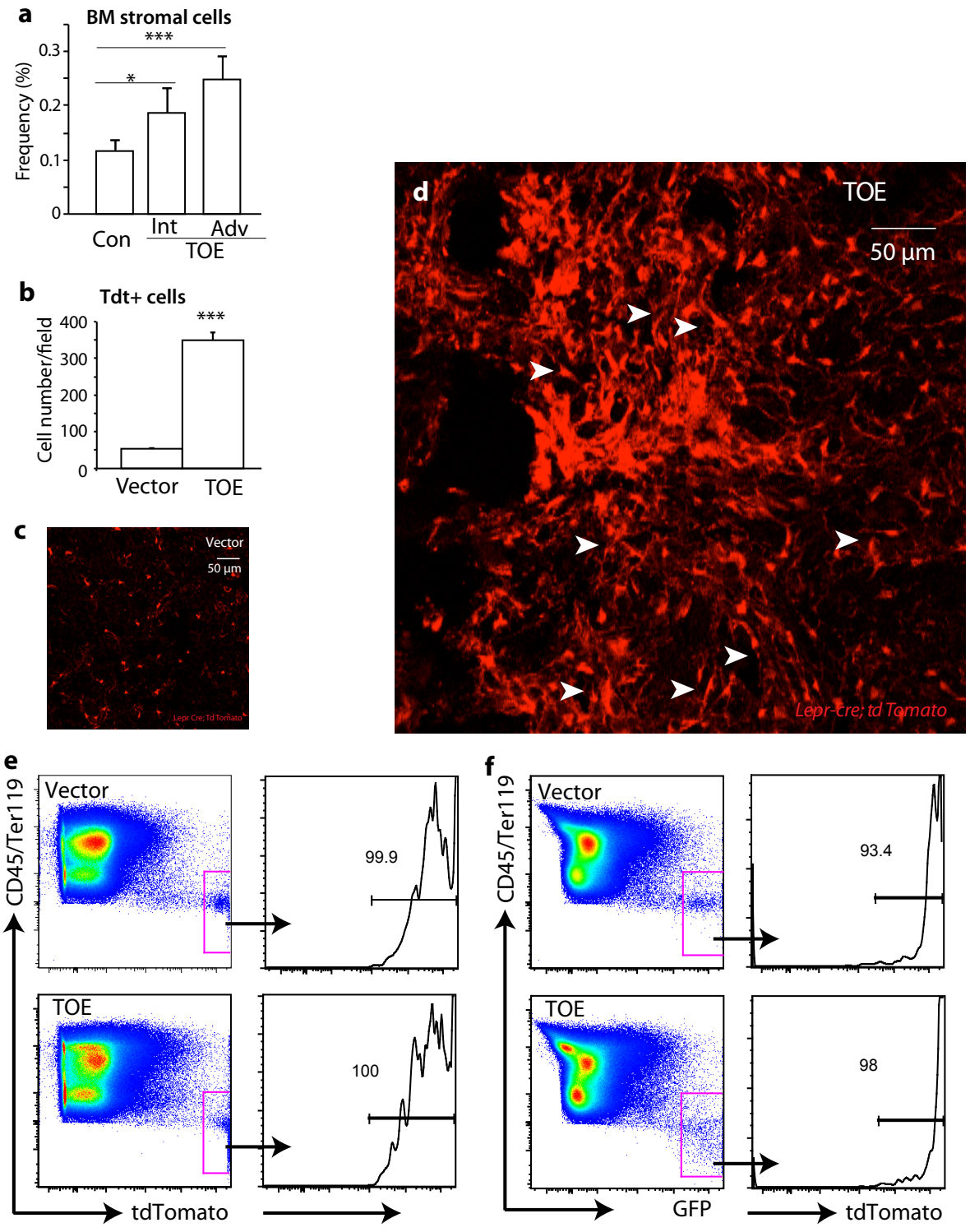

Figure 2.4 Bone marrow mesenchymal stromal lineage cells expand and assume a fibrotic cell fate

Figure 2.4 Bone marrow mesenchymal stromal lineage cells expand and assume a fibrotic cell fate

a. Bone marrow CD45/Ter119-CD140a^{+} mesenchymal stromal cell frequency increased as PMF developed from intermediate to advanced stages (n=17 mice for control, n=12 mice for intermediate TOE, n=8 mice for advanced TOE).

b. Bone marrow mesenchymal stromal lineage cells expanded 6.5 fold as quantified by counting TdTomato+ cells on bone marrow sections from vector control and TOE mice (n=4 images for control and TOE each; *p<0.05, ***p<0.001).

c-d. *Lepr-cre*-expressing mesenchymal stromal cells expanded extensively and displayed elongated fibroblast-like stromal cell morphology. Arrow heads point to elongated fibroblast-like cells.

e. In *Lepr-cre; loxptdTomato; Col-gfp* control or TOE mice, all tdTomato^{+} cells are GFP^{+}.

f. In *Lepr-cre; loxptdTomato; Col-gfp* control or TOE mice, nearly all GFP^{+} cells are tdTomato^{+}. Images are representative of at least 3 biological replicates.

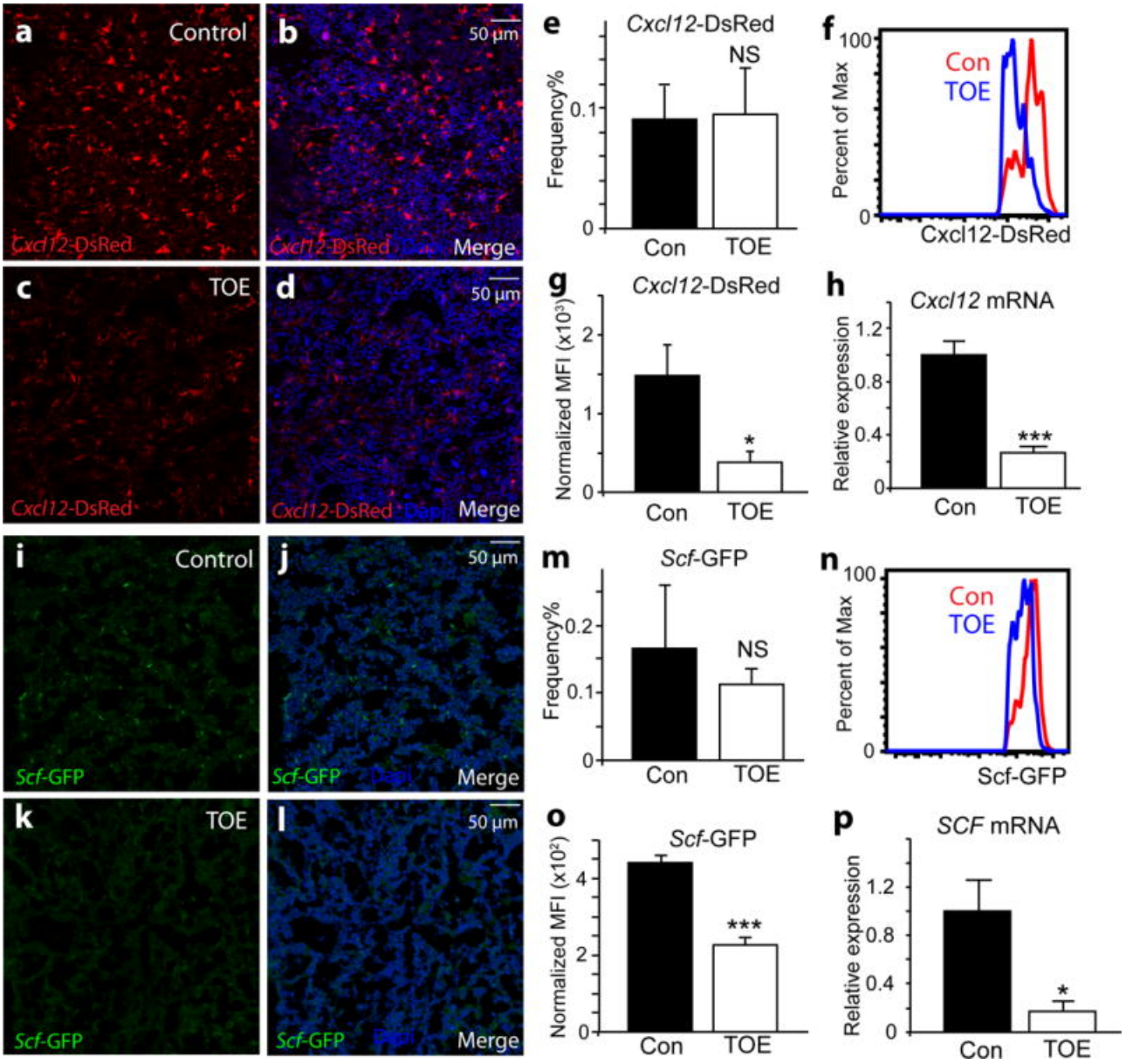

Figure 2.5 Bone marrow mesenchymal stromal cells down-regulate key HSC maintenance factors, CXCL12 and SCF

Figure 2.5 Bone marrow mesenchymal stromal cells down-regulate key HSC maintenance factors, CXCL12 and SCF

a–d. Confocal images showing *Cxcl12*-DsRed reporter expressing in the bone marrow of *Cxcl12*$^{DsRed/+}$ mice transplanted with control virus-infected bone marrow cells (**a-b**). The expression level of *Cxcl12*-DsRed reporter was dramatically down-regulated in the bone marrow of *Cxcl12*$^{DsRed/+}$ mice transplanted with Tpo-overexpressing virus-infected bone marrow cells (TOE) (**c-d**) compared with controls (**a-b**). Nuclei were stained with DAPI (blue).

e. The frequency of CD45/Ter119^{-}*Cxcl12*-DsRed^{+} mesenchymal stromal cells was not significantly altered in TOE mice compared with controls (n=4 mice for control and n=6 mice for TOE).

f–g. The fluorescent intensity of *Cxcl12*-DsRed was significantly reduced in TOE mice compared with controls as assessed by flow cytometry (n=4 mice for control and n=6 mice for TOE).

h. qPCR analysis revealed that *Cxcl12* transcripts were significantly decreased in sorted mesenchymal stromal cells from TOE mice compared with controls (n=3 mice for control and n=4 mice for TOE).

i–l. The expression level of *Scf*-GFP reporter was down-regulated in TOE mice. GFP (green) shows *Scf*-GFP^{+} cells. Nuclei were stained with DAPI (blue).

m. The frequency of CD45/Ter119^{-}*Scf*-GFP^{+} stromal cells was not significantly altered in TOE mice (n=3 mice for control and n=4 mice for TOE).

n–o. The fluorescent intensity of *Scf*-GFP was significantly reduced in TOE mice as assessed by flow cytometry (n=3 mice for control and n=4 mice for TOE).

p. qPCR analysis showed *Scf* transcripts were significantly decreased in sorted mesenchymal stromal cells (n=3 mice for control and n=4 mice for TOE). TOE, Tpo-overexpressing. Con, control vector virus. *$p<0.05$, ***$p<0.001$, NS, not significant. Images are representative of at least 3 biological replicates.

Mesenchymal stromal cells undergo fibrotic conversion/differentiation in PMF

We performed a genome-wide gene expression profiling to molecularly characterize the mesenchymal stromal cells in PMF. We sorted CD45/Ter119^{-}*Cxcl12*-DsRed^{+} mesenchymal stromal cells as *Cxcl12*expression is a direct marker for functional HSC niche cells. Although *Cxcl12*-DsRed is expressed by other bone marrow cells at low levels (Ding and Morrison, 2013) and its expression level was down-regulated ~ 4 fold (**Figure 2.5f-g**), our sorting strategy purified most mesenchymal stromal cells expressing high levels of DsRed (**Figure 2.6a**). As expected, these cells also expressed high levels of mesenchymal markers such as *Pdgfra (CD140a), Pdgfrb(CD140b)* and *Lepr* (**Figure 2.6b**). CD45/Ter119^{-}*Cxcl12*-DsRed^{+} cells expressed very little, if any, *Nestin* or *Ng2* (**Figure 2.6b**). Statistical analysis identified 480 up-regulated genes ($p<0.05$, fold>1.5) and 146 down-regulated genes ($p<0.05$, fold>1.5) from TOE mice compared with controls (**Figure 2.7a**). Gene ontology (GO) analysis using the Database for Annotation, Visualization and Integrated Discovery (DAVID) identified several significantly enriched processes, including extracellular matrix, cell adhesion and proteinaceous extracellular matrix **(Figure 2.7b**), suggesting a fibrotic conversion/differentiation of these cells.

To systematically test whether these cells underwent fibrotic conversion, we performed gene set enrichment analysis (GSEA). A mouse fibrosis gene set was obtained from Qiagen (www.qiagen.com), which includes 85 key genes involved in dysregulated tissue remodeling during the repair and healing of wounds (**Figure 2.6c**). We found that *Cxcl12*$^{+}$ mesenchymal stromal cells from PMF bone marrow expressed many genes associated with fibrosis (normalized enrichment score (NES)=3.32, false discovery rate (FDR) q=0 and p=0) (**Figure 2.7c**). Using a published fibrosis gene signature from *in vivo* fibrotic liver stellate cells (De Minicis et al.,

2007), we performed an independent GSEA analysis. Again, PMF mesenchymal stromal cells significantly expressed many genes associated with liver stellate cell fibrosis (NES=1.65, FDR q=0 and p=0), confirming their fibrotic conversion (**Figure 2.7d**). Since *Lepr*$^{+}$ stromal cells are the main source of bone formed in the adult bone marrow (Zhou et al., 2014) and osteosclerosis is a feature of myelofibrosis (Lataillade et al., 2008), we tested whether the PMF mesenchymal stromal cells globally up-regulated osteoblastic genes. A mouse osteogenesis gene set was obtained from Qiagen (www.qiagen.com), which includes 82 genes related to osteogenic differentiation (**Figure 2.6d**). A GSEA analysis revealed that PMF mesenchymal stromal cells significantly expressed many osteogenic genes (NES=1.7, FDR q=0 and p=0) (**Figure 2.7e**). Thus the mesenchymal stromal cells underwent global gene expression change to a fibrotic/osteogenic fate in the PMF bone marrow.

Genes that were significantly more highly expressed in PMF mesenchymal stromal cells included genes encoding extracellular matrix: *Acta2* (a-smooth muscle actin), *Fn* (fibronectin), several collagens (*Col12a1*, *Col1a1*, *Col1a2* and *Col3a1*) and integrins (*Itgbl1*, *Itga2* and *Itgb5*) (**Table 2.1**). Extracellular matrix remodeling enzymes were also up-regulated, including *Mmp9* (matrix metallopeptidase 9), *Timp1* (tissue inhibitor of metalloproteinase 1), *Mmp2* (matrix metallopeptidase 2), *Timp3* (tissue inhibitor of metalloproteinase 3) and *Mmp14* (matrix metallopeptidase 14) (**Table 2.1**). Several highly up-regulated genes associated with osteogenesis included *Postn* (periostin, osteoblast specific factor), *Spp1* (secreted phosphoprotein 1, osteopontin) and *Alpl* (alkaline phosphatase, liver/bone/kidney) (**Table 2.1**). We also observed a significant reduction of *Lepr* (**Table 2.1**), although the expression level was still high (**Figure 2.6b**). A recent study reported that LepR from bone marrow stromal cells promotes adipogenesis and inhibits osteogenesis (Yue et al., 2016). The down-regulation

of *Lepr* is consistent with the elevated osteogenesis of these cells in PMF. In line with our analysis on niche factor expression (**Figure 2.5**), we also observed downregulation of *Cxcl12* and *Scf* (**Figure 2.6b**). Altogether, these data demonstrate that bone marrow mesenchymal stromal cells undergo fibrotic conversion/differentiation and are thus likely the origin of myofibroblasts responsible for fibrosis in the PMF bone marrow.

a

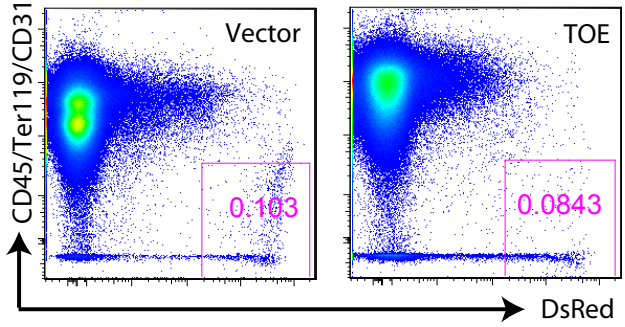

b

Genes	CON	TOE
Pdgfra	1373±988	2619±1113
Pdgfrb	1405±624	1886±759
Lepr	3599±769	2208±238
Nestin	35±3	36±1
Ng2	90±23	67±9
Cxcl12	7341±572	6186±898
Scf	3589±1454	2828±453

c

Mouse fibrosis genes

Acta2	Il5	Serpine1
Agt	Ilk	Serpinh1
Akt1	Inhbe	Smad2
Bcl2	Itga1	Smad3
Bmp7	Itga2	Smad4
Cav1	Itga3	Smad6
Ccl11	Itgav	Smad7
Ccl12	Itgb1	Snai1
Ccl3	Itgb3	Sp1
Ccr2	Itgb5	Stat1
Cebpb	Itgb6	Stat6
Col1a2	Itgb8	Tgfb1
Col3a1	Jun	Tgfb2
Ctgf	Lox	Tgfb3
Cxcr4	Ltbp1	Tgfbr1
Dcn	Mmp13	Tgfbr2
Edn1	Mmp14	Tgif1
Egf	Mmp1a	Thbs1
Eng	Mmp2	Thbs2
Fasl	Mmp3	Timp1
Grem1	Mmp8	Timp2
Gusb	Mmp9	Timp3
Hgf	Myc	Timp4
Ifng	Nfkb1	Tnf
Il10	Pdgfa	Vegfa
Il13	Pdgfb	
Il13ra2	Plat	
Il1a	Plau	
Il1b	Plg	
Il4	Serpina1a	

d

Mouse osteogenesis genes

Acvr1	Ctsk	Serpinh1
Ahsg	Dlx5	Smad1
Alpl	Egf	Smad2
Anxa5	Fgf1	Smad3
Bglap	Fgf2	Smad4
Bgn	Fgfr1	Smad5
Bmp1	Fgfr2	Sost
Bmp2	Flt1	Sox9
Bmp3	Fn1	Sp7
Bmp4	Gdf10	Spp1
Bmp5	Gli1	Tgfb1
Bmp6	Icam1	Tgfb2
Bmp7	Igf1	Tgfb3
Bmpr1a	Igf1r	Tgfbr1
Bmpr1b	Ihh	Tgfbr2
Bmpr2	Itga2	Tgfbr3
Cd36	Itga2b	Tnf
Cdh11	Itga3	Tnfsf11
Chrd	Itgam	Twist1
Col10a1	Itgav	Vacm1
Col14a1	Itgb1	Vegfa
Col1a1	Mmp10	Vegfb
Col2a1	Mmp2	
Col3a1	Mmp8	
Col4a1	Mmp9	
Col5a1	Nfkb1	
Comp	Nog	
Csf1	Pdgfa	
Csf2	Phex	
Csf3	Runx2	

Figure 2.6 Gene expression profiling analysis of mesenchymal stromal cells from PMF mice

Figure 2.6 Gene expression profiling analysis of mesenchymal stromal cells from PMF mice

a. Representative flow cytometric plots showing the gates to sort CD45/Ter119/CD31^{-}Cxcl12-DsRed^{+} stromal cells from PMF and control bone marrow. A total of three freshly double-sorted aliquots of cells (~5000) from PMF (from 5 mice) and control (from 3 mice) *Cxcl12*$^{DsRed/+}$ mice were used for gene expression analysis.

b. Normalized expression levels of mesenchymal cell markers and HSC niche factors by CD45/Ter119/CD31^{-}*Cxcl12*-DsRed^{+} stromal cells from PMF and control bone marrow. Values represent mean±s.d.. from three biological replicates.

c. List of fibrosis genes used to performed GSEA in Figure 2.7c.

d. List of osteogenic genes used to performed GSEA in Figure 2.7d.

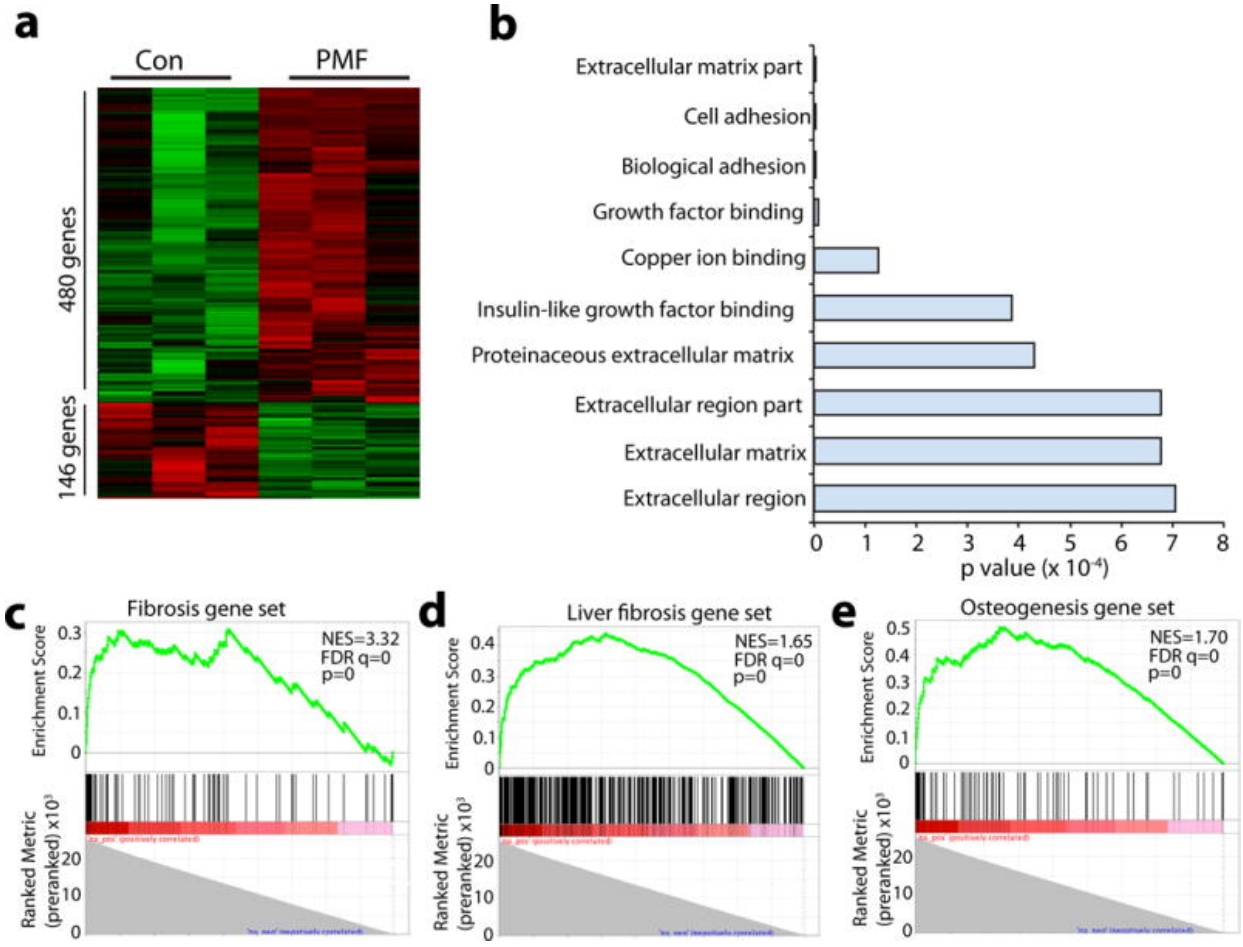

Figure 2.7 Mesenchymal stromal cells up-regulate fibrosis and osteogenesis genes in PMF

a. Heat map showed 480 significantly up-regulated and 146 significantly down-regulated genes in freshly sorted mesenchymal stromal cells from PMF mice compared with controls identified by gene expressing profiling analysis (n=3 mice for control and TOE each).

b. Gene ontology (GO) analysis showed biological processes significantly affected in mesenchymal stromal cells from PMF mice.

c–e. Gene set enrichment analysis (GESA) showed significant enrichment of fibrosis genes (**c** and **d**) and osteogenesis genes (**e**) in mesenchymal stromal cells from PMF mice. NES, normalized enrichment score. FDR, false discovery rate. p, nominal p value.

Gene	Fold PMF/Con	P value
Acta2	10	0
Itgbl1	8.1	0
Postn	8.5	0
Spp1	2.5	0
Col12a1	6.3	0
Fn1	10.1	0
Mmp9	8.9	0
Col6a3	5.7	0
Timp1	5.4	0
Dpt	12.3	0.00002
S100a4	5.2	0.0001
Col1a1	3	0.001
Itga2	2.1	0.001
Itgb5	2.5	0.002
Mmp2	7.8	0.003
Col1a2	2.3	0.008
Col3a1	2.7	0.008
Timp3	3.5	0.01
Alpl	2.7	0.02
Mmp14	3.7	0.02

Table 2.1 Significantly highly expressed genes in PMF mesenchymal stromal cells

PDGFRa in mesenchymal stromal cells in required for bone marrow fibrosis

The identification of *Lepr*$^{+}$ mesenchymal stromal lineage cells as bone marrow myofibroblasts in PMF provided us an opportunity to investigate the molecular pathways involved in their fibrotic conversion. Activation of PDGFRa has been implicated in fibrosis of multiple organs (Olson and Soriano, 2009; Iwayama et al., 2015). As *Lepr*$^{+}$mesenchymal stromal cells are the major cell type expressing PDGFRa in the bone marrow (Ding et al., 2012), we wondered whether PDGFRa in mesenchymal stromal cells is required for their fibrotic conversion. We conditionally deleted *Pdgfra* from bone marrow mesenchymal stromal cells by generating *Lepr-cre; Pdgfra*$^{fl/fl}$ or *Lepr-cre; Pdgfra*$^{fl/-}$ mice. PDGFRa was efficiently deleted from bone marrow mesenchymal stromal cells (**Figure 2.8a**). Bone marrow cells from these mice had normal reconstitution activity when transplanted into lethally irradiated recipient mice (**Figure 2.8b**). We induced PMF by transplanting TOE virus-infected bone marrow cells into *Lepr-cre; Pdgfra*$^{fl/fl}$and control mice. At 2–3 months after the bone marrow transplantation, HSC frequency from both *Lepr-cre; Pdgfra*$^{fl/fl}$ and control mice were similarly increased in the spleen (**Figure 2.9a**). This was accompanied by enlarged spleens with likely ongoing extramedullary haematopoiesis (**Figure 2.8c and Figure 2.9b-c**). Reticulin staining on spleen sections from *Lepr-cre; Pdgfra*$^{fl/fl}$ mice demonstrated excessive deposition of reticulin fibers to the same extent as those from control TOE mice (**Figure 2.8d**). These data revealed that *Lepr-cre; Pdgfra*$^{fl/fl}$ TOE mice developed many features of PMF in the spleen.

Myeloid proliferation and HSC expansion occurred similarly in *Lepr-cre; Pdgfra*$^{fl/fl}$ TOE and control TOE mice (**Figure 2.9d**). There was a significant rescue of the bone marrow

cellularity in *Lepr-cre; Pdgfra*$^{fl/fl}$ mice (**Figure 2.9e**), suggesting an improvement of the bone marrow niche function. Megakaryocyte hyperplasia was similar in *Lepr-cre; Pdgfra*$^{fl/fl}$ and control TOE mice (**Figure 2.8e**). We then examined bone marrow fibrosis by performing reticulin staining. Consistent with our earlier observation, excessive reticulin fiber deposition was observed in the bone marrow from control TOE mice (**Figure 2.8f** and **Figure 2.9f**, upper panels). In contrast, we did not observe reticulin staining in the bone marrow from *Lepr-cre; Pdgfra*$^{fl/fl}$ TOE mice (**Figure 2.8f** and **Figure 2.9f**, lower panels). Consistent with the ameliorated fibrosis, flushing the bone marrow cells out of the bone from *Lepr-cre; Pdgfra*$^{fl/fl}$ TOE mice was dramatically easier compared with fibrotic control TOE bone marrow likely due to the absence of excessive fibrosis and osteosclerosis. The increased frequency of mesenchymal stromal lineage cells was suppressed to almost vector control level in *Lepr-cre; Pdgfra*$^{fl/fl}$ TOE mice (**Figure 2.8g** and **Figure 2.9g**). Several fibrotic genes, such as *Col1a1, Col3a1* and *Acta2*, were significantly down-regulated in *Lepr-cre; Pdgfra*$^{fl/fl}$ TOE mice (**Figure 2.9i**). Thus, PDGFRa signaling in *Lepr*$^{+}$ mesenchymal stromal cells is required for bone marrow fibrosis in PMF. These data functionally show that bone marrow *Lepr*$^{+}$ mesenchymal stromal cells are the cell type responsible for fibrosis in PMF.

Imatinib effectively blocks the activity of several tyrosine kinases, including PDGFRa (Lydon and Druker, 2004). We assessed whether imatinib treatment would alleviate bone marrow fibrosis. PMF was induced in TOE mice and then imatinib was administrated through chow. Imatinib effectively rescued bone marrow hypocellularity and blocked mesenchymal stromal cell expansion, fibrotic conversion, and bone marrow fibrosis **(Figure 2.9e,g-i**). Imatinib also effectively suppressed spleen extramedulary haematopoiesis and fibrosis, suggesting that other cell types and/or pathways may mediate PMF spleen pathogenesis (**Figure 2.8c,h** and

Figure 2.9a-c). Our results suggest that targeting PDGFRa pathway in mesenchymal stromal cells may be beneficial in treating bone marrow fibrosis.

Activation of PDGFRa in *Lepr*$^{+}$ bone marrow mesenchymal stromal cells leads to their expansion and extramedullary hematopoiesis

To directly test whether activation of the PDGFRa pathway in mesenchymal stromal cells has an impact on PMF pathogenesis, we conditionally activated PDGFRa by generating *Lepr-cre; Pdgfra*$^{D842V/+}$*; tdTomato* mice (**Figure 2.10a**). The *Pdgfra*^{D842V} allele allows for cell-type specific activation of PDGFRa pathway under the control of its endogenous promoter (Olson and Soriano, 2009; Iwayama et al., 2015). By flow cytometry, bone marrow stromal cell frequency was largely unchanged in *Lepr-cre; Pdgfra*$^{D842V/+}$ mice (**Figure 2.11a**). However, by confocal microscopy, we observed foci with a significant increase of tdTomato^{+} stromal cells in the trabecular bone region of *Lepr-cre; Pdgfra*$^{D842V/+}$*; tdTomato* mice (**Figure 2.10b-d**). We also observed excessive osteogenesis in the diaphysis region of these mice (**Figure 2.10e-f**). However, no excessive bone marrow fibrosis was observed (**Figure 2.11b**).

Lepr-cre; Pdgfra$^{D842V/+}$ mice had normal bone marrow cellularity and HSC frequency (**Figure 2.10g** and **Figure 2.11c**). However, these mice had increased HSC and haematopoietic progenitor frequencies in the spleens and livers (**Figure 2.10h-j** and **Figure 2.11d**). These results suggest that activation of PDGFRa pathway in *Lepr*$^{+}$ cells is sufficient to cause some features of PMF: mesenchymal stromal cell expansion, osteogenesis and HSC mobilization.

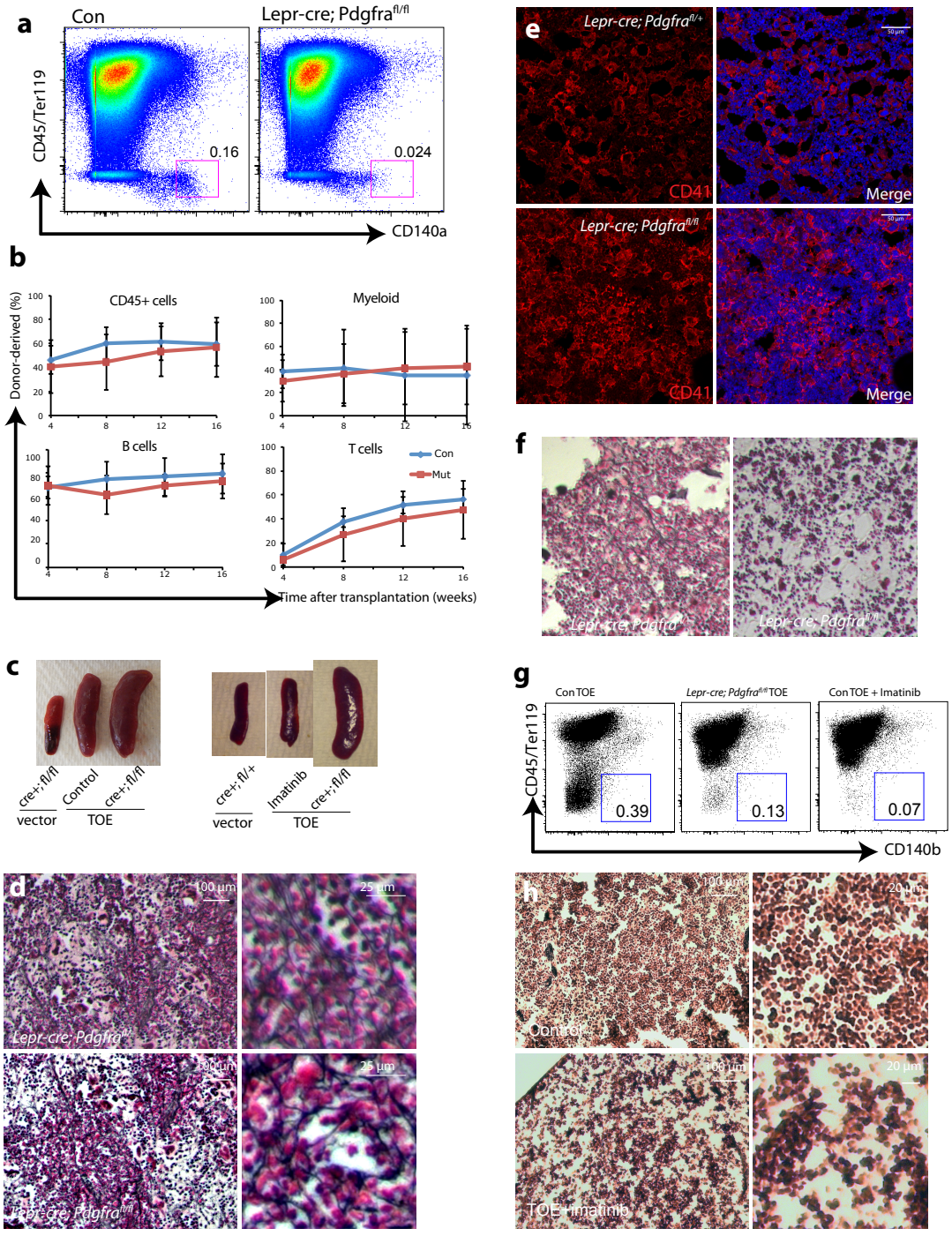

Figure 2.8 *Lepr-cre; Pdgfra*$^{fl/-}$ mice have normal HSC function and *Lepr-cre; Pdgfra*$^{fl/fl}$ TOE mice fail to develop bone marrow fibrosis

Figure 2.8 *Lepr-cre; Pdgfra*$^{fl/-}$ mice have normal HSC function and *Lepr-cre; Pdgfra*$^{fl/fl}$ TOE mice fail to develop bone marrow fibrosis

a. Flow cytometry plots showing efficient deletion of PDGFRa.

b. A competitive reconstitution assay for *Lepr-cre; Pdgfra*$^{fl/-}$ and control mice. $5x10^5$ donor bone marrow cells from *Lepr-cre; Pdgfra*$^{fl/-}$ adult mice or control *Lepr-cre; Pdgfra*$^{fl+}$ mice were competitively transplanted with $5x10^5$ recipient bone marrow cells into irradiated recipient mice. The percentages of donor-derived Mac-1^+ myeloid, $CD3^+$ T, and $B220^+$ B cells in the blood were analyzed for 16 weeks after transplantation (n=5 recipient mice for each genotype).

c. *Lepr-cre; Pdgfra*$^{fl/fl}$ TOE mice displayed enlarged spleens and imatinib-treated TOE mice showed normal sized spleens.

d. Representative reticulin staining on spleen sections from *Lepr-cre; Pdgfra*$^{fl/fl}$ TOE mice revealed excessive deposition of reticulin fibers, similar to control TOE mice.

e. Confocal images showing similar levels of megakaryocyte hyperplasia in the bone marrow from *Lepr-cre; Pdgfra*$^{fl/fl}$ and control TOE mice. CD41 is a marker for megakaryocytes (red). Nuclei were stained with DAPI (blue)

f. Bone marrow sections from *Lepr-cre; Pdgfra*$^{fl/fl}$ and control TOE mice were subjected to reticulin staining. While control TOE mice robustly developed bone marrow fibrosis, none of the *Lepr-cre; Pdgfra*$^{fl/fl}$ TOE mice had bone marrow fibrosis.

g. Representative flow cytometry plots showing effective suppression of bone marrow stromal cell expansion in *Lepr-cre; Pdgfra*$^{fl/fl}$ TOE and imatinib-treated TOE mice.

h. Spleen sections from control and TOE+ imatinib were subjected to reticulin staining. Images are representative of at least 3 biological replicates.

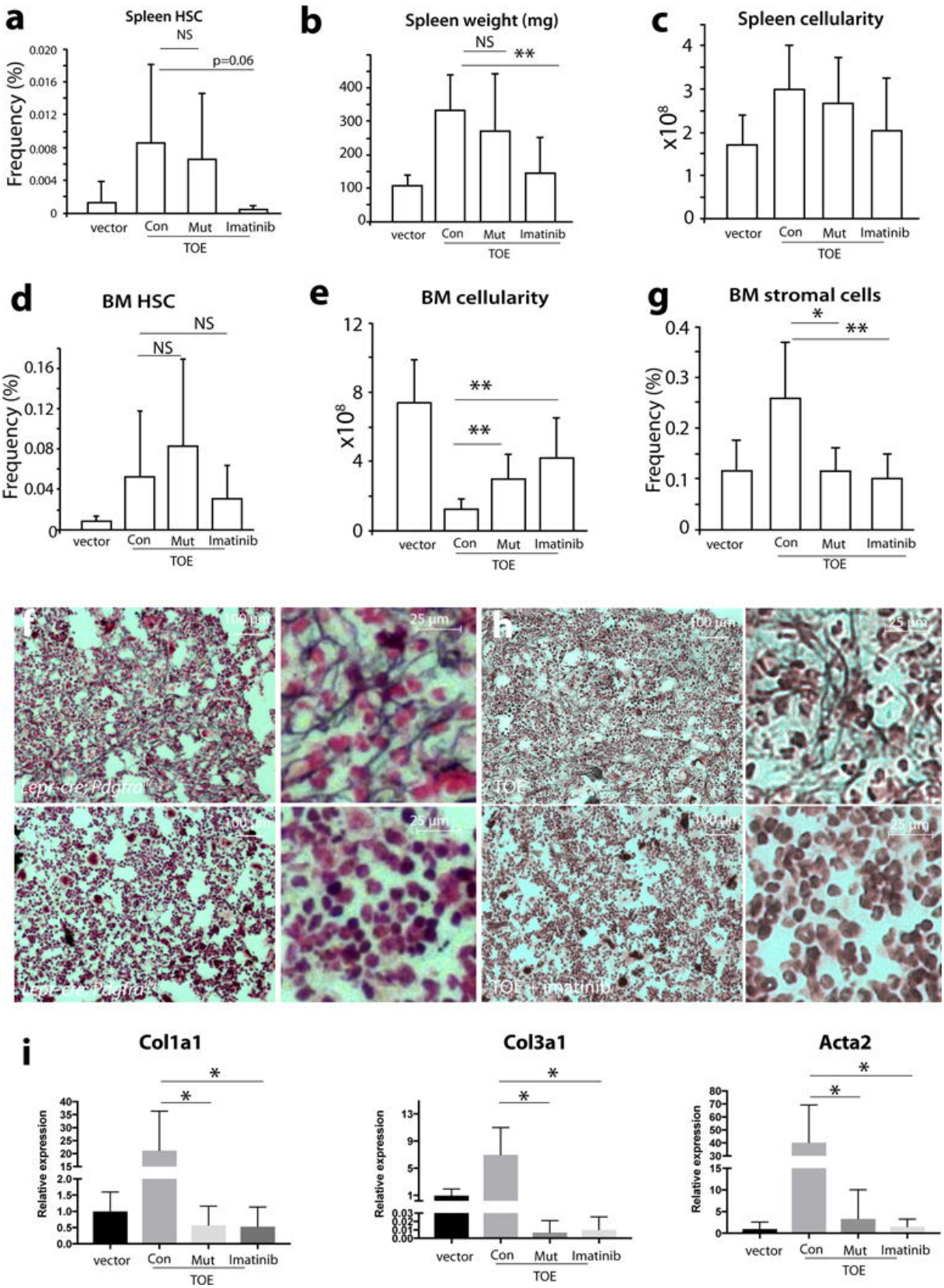

Figure 2.9 Deletion of *Pdgfra* from mesenchymal stromal cells or administration of imatinib ameliorates bone marrow fibrosis

Figure 2.9 Deletion of *Pdgfra* from mesenchymal stromal cells or administration of imatinib ameliorates bone marrow fibrosis

a. *Lepr-cre; Pdgfra*$^{fl/fl}$ TOE mice had an increase of spleen HSC frequency similar to control TOE mice while imatinib suppresses HSC mobilization (n=22 mice for vector, n=10 mice for Con, n=8 mice for Mut, n=7 mice for imatinib). vector = vector in control; Con = TOE in control; Mut = TOE in *Lepr-cre; Pdgfra*$^{fl/fl}$; imatinib = TOE treated with imatinib.

b–c. *Lepr-cre; Pdgfra*$^{fl/fl}$ TOE mice but not imatinib-treated TOE mice displayed increased spleen weight (**b**, n=18 mice for vector, n=8 mice for Con, n=7 mice for Mut, n=7 mice for imatinib) and cellularity (**c**, n=15 mice for vector, n=7 mice for Con, n=7 mice for Mut, n=7 mice for imatinib) compared with control TOE mice.

d. Bone marrow from *Lepr-cre; Pdgfra*$^{fl/fl}$ TOE or imatinib-treated TOE mice had no significant change in HSC frequency, compared with control TOE mice (n=21 mice for vector, n=10 mice for Con, n=8 mice for Mut, n=7 mice for imatinib).

e. *Lepr-cre; Pdgfra*$^{fl/fl}$ TOE and imatinib-treated TOE mice had significant increase of bone marrow cellularity compared with control TOE mice (n=21 mice for vector, n=10 mice for Con, n=8 mice for Mut, n=7 mice for imatinib).

f. Deletion of *Pdgfra* from mesenchymal stromal cells led to blockage of reticulin deposition in the bone marrow from *Lepr-cre; Pdgfra*$^{fl/fl}$ TOE mice.

g. Deletion of *Pdgfra* from *Lepr*$^{+}$ stromal cells or administration of imatinib led to suppression of the overproliferation of bone marrow CD45/Ter119^{-}PDGFRb^{+} mesenchymal stromal cells in TOE mice (n=17 mice for vector, n=8 mice for Con, n=6 mice for Mut, n=7 mice for imatinib).

h, Administration of imatinib led to blockage of reticulin fiber deposition in the bone marrow of TOE mice.

i, Deletion of *Pdgfra* from *Lepr*$^{+}$ stromal cells or administration of imatinib suppresses fibrotic genes in bone marrow mesenchymal stromal cells (n=4 mice for vector, n=4 mice for Con, n=4 mice for Mut, n=4 mice for imatinib). *$p<0.05$, **$p<0.01$, NS, not significant.

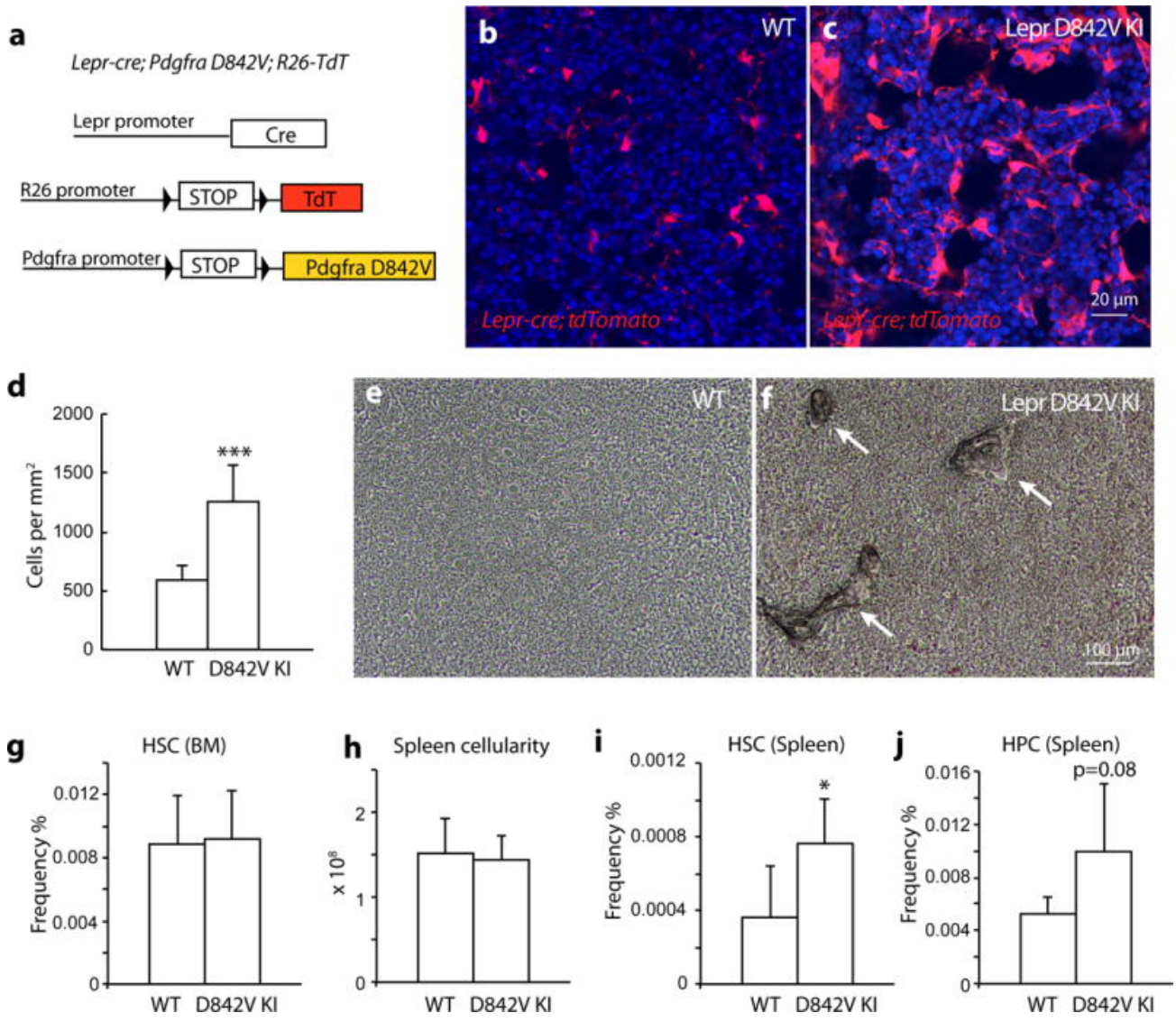

Figure 2.10 Activation of PDGFRa pathway in *Lepr*$^{+}$ cells leads to mesenchymal stromal cell expansion and HSC mobilization

Figure 2.10 Activation of PDGFRa pathway in *Lepr*$^{+}$ cells leads to mesenchymal stromal cell expansion and HSC mobilization

a. A scheme depicting the *in vivo* lineage tracing experiments with *Lepr-cre; Pdgfra*$^{D842V/+}$*; tdTomato* mice.

b–c. Confocal images showing expansion of tdTomato^{+} stromal cells in the trabecular region of bone marrow from *Lepr-cre; Pdgfra*$^{D842V/+}$*; tdTomato* mice.

d. Quantification of tdTomato^{+} cells on bone marrow images from trabecular region showing that tdTomato^{+} cells were significantly expanded in *Lepr-cre; Pdgfra*$^{D842V/+}$*; tdTomato* mice compared with controls (n=12 representative confocal images from 3 independent mice each).

e–f. Bright-field images of the diaphysis region showing excessive bone formation in *Lepr-cre; Pdgfra*$^{D842V/+}$ mice. Arrows point to bone.

g–h. *Lepr-cre; Pdgfra*$^{D842V/+}$ mice had normal bone marrow HSC frequency (**g**, n=4 mice for control, n=5 mice for D842V) and spleen cellularity (**h**, n=5 mice for control, n=6 mice for D842V).

i–j. *Lepr-cre; Pdgfra*$^{D842V/+}$ mice displayed increased HSC (**i**, n=5 mice for control, n=6 mice for D842V) and haematopoietic progenitor HPC (LSK) (**j**, n=5 mice for control, n=6 mice for D842V) frequencies in the spleen.

*p<0.05, ***p<0.001. Images are representative of at least 3 biological replicates.

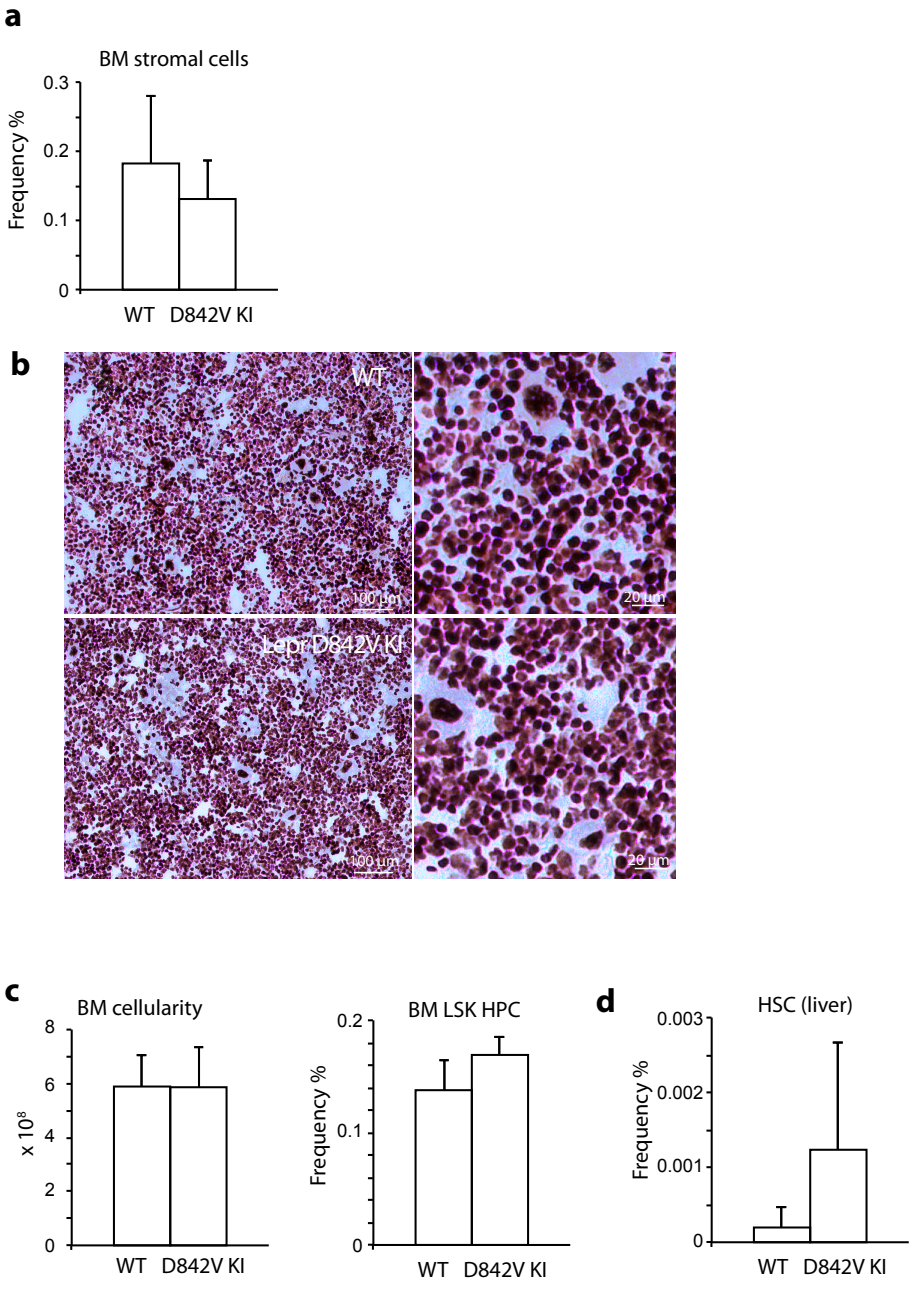

Figure 2.11 *Lepr-cre; Pdgfra*$^{D842V/+}$ mice do not have frank fibrosis but show HSC mobilization

Figure 2.11 *Lepr-cre; Pdgfra*$^{D842V/+}$ mice do not have frank fibrosis but show HSC mobilization

a. Flow cytometry analysis revealed normal bone marrow stromal cell frequency from *Lepr-cre; Pdgfra*$^{D842V/+}$ mice (n=3 mice for control, n=4 mice for D842V KI).

b. Representative reticulin staining on bone marrow sections from *Lepr-cre; Pdgfra*$^{D842V/+}$ and control mice.

c. Normal bone marrow cellularity (n=4 mice for control, n=5 mice for D842V KI) and HPC frequency of *Lepr-cre; Pdgfra*$^{D842V/+}$ mice (n=5 mice for control, n=6 mice for D842V KI).

d. HSC frequency in livers from *Lepr-cre; Pdgfra*$^{D842V/+}$ mice (n=5 mice for control, n=6 mice for D842V KI). Images are representative of at least 3 biological replicates.

DISCUSSION

Although PMF has been recognized as a hematological disease originating from abnormal HSCs, its clinical features suggest a more complex pathogenesis. The bone marrow fibrosis associated with PMF has been hypothesized as a stromal reaction to the overproliferative hematopoietic clones, but the precise identity of the reactive myofibroblasts had not previously been identified. Our fate mapping data demonstrate that *Lepr*$^{+}$ mesenchymal stromal cells are the cells of origin of myofibroblasts responsible for collagen fiber generation and deposition in PMF. The identification of these cells warrants further detailed investigation aimed at developing targeted therapies to treat bone marrow fibrosis.

In this study we observed expansion of bone marrow *Lepr*$^{+}$ mesenchymal stromal lineage cells in PMF. A report using *Nestin* as a marker suggests that bone marrow stromal cell number is reduced in Jak2^{V617F} mice (Arranz et al., 2014). The authors performed *Nestin*-creER fate mapping and did not observe contribution from this lineage to myofibroblasts. Several previous studies have shown that *Nestin*-cre or *Nestin*-creER recombines in only rare bone marrow stromal cells (Ding et al., 2012; Zhou et al., 2014; Worthley et al., 2015). These cells are not CFU-Fs and contribute little, if any, to skeletal tissues (Zhou et al., 2014; Worthley et al., 2015). Thus, it is unlikely that *Nestin*-creER targets mesenchymal stromal cells. It should be noted that although low expression of a *Nestin*-GFP transgene is a marker for CFU-F, the expression of endogenous *Nestin*, or other *Nestin* transgenic lines (including *Nestin*-cre or *Nestin*-CreER) does not mark the same mesenchymal stromal cells (Ding et al., 2012; Zhou et al., 2014; Worthley et al., 2015). Thus, our data are consistent with the notion that *Lepr*$^{+}$ stromal cells but not *Nestin*$^{+}$, *Nestin*-cre^{+} or *Nestin*-creER^{+} cells are the source of bone marrow myofibroblasts in PMF.

NG2$^+$ cells have been reported to contain bone marrow CFU-Fs (Kunisaki et al., 2013). However, a fate-mapping experiment demonstrated *Ng2*-creER$^+$ cells did not contribute to PDGFRa$^+$ stromal cells (Kunisaki et al., 2013), suggesting these cells are unlikely the source of bone marrow fibrosis. Gli1$^+$ and Gremlin-1$^+$ bone marrow stromal cells also contain CFU-Fs (Kramann et al., 2015; Worthley et al., 2015). Their contributions to bone marrow fibrosis are unknown. The contributions to bone marrow fibrosis by distinct yet overlapping mesenchymal stromal cells bearing different markers require further investigations.

Our *Lepr-cre; Pdgfra$^{fl/fl}$* TOE mice still developed severe spleen fibrosis. It could be that *Lepr-cre* does not target all of the spleen fibrogenic cells and/or that PDGFRa is not required for spleen fibrosis. Over-activation of PDGFRa is sufficient to drive fibrosis in diverse organs (Olson and Soriano, 2009; Iwayama et al., 2015). We thus favor the first possibility. Identification of the spleen fibrogenic cells will directly distinguish these possibilities. Recently, spleen *Tcf21*$^+$ perivascular stromal cells have been identified as an important component of the spleen niche (Inra et al., 2015). It will be interesting to determine the relative contributions of the *Tcf21*$^+$ and *Lepr*$^+$ cells to spleen fibrosis. Imatinib exerted more potent effects against bone marrow fibrosis and HSC mobilization than genetic deletion of *Pdgfra* from *Lepr*$^+$ cells. Given that imatinib targets several tyrosine kinases including BCR-ABL, PDGFR and c-KIT, it is likely that the additional molecular and cellular targets account for the stronger effects of the drug.

Lepr-cre; Pdgfra$^{D842V/+}$ mice showed regional stromal cell expansion and HSC mobilization (**Figure 2.10**). But the phenotypes were not as pronounced as the TOE model. This could reflect the partial activation of the PDGFRa pathway in the D842V model (Olson and Soriano, 2009). However, other pathways could be co-operating in TOE to induce more

prominent PMF pathology. Further elucidation of the PDGFRa and other pathways in PMF will deepen our understanding of the pathogenesis.

The modification of the bone marrow niche by abnormal hematopoietic cells is a critical contributor to many hematological diseases (Schepers et al., 2015). Consistent with early observations [15], our data suggest that hyperplastic megakaryocytes are the source of PDGF and other cytokines promoting bone marrow mesenchymal stromal cell fibrosis and HSC niche dysfunction. Current therapies for PMF focused on the hematopoietic compartment by targeting the mutant hematopoietic clones. But the overall benefits are limited. Imatinib mesylate have been preliminarily explored in PMF (Tefferi et al., 2002; Hasselbalch et al., 2003) but its clinical benefits were limited due to side effects. Our results call for additional detailed study. We propose that combined therapy against both mutant hematopoietic clone (e.g. with JAK inhibitors) and dysfunctional, fibrotic bone marrow niche (e.g. with imatinib or other PDGFRa inhibitors) with careful treatment regimen may lead to better outcome.

EXPERIMENTAL METHODS

Mice

Lepr-cre (DeFalco et al., 2001), *LoxptdTomato* (Madisen et al., 2010), and *Pdgfra*^{fl} (Tallquist and Soriano, 2003) mice were obtained from the Jackson Laboratory. *Scf*^{gfp}, *Cxcl12*^{DsRed} and *Col-gfp* mice were described previously (Yata et al., 2003; Ding and Morrison, 2013; Ding et al., 2012). *Pdgfra*^{D842V} mice (Olson and Soriano, 2009; Iwayama et al., 2015) were kindly provided by Drs. Lorin Olson and Philippe Soriano. All mice were maintained on C57BL/6 background. Experiments were started on 8-week-old young adult mice and gender was not selected. Mice were housed in specific pathogen-free, Association for the Assessment and Accreditation of Laboratory Animal Care (AAALAC)- approved facilities at the Columbia University Medical Center. All protocols were approved by the Institute Animal Care and Use Committee of Columbia University and were under the Animal Welfare Assurance A3007-01.

Retroviral production and infection of bone marrow cells

Mouse Tpo mRNA was cloned into pMIG retroviral vector. A DsRed version and a 'colorless' version of pMIG-Tpo were generated by replacing GFP reporter with DsRed or deleting GFP gene in pMIG, respectively. These versions of retroviral vectors allowed tracing of infected bone marrow cells in recipient mice. Retroviruses were produced by transfecting 293T cells with pMIG-Tpo or pMIG vectors along with pCL-Eco. Fluorouracil (5-FU) (150mg/kg) was injected into donor mice via I.V. route. Four to five days later, mice were euthanized and bone marrow cells were collected. DMEM with 15% heat-inactivated fetal bovine serum, 100ng/ml SCF, 10ng/ml IL-3, 10ng/ml IL-6 (from Peprotech) and 50um 2-mercaptoethanol was used to pre-

stimulate 5-FU-treated bone marrow cells overnight. Two spin infections were carried out before bone marrow cells were transplanted into lethally irradiated recipient mice at 1–10 million cells /mouse.

Bone marrow transplantation

Adult recipient mice were lethally irradiated by a Cesium 137 Irradiator (JL Shepherd and Associates) at 300 rad/minute with two doses of 540 rad (total 1080 rad) delivered at least 2h apart. Cells were transplanted by retro-orbital venous sinus injection of anesthetized mice. Mice were maintained on antibiotic water (Baytril 0.17g/L) for 14 days then switched to regular water. Recipient mice were periodically bled to assess the level of donor-derived blood cells (by flow cytometry), platelet (by CBC count) and serum TPO level (by ELISA).

Flow cytometry

Bone marrow cells were isolated by flushing the long bones or by crushing the long bones with mortal and pestle in Ca^{2+} and Mg^{2+} free HBSS with 2% heat-inactivated bovine serum. Spleen cells were obtained by crushing the spleen between two glass slides. The cells were drawn by passing through a 25G needle several times and filtered with a 70μm nylon mesh. The following antibodies were used to stain HSCs: anti-CD150 (TC15-12F12.2, Biolegend, Cat#115903 or 115911, 1:200), anti-CD48 (HM48-1, Biolegend, Cat#103411, 1:200), anti-Sca-1 (E13-161.7, Biolegend, Cat#122513, 1:200), anti-cKit (2B8, Biolegend, Cat#105825, 1:200), lineage markers (anti-Ter119, Biolegend, Cat#116205 or 116207, 1:200; anti-B220 (6B2), Biolegend, Cat#103205 or 103207, 1:400; anti-Gr1 (8C5), Biolegend, Cat#108405 or 108407, 1:400; anti-

CD2 (RM2-5), Biolegend, Cat#100105 or 100107, 1:200; anti-CD3 (17A2), Biolegend, Cat#100203 or 100205, 1:200; anti-CD5 (53-7.3), Biolegend, Cat#100605 or 100607, 1:400 and anti-CD8 (53-6.7), Biolegend, Cat#100705 or 100707, 1:400). DAPI was used to exclude dead cells. For flow cytometric analysis of stromal cells, bone marrow was flushed using HBSS- with 2% bovine serum. Then the whole bone marrow was digested with Collagenase IV (200U/ml) and DNase I (200U/ml) at 37°C for 20 min. Samples were then stained with antibodies and analyzed by flow cytometry. Anti-CD140a (APA5), Biolegend, Cat#135909, 1:100; anti-CD140b (APB5), Biolegend, Cat#136009, 1:100; anti-CD45 (30-F11), Biolegend, Cat#103111, 1:400 and anti-Ter119, Biolegend, Cat#116211, 1:200 antibodies were used to stain mesenchymal stromal cells. For flow cytometric analysis of peripheral blood chimera levels, peripheral blood was subjected to ammonium chloride potassium red cell lysis before antibody staining. Antibodies including anti-CD45.2 (104), Biolegend, Cat#109805, 1:400; anti-CD45.1 (A20), Biolegend, Cat#110715, 1:200; anti-Gr1 (8C5), Biolegend, Cat#108415, 1:400; anti-Mac-1 (M1/70), Biolegend, Cat#101211, 1:400; anti-B220 (6B2), Biolegend, Cat#103209, 1:400 and anti-CD3 (17A2), Biolegend, Cat#100205, 1:200 were then added to stain cells. Samples were run on FACSAria II, LSRII or FACSCanto II flow cytometers. Data were analyzed by FACSDiva (BD) or FlowJo (Tree Star) software.

Bone section and immunostaining

Freshly dissected long bones were fixed in a Formalin-based fixative at 4°C for 3 hours. Then the bones were embedded in 8% gelatin in PBS. Samples were snap frozen with liquid N_2 and stored at −80°C. Bones were sectioned using a CryoJane system (Instrumedics). Sections were dried overnight at room temperature (RT) and stored at −80°C. Sections were re-hydrated in PBS

for 5 min before immunostaining. 5% goat serum in PBS was used to block the sections. Primary antibodies were applied to the slides for 1h at RT followed by secondary antibody incubation for 30min at RT with repetitive washes in between. Slides were mounted with anti-fade prolong gold (Life Tech) and images were acquired on a Zeiss 710 confocal microscope. Rat-anti-CD41 (eBioscience, eBioMWReg30, Cat#13-0411, 1:100) was used as primary antibody.

Reticulin staining

Bone sections prepared as above were stained with Reticulin Stain Kit (Polysciences, Inc.) per manufacture's instruction. Images were taken on a Zeiss Axio Observer microscope.

Cell cycle analysis

For BrdU incorporation analysis, mice were given an intraperitoneal injection of 0.1mg BrdU in PBS per g of body weight. Then the mice were maintained on 0.5mg/ml BrdU water for 5 days before the analysis. The frequency of $BrdU^+$ cells was determined by flow cytometry using an APC BrdU Flow Kit (BD Biosciences).

Quantitative reverse transcription PCR

Cells were double-sorted directly into Trizol. Total RNA was extracted according to manufacture's instructions. Quantitative real-time PCR was run using SYBR green on a StepOne Plus (Life Tech) or a CFX Connect Real-time PCR machine (BioRad). β-actin was used to normalize the RNA content of samples. Primers used in this study were: *Scf*: OLD405: 5′-

TTGTTACCTTCGCACAGTGG-3′ and OLD406: 5′-AATTCAGTGCAGGGTTCACA-3′; *Cxcl12*: OLD35: 5′-TGCATCAGTGACGGTAAACCA-3′ and OLD36: 5′-GTTGTTCTTCAGCCGTGCAA-3′; β-actin: OLD27: GCTCTTTTCCAGCCTTCCTT-3′ and OLD28: 5′-CTTCTGCATCCTGTCAGCAA-3′; *Col1a1*: OLD826: ACGGCTGCACGAGTCACAC and OLD827: GGCAGGCGGGAGGTCTT; *Col3a1*: OLD828: 5′-AGGCTGAAGGAAACAGCAAA-3′ and OLD829: 5′-TAGTCTCATTGCCTTGCGTG-3′; *Acta2*: OLD830: ACTGGGACGACATGGAAAAG and OLD831: GTTCAGTGGTGCCTCTGTCA.

Gene expression profiling and analysis

Three independent, fresh isolated aliquots of approximately 5,000 *Cxcl12-DsRed*$^{+}$ cells from bone marrow of from *Cxcl12*$^{DsRed/+}$ recipient mice transplanted with Tpo-overexpressing virus-infected bone marrow cells or control virus-infected bone marrow cells were flow cytometrically sorted into Trizol. Total RNA was extracted and amplified using the WT-Ovation Pico RNA Amplification system (Nugen) following manufacture's instructions. Sense strand cDNA was generated using the WT-Ovation Exon Module (Nugen). Then, cDNA was fragmented and labeled using FL-Ovation DNA Biotin Module V2 (Nugen). The labeled cDNA was hybridized to Affymetrix Mouse Gene ST 1.0 chips following the manufacturer's instructions. Expression values for all probes were normalized and determined using the robust multi-array average (RMA) method via Affymetrix Expression Console. Normalized data were analyzed using NIA Array Analysis (Sharov et al., 2005). Significantly up- or down-regulated genes ($p<0.05$ and fold>1.5) were used to performed gene ontology analysis using the Database for Annotation, Visualization and Integrated Discovery (DAVID) online tools (Huang et al., 2009a, 2009b). For

gene set enrichment analysis (GSEA), the complete gene expression profiles were ranked based on p values from NIA Array Analysis and used as metric. Gene sets associated with fibrogenesis and osteogenesis were obtained from www.qiagen.com. The analyses were performed as described (Mootha et al., 2003; Subramanian et al., 2005).

Imatinib administration

Imatinib meslyate (0.5g/kg) (Biotang INC) chow was custom made by Envigo. One month after bone marrow transplantation (Tpo overexpression), mice were started on imatinib chow for 2 additional months before analysis.

Statistics and reproducibility

Sample size was not based on power calculations. No animals were excluded from the analysis. The experiments were not randomized. The investigators were not blinded to allocation during experiments and result assessment. Pairwise statistical significance was evaluated by two-tailed Student's t-test. One-way ANOVA was used to analyze microarray data. All data and statistics were derived from at least three biological replicates. 293T cells were used to generate retrovirus in this study. No cell lines used in this study were found in the database of commonly misidentified cell lines that is maintained by ICLAC and NCBI Biosample. The cell lines were not authenticated. The cell lines were not tested for mycoplasma contamination.

Data availability

Microarray data that support the findings of this study have been deposited in the Gene Expression Omnibus (GEO) under accession code GSE84387. Previously published expression data that were re-analyzed here are available online (De Minicis et al., 2007). All other data supporting the findings of this study are available from the corresponding author upon reasonable request.

ACKNOWLEDGEMENTS

This work was supported by the MPN Research Foundation. L.D., J.L. were supported by the Rita Allen Foundation and the National Heart, Lung and Blood Institute (1R01HL132074). Flow cytometry was partly supported by the NIH (S10RR027050 and S10OD020056). We thank Dr. R. Schwabe at Columbia and Dr. D. Brenner at UC San Diego for providing *Col-gfp* mice. We thank Dr. Lorin Olson at Oklahoma Medical Research Foundation and Dr. Philippe Soriano at Icahn School of Medicine at Mount Sinai for providing *Pdgfra*^{D842V} mice. We thank S. Weyn-Vanhentenryck, C. Zhang and R. Schwabe at Columbia for help on analyzing gene expression data. We thank S. Ho and A. Figueroa for help on flow cytometry.

Chapter 3

Hepatic thrombopoietin is required for bone marrow hematopoietic stem cell maintenance

The work described in this chapter is published:

Matthew Decker, Juliana Leslie, Qingxue Liu and Lei Ding (2018)

Hepatic thrombopoietin is required for bone marrow hematopoietic stem cell maintenance

Science, Vol 360, Issue 6384, p106-110

M.D and L.D. performed all the experiments with the help of Q.L. and J.L. M.D. and L.D. designed the experiments, interpreted the results, and wrote the manuscript

SUMMARY

Hematopoietic stem cell (HSC) maintenance depends on extrinsic cues. Currently, only local signals arising from the bone marrow niche have been shown to maintain HSCs. However, it is not known whether systemic factors also sustain HSCs. Here, we assess the physiological source of thrombopoietin (TPO), a key cytokine required for maintaining HSCs. Using $Tpo^{DsRed\text{-}CreER}$ knockin mice, we show that TPO is expressed by hepatocytes but not by bone marrow cells. Deletion of *Tpo* from hematopoietic cells, osteoblasts, or bone marrow mesenchymal stromal cells does not affect HSC number or function. However, when *Tpo* is deleted from hepatocytes, bone marrow HSCs are depleted. Thus, the adult bone marrow niche is unable to maintain HSCs in the absence of circulating hepatic TPO, demonstrating cross-organ dependence of a tissue-specific stem cell population. Our results suggest that systemic factors are a critical extrinsic regulatory component of HSCs.

INTRODUCTION

HSCs primarily reside in the bone marrow and are maintained by extrinsic cues that arise from supporting niche cells (Morrison and Scadden, 2014). Endothelial cells (Ding et al., 2012; Ding and Morrison, 2013) and perivascular mesenchymal stromal cells (Sugiyama et al., 2006; Méndez-Ferrer et al., 2010; Ding et al., 2012; Ding and Morrison, 2013; Greenbaum et al., 2013) are critical components of the bone marrow niche. Growing functional genetic evidence suggests that HSCs may be largely maintained through signals arising directly from, or mediated through, these local niche cells (Scadden, 2014). However, olfaction maintains hematopoietic progenitors through systemic GABA levels in *Drosophila* (Shim et al., 2013), suggesting that long-range signals may likewise be able to directly maintain mammalian HSCs.

No such distal maintenance factors have yet been identified in the mammalian hematopoietic system, although long-range cues, such as estrogen from the ovaries and erythropoietin from the kidney, can acutely stimulate HSC proliferation and dictate HSC and progenitor differentiation (Grover et al., 2014; Nakada et al., 2014). Neurotransmitters from the nervous system can mobilize HSCs, but this effect is mediated through mesenchymal stromal cells in the niche (Méndez-Ferrer et al., 2008). Therefore, current evidence describes roles for long-range cues that modify HSC behavior, but direct evidence for constant maintenance of HSCs by a cross-organ long-range systemic factor is lacking.

Signaling of the hematopoietic cytokine TPO through its receptor c-MPL is essential for thrombopoiesis (Kaushansky et al., 1994; Lok et al., 1994; de Sauvage et al., 1994) and HSC maintenance (Kimura et al., 1998; Qian et al., 2007; Yoshihara et al., 2007). Patients with loss-of-function mutations in c-MPL or TPO develop congenital amegakaryocytic thrombocytopenia and display subsequent bone marrow failure (Ballmaier et al., 2003; Dasouki et al., 2013; Seo et al., 2017). *Tpo* mRNA is expressed through multiple cell types, including hepatocytes (de Sauvage et al., 1994; Sungaran et al., 1997), osteoblasts (Yoshihara et al., 2007), megakaryocytes (Nakamura-Ishizu et al., 2014, 2015) and stromal cells (Sungaran et al., 1997; McIntosh and Kaushansky, 2008). However, *Tpo* is under stringent translational control by inhibitory elements in the 5'-untranslated region (Ghilardi et al., 1998) so it is not clear whether any of the above cell types actually synthesize TPO protein. *Tpo* has not been conditionally deleted from any cell types to assess the functional source required for HSC maintenance. Thus it is not clear how TPO maintains bone marrow HSCs *in vivo*. Intriguingly, loss of hepatic TPO leads to low platelets (Qian et al., 1998), showing that TPO from the liver regulates thrombopoiesis.

RESULTS

TPO is robustly translated by hepatocytes but not by bone marrow cells

Using quantitative reverse transcription PCR (qRT-PCR) analysis, we found that *Tpo* transcripts are enriched in osteoblasts, mesenchymal stromal cells, and the liver (**Figure 3.1a** and **Figure 3.2a-b**), consistent with previous reports. To systemically assess the expression of TPO protein, we generated $Tpo^{DsRed\text{-}CreER}$ knockin mice by replacing the stop codon of *Tpo* with a *P2A-DsRed-P2A-CreER* cassette (**Figure 3.2c-f**). The P2A elements allow the translation of TPO, DsRed and CreER recombinase under the control of *Tpo* endogenous regulatory elements. This enables us to monitor the translational expression of TPO *in vivo*. We generated $Tpo^{DsRed\text{-}CreER}$*; loxpZsGreen* mice (**Figure 3.1b**). Consistent with the low expression level of *Tpo in vivo* (Ghilardi et al., 1998), no DsRed fluorescence was detected (**Figure 3.1c-f**). However, upon tamoxifen administration to 8-week old mice, there was broad and specific expression of ZsGreen in hepatocytes (**Figure 3.1g-j** and **Figure 3.2g-o**). We also observed rare $ZsGreen^{+}$ cells in the kidney (**Figure 3.2p**). However, no $ZsGreen^{+}$ bone marrow cells could be detected (**Figure 3.1k-n and Figure3.2q**). Thus, TPO is robustly translated by hepatocytes but not by cells in the bone marrow.

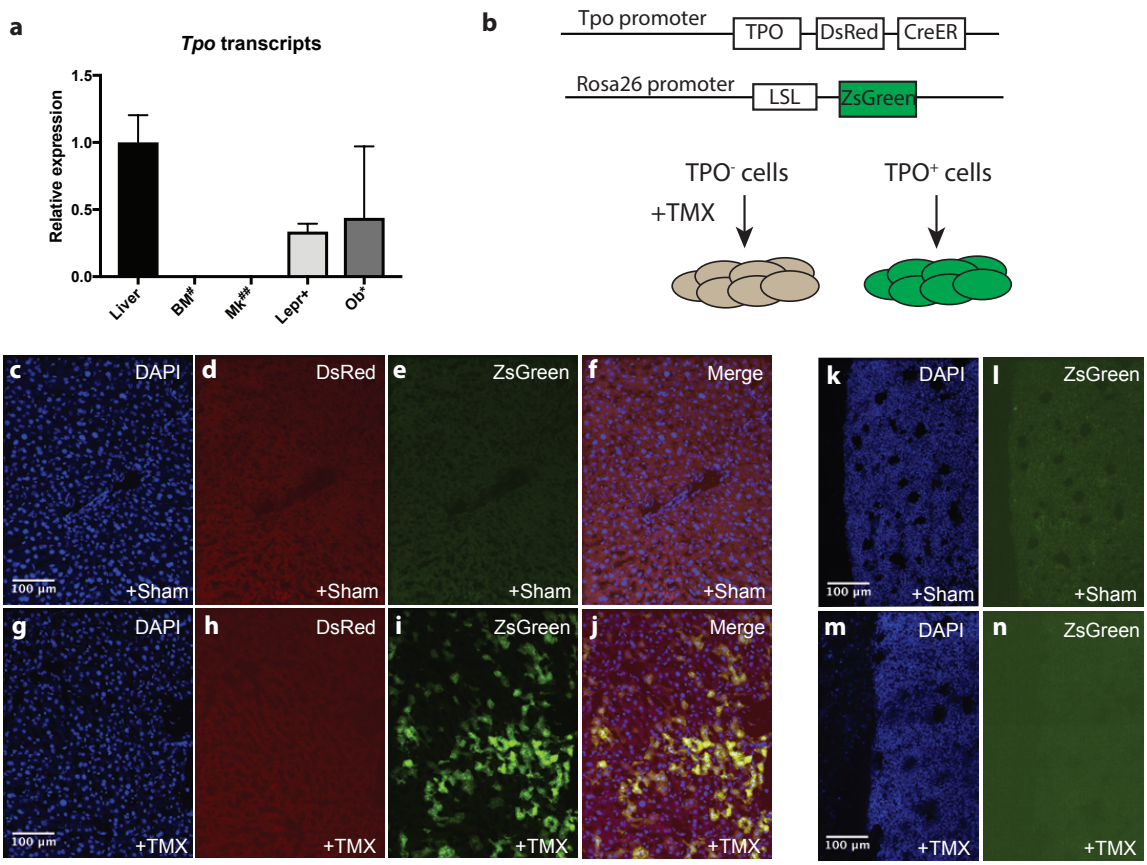

Figure 3.1 TPO is expressed by hepatocytes but not bone marrow cells

Figure 3.1 TPO is expressed by hepatocytes but not bone marrow cells

a. qRT-PCR analysis of *Tpo* transcript levels in whole liver lysate, whole bone marrow lysate, and purified bone marrow populations (n = 3). BM = whole bone marrow, Mk = megakaryocytes, Lepr+ = *Lepr*+ mesenchymal stromal cells, Ob = osteoblasts.

b. Schema of TPO expression analysis in $Tpo^{DsRed\text{-}CreER}$*; loxpZsGreen* reporter mice.

c-f. Confocal images of liver sections from sham-treated (Sham) $Tpo^{DsRed\text{-}CreER}$*; loxpZsGreen* mice. There was no apparent ZsGreen expression in hepatocytes (green). DsRed fluorescence could not be appreciated (red). Nuclei were stained with DAPI (blue).

g-j. Confocal images of liver sections from tamoxifen-treated (TMX) $Tpo^{DsRed\text{-}CreER}$*; loxpZsGreen* mice. There was prominent ZsGreen expression in the liver (green) while DsRed fluorescence could not be appreciated (red). Nuclei were stained with DAPI (blue).

k-n. Confocal images of femur sections from sham-treated (Sham) or tamoxifen-treated (TMX) $Tpo^{DsRed\text{-}CreER}$*; loxpZsGreen* mice. There was no apparent ZsGreen expression in the bone marrow (green). Nuclei were stained with DAPI (blue).

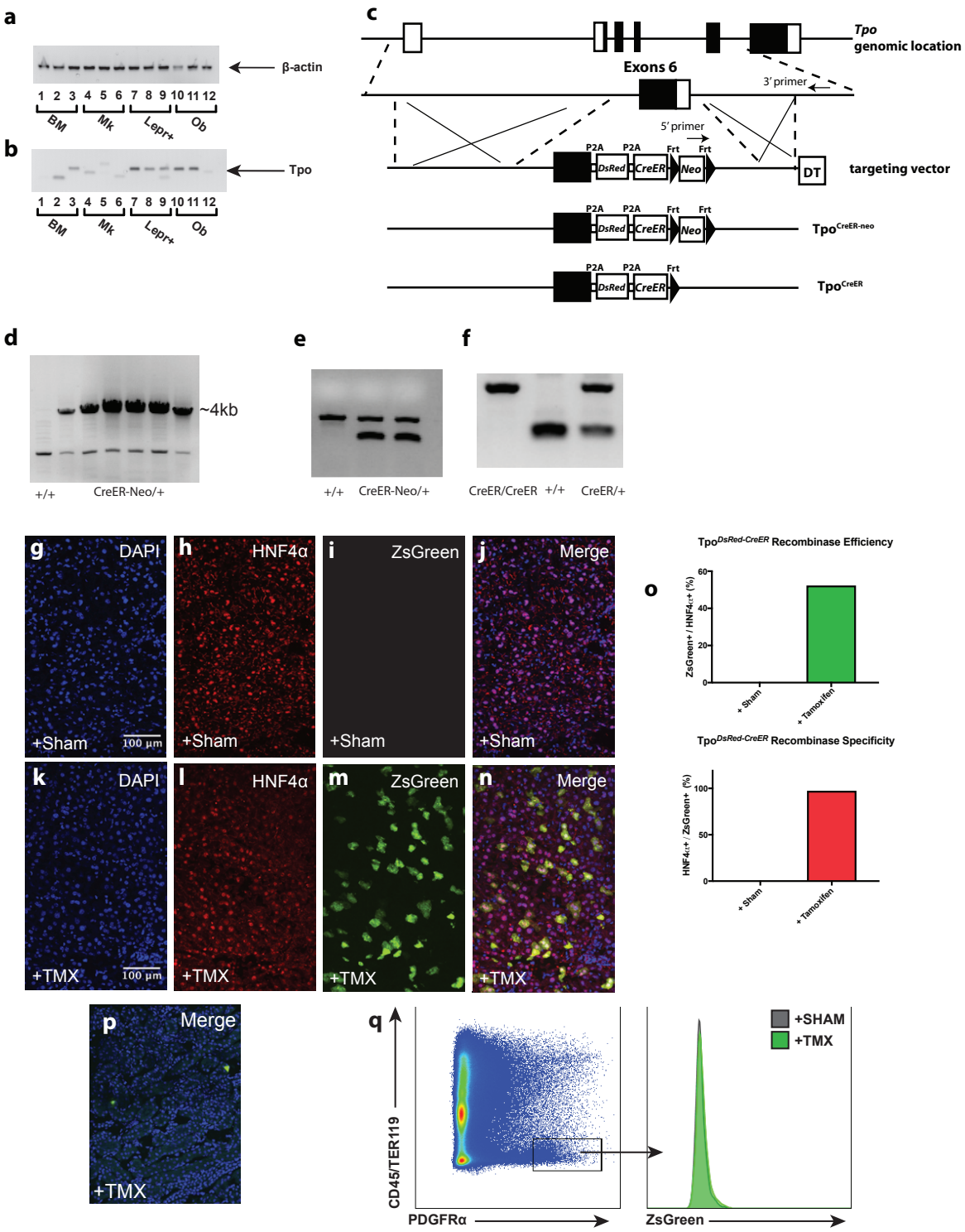

Figure 3.2 *Tpo*$^{DsRed\text{-}CreER}$ reporter mice show translational expression of TPO in hepatocytes but not in the bone marrow

Figure 3.2 *Tpo*$^{DsRed\text{-}CreER}$ reporter mice show translational expression of TPO in heaptocytes but not in the bone marrow

a-b. Image of gels loaded with PCR product from amplification with β-actin (A) and *Tpo* (B) primers. BM = whole bone marrow (lanes 1-3), Mk = CD41^{+} megakaryocytes (lanes 4-6), Lepr+ = Lepr+ mesenchymal stromal cells (lanes 7-9), Ob = Col2.3-GFP^{+} osteoblasts (lanes 10-12).

c. Targeting strategy for the generation of *Tpo*$^{DsRed\text{-}CreER}$ allele.

d. PCR screen of ES cell lysates showing correct insertion of the targeting vector.

e. Genotyping PCR showing germline transmission of the *Tpo*$^{DsRed\text{-}CreER}$ allele.

f. Genotyping PCR showing successful generation of homozygosity of the *Tpo*$^{DsRed\text{-}CreER}$ allele.

g-j. Confocal images of liver sections from sham-treated (Sham) *Tpo*$^{DsRed\text{-}CreER}$*; loxpZsGreen* mice. Hepatocytes were stained with an antibody against HNF4α (red). There was no apparent ZsGreen expression in hepatocytes (green). Nuclei were stained with DAPI (blue).

k-n. Confocal images of liver sections from tamoxifen-treated (TMX) *Tpo*$^{DsRed\text{-}CreER}$*; loxpZsGreen* mice. Hepatocytes were stained with an antibody against HNF4α (red). There is prominent ZsGreen in hepatocytes (green). Nuclei were stained with DAPI (blue).

o. Quantification of hepatic efficiency and specificity of the inducible Cre recombinase in tamoxifen-treated (+Tamoxifen) *Tpo*$^{DsRed\text{-}CreER}$*; loxpZsGreen* mice. Three representative 20x images from three different mice were counted for each condition.

p. Confocal image showing a kidney section from a tamoxifen-treated (TMX) *Tpo*$^{DsRed\text{-}CreER}$*; loxpZsGreen* mouse. There is apparent CreER activity in two kidney cells.

q. A representative flow cytometric plot showing no ZsGreen^{+} cells in CD45/Ter119^{-} Pdgfra^{+} stromal cells from *Tpo*$^{DsRed\text{-}CreER}$*; loxpZsGreen* mice after treatment with tamoxifen.

Whole body loss of TPO depletes HSCs and megakaryocyte-lineage cells

We generated a loss-of-function allele of *Tpo* (*Tpo*^{gfp}) by recombining enhanced green fluorescent protein (*gfp*) into the start codon of *Tpo* (**Figure 3.3a-c**). As expected, *Tpo* transcripts were depleted from *Tpo*$^{gfp/gfp}$ mouse livers (**Figure 3.3d**). Consistent with earlier reports (Gurney et al., 1994; Alexander et al., 1996), whole body loss of TPO led to reduced platelets (**Figure 3.4a-c**) and reduced megakaryocytes (**Figure 3.4d-j**). Bone marrow from *Tpo*$^{gfp/gfp}$ mice had normal cellularity, but CD150^{+}CD48^{-}Lin^{-}Sca1^{+}cKit^{+} HSC frequency (percentage of live whole bone marrow cells) decreased about 70-fold compared with *Tpo*$^{+/+}$ controls (**Figure 3.4k-m**). CD150^{-}CD48^{-} Lin^{-}Sca1^{+}cKit^{+} multipotent progenitor (MPP) and Lin^{-}Sca1^{+}cKit^{+} (LSK) hematopoietic progenitor frequencies declined by 10-fold and 3-fold, respectively (**Figure 3.4n-o**). Lineage-restricted hematopoietic progenitors appeared normal, except that CD34^{+}FcγR^{-} Lineage^{-}Sca1^{-}cKit^{+} common myeloid progenitors (CMPs) were reduced (**Figure 3.4p**). Bone marrow and spleen cells from *Tpo*$^{gfp/gfp}$ mice formed fewer colonies in methylcellulose (**Figure 3.4q**). There was no change in spleen cellularity but spleen HSC frequency was reduced (**Figure 3.4r-s**). *Tpo*$^{+/gfp}$ heterozygous mice displayed intermediate phenotypes (**Figure 3.4**). Thus, TPO is a major factor required for HSC maintenance.

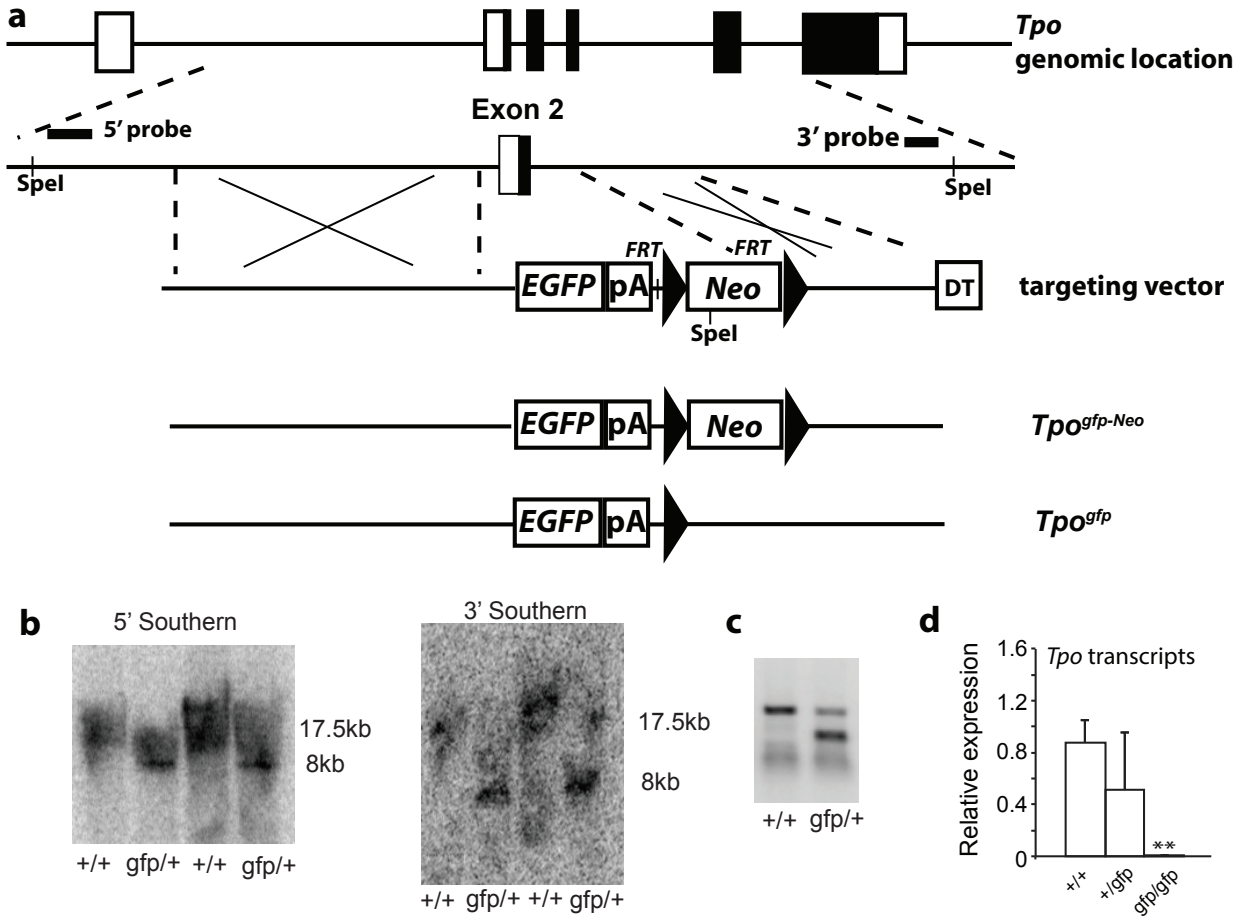

Figure 3.3 *Tpo*^{gfp} mice show loss of *Tpo* expression

a. Targeting strategy for the generation of a *Tpo*^{gfp} allele.

b. Southern blots showing correct insertion of targeting vector into the endogenous *Tpo* locus.

c. Genotyping PCR showing germline transmission of the *Tpo*^{gfp} allele.

d. qPCR showing significant loss of *Tpo* expression in *Tpo*$^{gfp/gfp}$ (gfp/gfp) mouse liver lysate relative to *Tpo*$^{+/+}$ and *Tpo*$^{+/gfp}$ control liver lysate.

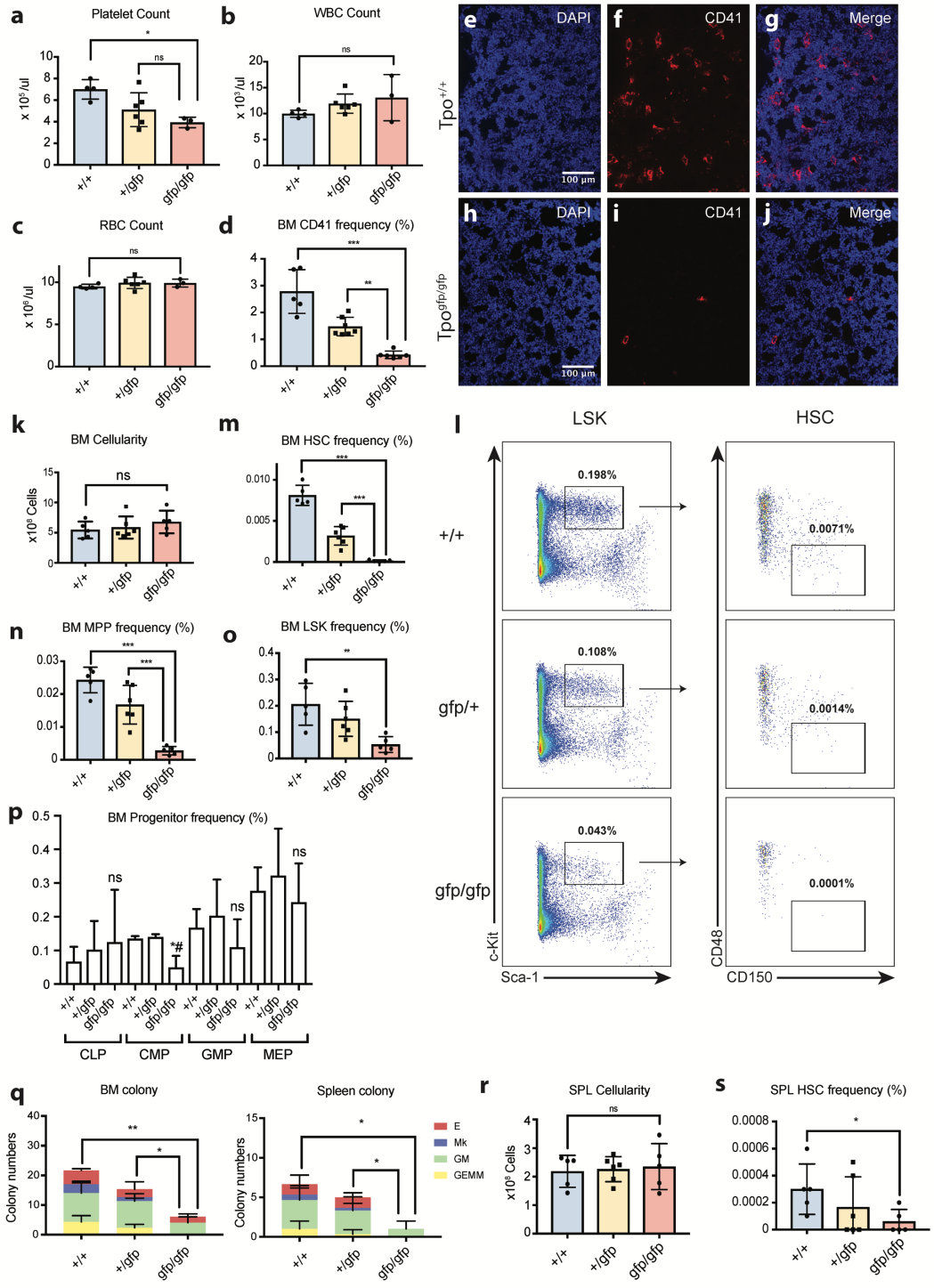

Figure 3.4 *Tpo* is required for HSC maintenance and normal thrombopoiesis

Figure 3.4 *Tpo* is required for HSC maintenance and normal thrombopoiesis

a-c. Peripheral blood count analysis of $Tpo^{+/+}$, $Tpo^{+/gfp}$, and $Tpo^{gfp/gfp}$ mice showed decreased platelet levels (a) in $Tpo^{gfp/gfp}$ animals but no change in white blood cell (b) or red blood cell (c) counts (n = 4 for $Tpo^{+/+}$, n = 6 for $Tpo^{+/gfp}$, n = 3 for $Tpo^{gfp/gfp}$).

d. Bone marrow $CD41^+$ megakaryocyte lineage cell frequency was significantly decreased in $Tpo^{gfp/gfp}$ mice relative to both $Tpo^{+/+}$ and $Tpo^{+/gfp}$ animals (n = 5 for $Tpo^{+/+}$, n = 7 for $Tpo^{+/gfp}$, n = 6 for $Tpo^{gfp/gfp}$).

e-j. Confocal images of femur sections from $Tpo^{+/+}$ (e-g) and $Tpo^{gfp/gfp}$ (h-j) mice showing a depletion of $CD41^+$ megakaryocyte lineage cells in $Tpo^{gfp/gfp}$ mice. CD41 was stained red. Nuclei were stained with DAPI (blue).

k. Bone marrow cellularity was normal in $Tpo^{gfp/gfp}$ mice (n = 5 for $Tpo^{+/+}$, n = 6 for $Tpo^{+/gfp}$, n = 5 for $Tpo^{gfp/gfp}$).

l. Representative flow cytometric plots showing decreased Lin^- $Sca1^+cKit^+$ (LSK) and Lin^- $Sca1^+cKit^+CD150^+CD48^-$ HSC frequency in bone marrow from $Tpo^{+/gfp}$ and $Tpo^{gfp/gfp}$ mice.

m-o. Bone marrow HSC, Lin^- $Sca1^+cKit^+CD150^-CD48^-$ multipotent progenitor (MPP) and LSK frequencies were decreased in $Tpo^{gfp/gfp}$ mice relative to both $Tpo^{+/+}$ and $Tpo^{+/gfp}$ animals (n = 5 for $Tpo^{+/+}$, n = 6 for $Tpo^{+/gfp}$, n = 5 for $Tpo^{gfp/gfp}$).

p. Bone marrow lineage-committed progenitor frequencies were not significantly affected in $Tpo^{gfp/gfp}$ mice relative to controls except CMP (n = 3 each genotype). MEP: myeloerythroid progenitor, GMP: granulocyte-macrophage progenitor, CMP: common myeloid progenitor, CLP: common lymphoid progenitor.

q. Myeloerythroid colony-forming cell frequency was significantly decreased in the bone marrow and spleens from $Tpo^{gfp/gfp}$ mice relative to controls. (n=3 for each genotype).

r. Spleen cellularity was normal in *Tpo*$^{gfp/gfp}$ mice (n = 5 for *Tpo*$^{+/+}$, n = 6 for *Tpo*$^{+/gfp}$, n = 5 for *Tpo*$^{gfp/gfp}$).

s. Spleen HSC frequency was reduced in *Tpo*$^{gfp/gfp}$ mice (n = 5 for *Tpo*$^{+/+}$, n = 6 for *Tpo*$^{+/gfp}$, n = 5 for *Tpo*$^{gfp/gfp}$).

+/+: *Tpo*$^{+/+}$, +/gfp: *Tpo*$^{+/gfp}$, gfp/gfp: *Tpo*$^{gfp/gfp}$. All data represent mean ± s.d. ns, not significant. * P<0.05, ** P<0.01, ***, P<0.001.

Conditional deletion of TPO from megakaryocytes, osteoblasts, and mesenchymal stromal cells does not affect HSC function

We generated a floxed allele of *Tpo* (*Tpo*^{fl}) by inserting *loxp* sequences flanking exons 2-4 of *Tpo* (**Figure 3.5a-c**). Recombination of the *loxp* sites will lead to the deletion of the start codon and the generation of a frameshift. We recombined the *Tpo*^{fl} allele in the germline to generate *Tpo*$^{-}$ by mating with *EIIa-cre* (**Figure 3.5d**). As expected, *Tpo* transcripts were absent from homozygous *Tpo*$^{-/-}$ mice (**Figure 3.5e**). *Tpo*$^{-/-}$ mice had significant reduction of HSCs, MPPs, and megakaryocytes (**Figure 3.5f-h**), nearly identical to the *Tpo*$^{gfp/gfp}$ mice (**Figure 3.4**). Recombination of the *Tpo*^{fl} allele therefore gave a strong loss of *Tpo* function.

Megakaryocytes have been proposed to be a major source of TPO for HSCs (Nakamura-Ishizu et al., 2014, 2015). However, we did not detect any *Tpo* expression in megakaryocytes by qRT-PCR (**Figure 3.1a**) or by reporter mice (**Figure 3.1k-n**). Nonetheless, we directly tested whether megakaryocytes (or any hematopoietic cells) are sources of TPO for HSC maintenance *in vivo* by generating *Vav1-cre; Tpo*$^{fl/gfp}$ mice. *Vav1-cre* efficiently deleted *Tpo* from the hematopoietic system (**Figure 3.6a**). Eight-week-old *Vav1-cre; Tpo*$^{fl/gfp}$ mice had normal blood counts, cellularity, and HSC frequency (**Figure 3.6b-d**) and normal restricted hematopoietic progenitors and megakaryocytic cells in the bone marrow (**Figure 3.6e-h**). Spleen cellularity, HSC frequency, and megakaryocytic cells were also unaffected (**Figure 3.6i-k**). Bone marrow cells from *Vav1-cre*; *Tpo*$^{fl/gfp}$ mice formed normal number of colonies in methylcellulose and reconstituted irradiated recipients normally (**Figure 3.6l-m**). Thus, hematopoietic cells, including megakaryocytes, are not a critical source of TPO for HSC maintenance.

Osteoblasts have also previously been proposed to be the main source of TPO in the bone marrow (Yoshihara et al., 2007) and osteoblasts express *Tpo* transcripts (**Figure 3.1a**); however, we could not detect any *Tpo* translational activity in osteoblasts from our reporter mice (**Figure**

3.1k-n). We directly tested whether deletion of *Tpo* from osteoblasts affects HSCs. Consistent with previous reports (Ding et al., 2012; Ding and Morrison, 2013), *Col2.3-cre* recombined efficiently in bone-lining osteoblasts (**Figure 3.7a-f**). Eight-week-old *Col2.3-cre; Tpo*$^{fl/gfp}$ mice had normal platelet counts (**Figure 3.7g**), cellularity and HSC frequency in the bone marrow and spleens (**Figure 3.7h-i** and **Figure 3.7k-l**). There was no effect on the capacity of bone marrow or spleen cells to form colonies in methylcellulose (**Figure 3.7j** and **Figure 3.7m**). *Col2.3-cre; Tpo*$^{fl/gfp}$ bone marrow cells had normal capacities to reconstitute irradiated recipients (**Figure 3.7n-o**). Thus, osteoblasts are not a critical source of TPO for HSC maintenance.

Bone marrow *Lepr*$^{+}$ mesenchymal stromal cells are a critical source of HSC niche factors, including SCF and CXCL12 (Ding et al., 2012; Ding and Morrison, 2013). These cells express *Tpo* transcripts (**Figure 3.1a**), although we could not detect *Tpo* translational activity (**Figure 3.1k-n**). We conditionally deleted *Tpo* from mesenchymal stromal cell by generating *Lepr-cre*; *Tpo*$^{fl/gfp}$ mice. *Tpo* was efficiently deleted from these cells (**Figure 3.8a-f**) . Eight-week-old *Lepr-cre*; *Tpo*$^{fl/gfp}$ had normal platelet counts (**Figure 3.8g**), cellularity, and HSC frequency in the bone marrow and spleens (**Figure 3.7h-i** and **Figure 3.7k-l**). Bone marrow and spleen cells from *Lepr-cre; Tpo*$^{fl/gfp}$ mice formed normal numbers of hematopoietic colonies in methylcellulose (**Figures 3.7j** and **Figure 3.7m**). Bone marrow cells from *Lepr-cre*; *Tpo*$^{fl/gfp}$ mice reconstituted irradiated recipient mice normally (**Figures 3.7n-o**). Thus, bone marrow mesenchymal stromal cells are not a critical source of TPO for HSC maintenance.

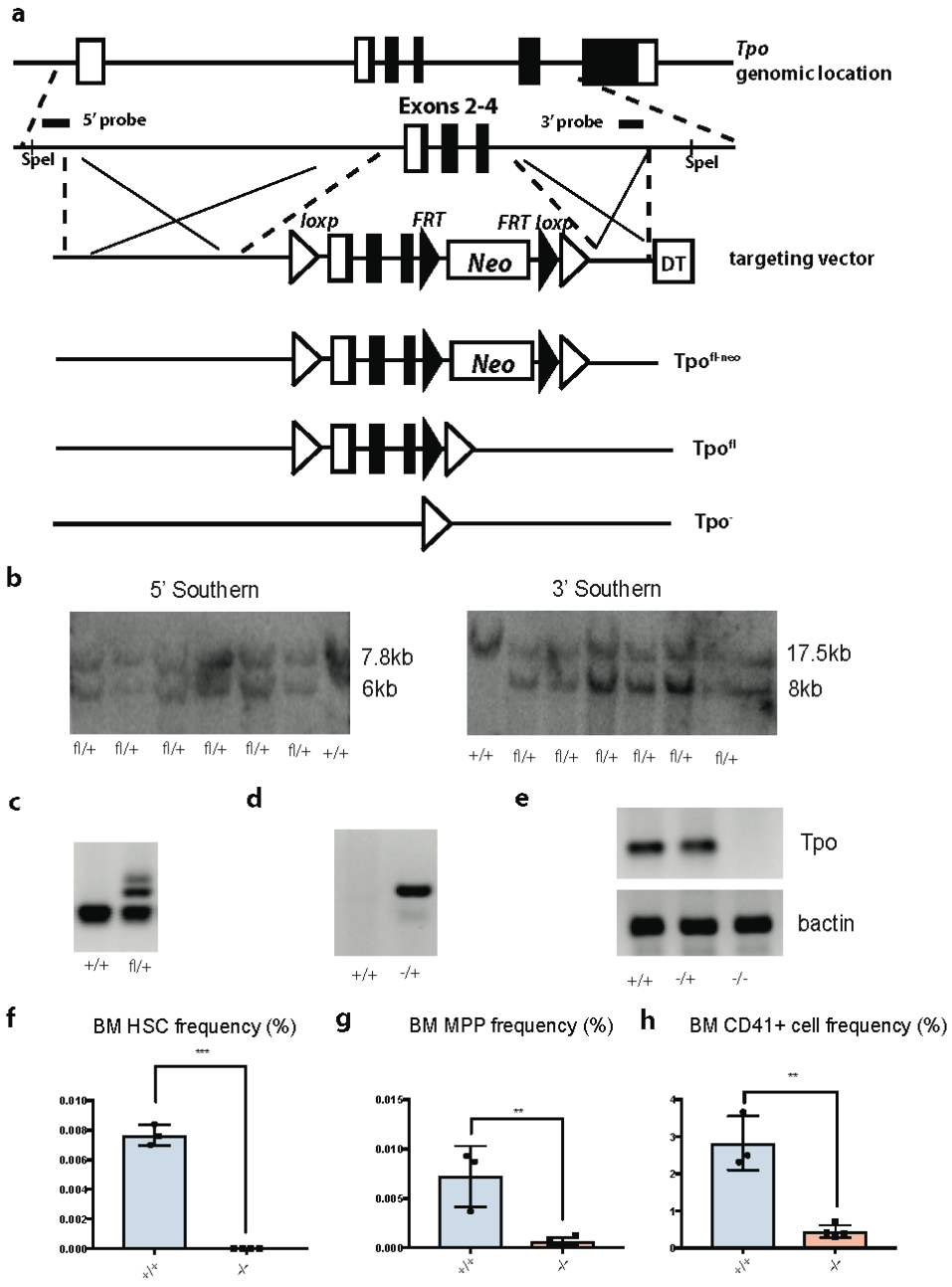

Figure 3.5 Germline recombination of *Tpo*^{fl} allele causes loss of *Tpo* expression and decreased HSC, MPP, and CD41^{+} cell frequencies

Figure 3.5 Germline recombination of *Tpo*^{fl} allele causes loss of *Tpo* expression and decreased HSC, MPP, and CD41^{+} cell frequencies

a. Targeting strategy for the generation of a *Tpo*^{fl} allele.

b. Southern blots showing correct insertion of targeting vector into the *Tpo* endogenous locus.

c. Genotyping PCR showing germline transmission of the *Tpo*^{fl} allele.

d. Genotyping PCR showing the detection of *Tpo*$^{-}$ allele in the progeny of *EIIA Cre* x *Tpo*$^{fl/+}$ mating.

e. RT-PCR showing the loss of *Tpo* transcripts in *Tpo*$^{-/-}$ mouse liver.

f-h. Bone marrow HSC frequency (F), MPP frequency (G), and megakaryocyte frequency (H) were all significantly decreased in *Tpo*$^{-/-}$ (-/-) mice relative to *Tpo*$^{+/+}$ (+/+) controls (n = 4 for *Tpo*$^{-/-}$, n = 3 for *Tpo*$^{+/+}$). All data represent mean ± s.d. ** P<0.01, ***, P<0.001.

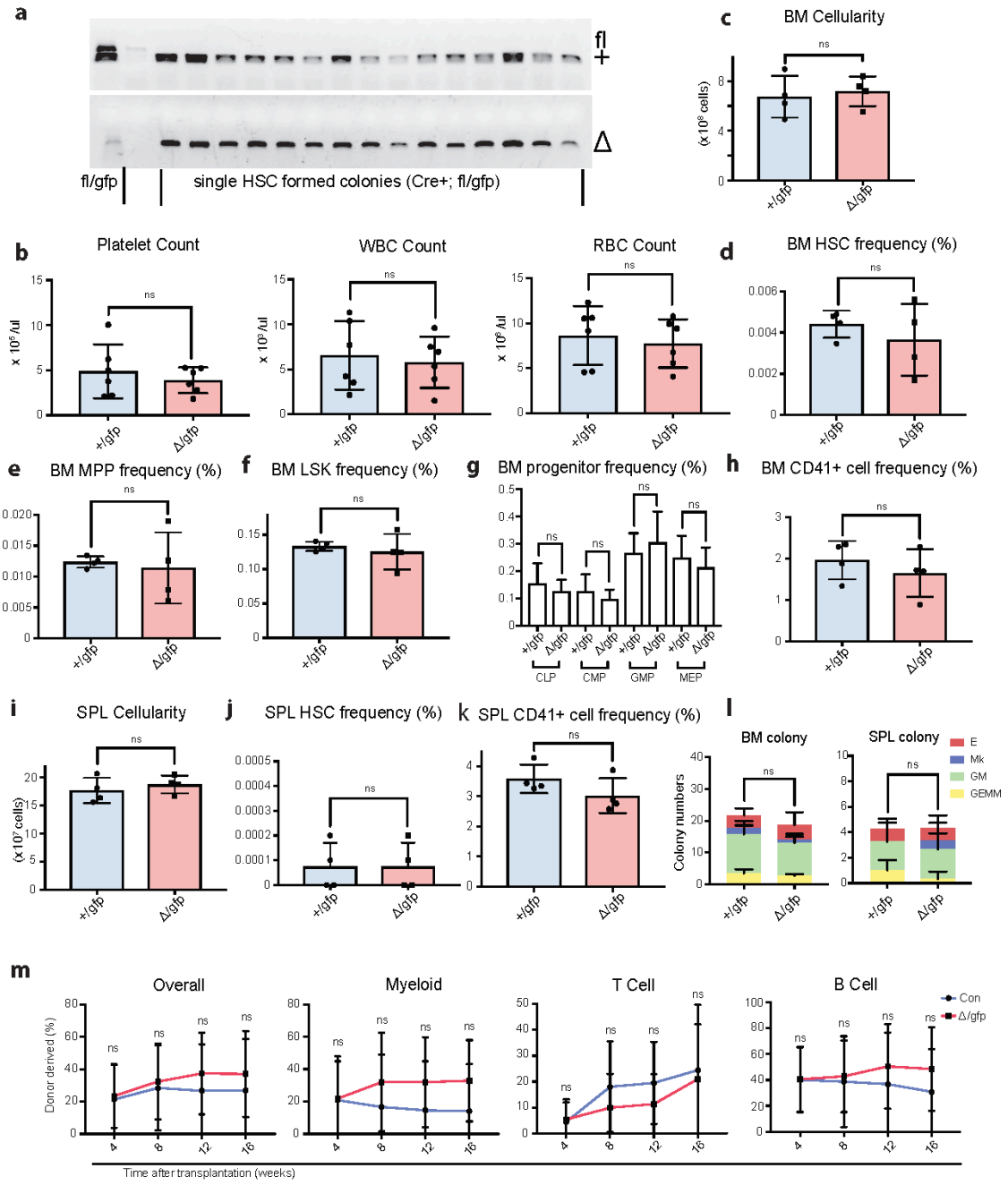

Figure 3.6 Efficient deletion of *Tpo* from hematopoietic cells does not perturb hematopoiesis or thrombopoiesis

Figure 3.6 Efficient deletion of *Tpo* from hematopoietic cells does not perturb hematopoiesis or thrombopoiesis

a. Representative genotyping results for quantifying deletion efficiency in hematopoietic colonies formed by individual sorted HSCs.

b. No significant differences were observed in platelet, white and red cell counts in *Vav1-cre; $Tpo^{fl/gfp}$* mice compared with controls (n = 6 for controls and *Vav1-cre; $Tpo^{fl/gfp}$* each).

c-h. No significant differences were observed in cellularity (C), HSC frequency (D), MPP frequency (E), LSK frequency (F), MEP, GMP, CMP, CLP frequencies (G) and $CD41^+$ megakaryocyte lineage cell frequency (H) in the bone marrow from *Vav1-cre; $Tpo^{fl/gfp}$* mice compared with controls (n = 4 for controls and *Vav1-cre; $Tpo^{fl/gfp}$* each).

i-k. No significant differences were observed in cellularity (I), HSC frequency (J) and $CD41^+$ megakaryocyte lineage cell frequency (K) in the spleen from *Vav1-cre; $Tpo^{fl/gfp}$* mice compared with controls (n = 4 for controls and *Vav1-cre; $Tpo^{fl/gfp}$* each).

l. Cells from bone marrow or spleens of *Vav1-cre; $Tpo^{fl/gfp}$* mice formed normal number of colonies in methylcellulose (n= 4 for controls and 5 for *Vav1-cre; $Tpo^{fl/gfp}$*).

m. 5 x 10^5 bone marrow cells from *Vav1-cre; $Tpo^{fl/gfp}$* mice gave similar levels of donor cell reconstitution relative to controls (two experiments with a total of 7 recipient mice for controls and 8 recipient mice for *Vav1-cre; $Tpo^{fl/gfp}$*).

Con: *Vav1-cre; $Tpo^{+/gfp}$* or *$Tpo^{fl/gfp}$*. Δ/gfp: *Vav1-cre; $Tpo^{fl/gfp}$*. All data represent mean ± s.d. ns, not significant.

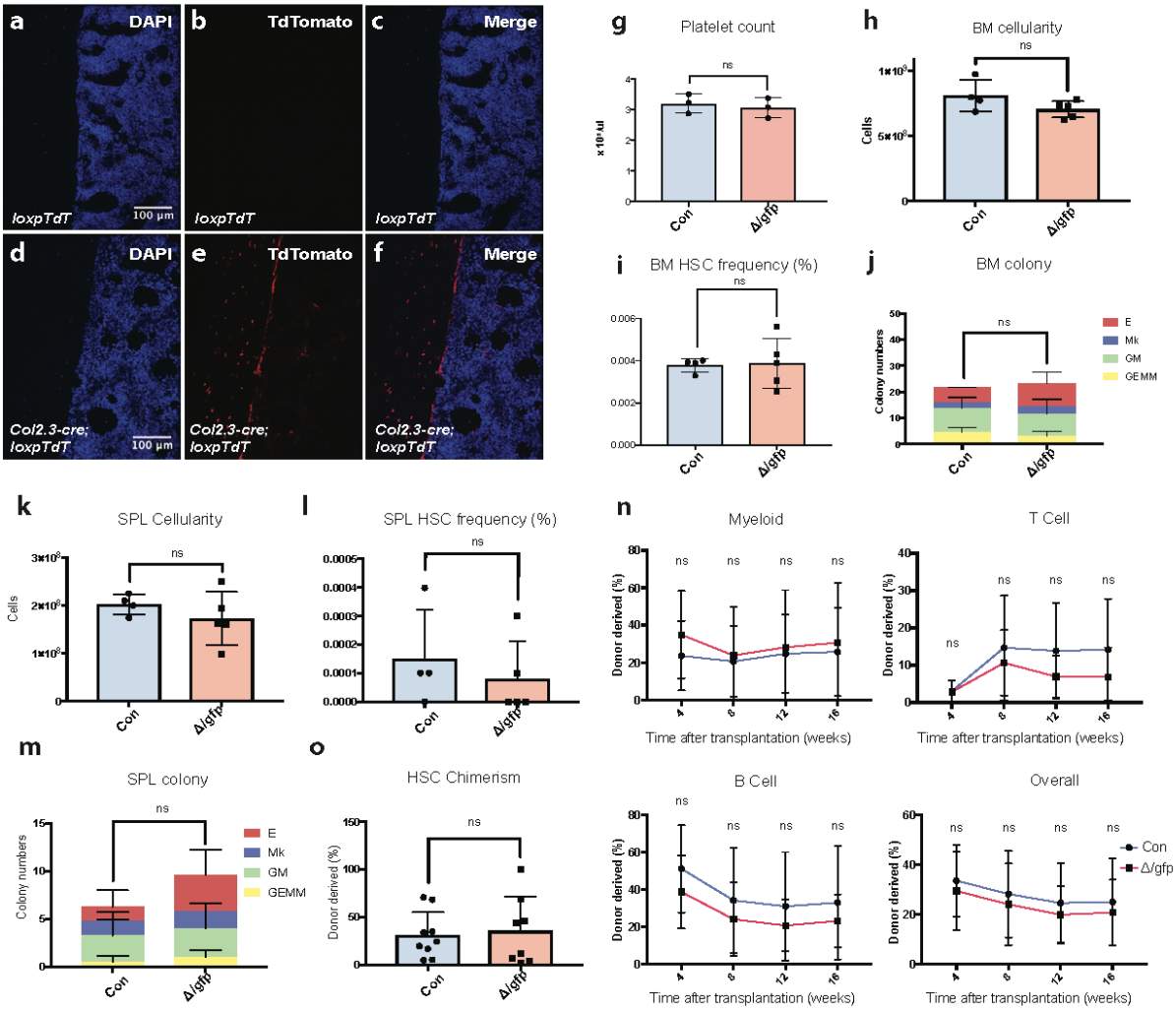

Figure 3.7 Osteoblasts are not a critical source of TPO for HSC maintenance

Figure 3.7 Osteoblasts are not a critical source of TPO for HSC maintenance

a-f. Confocal images of femur sections from *Col2.3-cre; loxpTdTomato* mice showing efficient recombination in osteoblasts. Nuclei were stained with DAPI (blue).

g. Peripheral blood platelet counts were not significantly affected in *Col2.3-cre;* $Tpo^{fl/gfp}$ mice relative to controls (n = 3 for each genotype).

h-j. Bone marrow cellularity (H), HSC frequency (I), and myeloerythroid-colony-forming cell frequency (J) were not significantly affected in *Col2.3-cre;* $Tpo^{fl/gfp}$ mice relative to controls (n = 4 for controls, n = 5 for *Col2.3-cre;* $Tpo^{fl/gfp}$).

k-m. Spleen cellularity (K), HSC frequency (L), and myeloerythroid-colony-forming cell frequency (M) were not significantly affected in *Col2.3-cre;* $Tpo^{fl/gfp}$ mice relative to controls (n = 4 for controls, n = 5 for *Col2.3-cre;* $Tpo^{fl/gfp}$).

n. 5 x 10^5 bone marrow cells from *Col2.3-cre;* $Tpo^{fl/gfp}$ mice gave similar levels of donor cell reconstitution in major hematopoietic lineages (B, T and myeloid) relative to controls (two experiments with a total of 8-9 recipient mice per genotype).

o. Similar HSC chimerism levels were in the recipient bone marrow 16 weeks after bone marrow transplantation relative to controls (n=9 for controls, n=8 for *Col2.3-cre;* $Tpo^{fl/gfp}$).

Con: *Col2.3-cre;* $Tpo^{+/gfp}$ or $Tpo^{fl/gfp}$. Δ/gfp: *Col2.3-cre;* $Tpo^{fl/gfp}$. All data represent mean ± s.d. ns, not significant. * P<0.05, ** P<0.01, ***, P<0.001

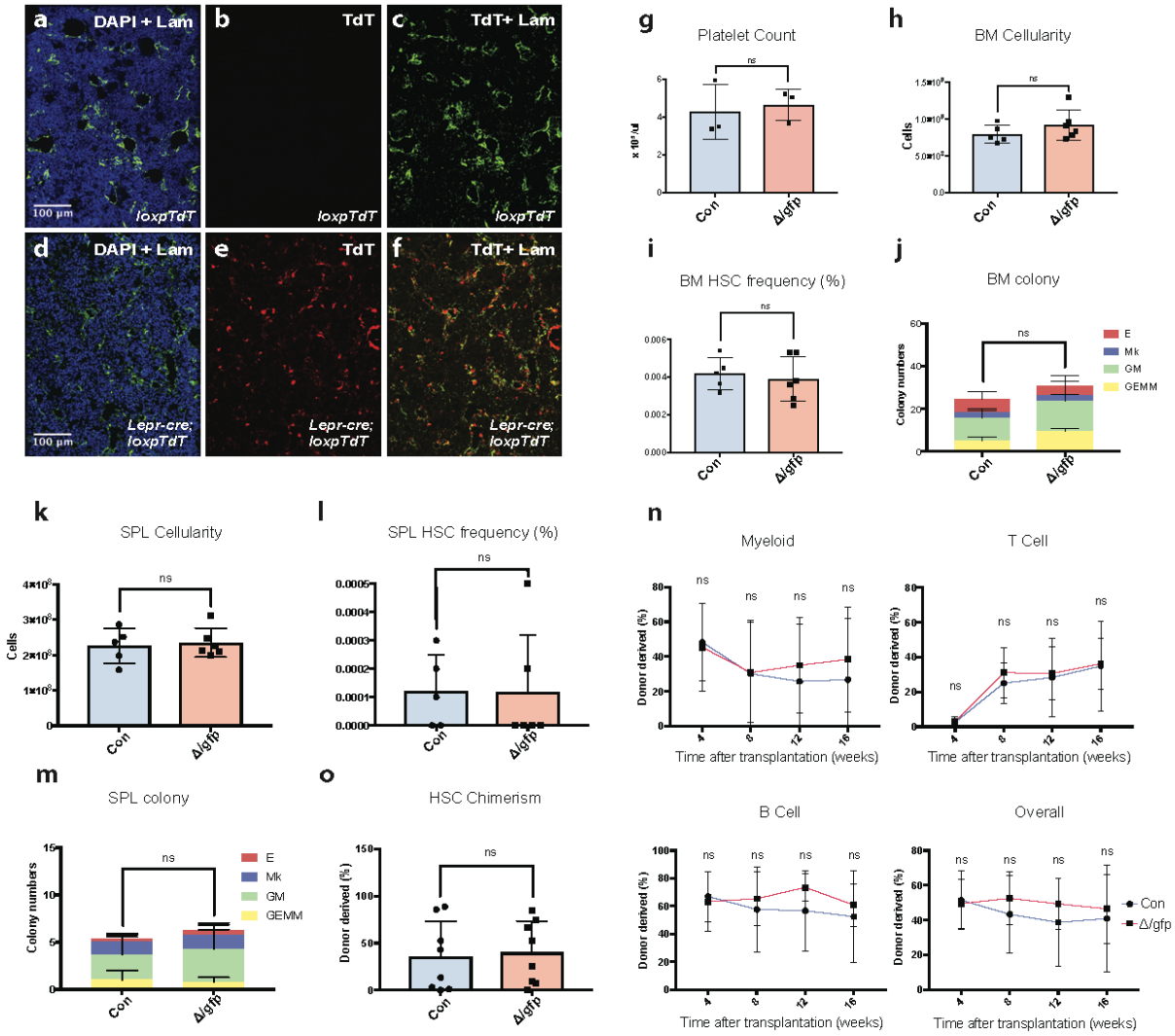

Figure 3.8 *Lepr*$^{+}$ mesenchymal stromal cells are not a critical source of TPO for HSC maintenance

Figure 3.8 *Lepr*$^{+}$ mesenchymal stromal cells are not a critical source of TPO for HSC maintenance

a-f. Confocal images of femur sections from *Lepr-cre; loxpTdTomato* mice showing specific recombination in bone marrow perivascular stromal cells. Vasculature was stained with an antibody against Laminin (green). Nuclei were stained with DAPI (blue).

g. Platelet counts were not significantly affected in *Lepr-cre; Tpo*$^{fl/gfp}$ mice relative to controls (n = 3 for controls, n =3 for *Lepr-cre; Tpo*$^{fl/gfp}$).

h-i. Bone marrow cellularity (H) and HSC frequency (I), were not significantly affected in *Lepr-cre; Tpo*$^{fl/gfp}$ mice relative to controls (n = 5 for controls, n =6 for *Lepr-cre; Tpo*$^{fl/gfp}$).

j. Bone marrow cells from *Lepr-cre; Tpo*$^{fl/gfp}$ mice formed similar number of myeloerythroid colonies relative to controls (n = 3 for each genotype).

k-l. Spleen cellularity (K) and HSC frequency (L) were not significantly affected in *Lepr-cre; Tpo*$^{fl/gfp}$ mice relative to controls (n = 5 for controls, n =6 for *Lepr-cre; Tpo*$^{fl/gfp}$).

m. Spleen cells from *Tpo*$^{fl/gfp}$ mice formed similar number of myeloerythroid colonies relative to controls (n =3 for each genotype).

n. 5 x 10^5 bone marrow cells from *Lepr-cre; Tpo*$^{fl/gfp}$ mice gave similar levels of donor cell reconstitution in multiple major hematopoietic lineages relative to controls (two experiments with a total of 8 recipient mice per genotype).

o. Recipient mice who received *Lepr-cre; Tpo*$^{fl/gfp}$ bone marrow cells showed similar donor bone marrow HSC chimerism sixteen weeks post-transplant relative to controls (n = 8 mice per genotype).

Con: *Lepr-cre; Tpo*$^{+/gfp}$ or *Tpo*$^{fl/gfp}$. Δ/gfp: *Lepr-cre; Tpo*$^{fl/gfp}$. All data represent mean ± s.d. ns, not significant. * P<0.05, ** P<0.01, ***, P<0.001.

Hepatocyte-derived TPO is required for HSC maintenance

The above data suggest that TPO produced locally by osteoblasts or mesenchymal stromal cells is not required for HSC maintenance. To test whether systemic TPO generated by the liver is important for HSC maintenance, we generated *Alb-cre; Tpo*$^{fl/fl}$ mice. As expected (Postic et al., 1999), *Alb-cre* recombined specifically and efficiently in hepatocytes but not in the bone marrow (**Figure 3.9a-d**). Eight-week-old *Alb-cre*; *Tpo*$^{fl/fl}$ mice had a 5-fold reduction of platelet count (**Figure 3.9e**), and a 5-fold reduction of megakaryocytic cells in the bone marrow (**Figure 3.9f**). *Alb-cre*; *Tpo*$^{fl/fl}$ mice exhibited normal bone marrow and spleen cellularity (**Figure 3.9g**). The frequency of bone marrow HSCs was reduced 24-fold compared to controls (**Figure 3.9h**). Bone marrow and spleen cells from *Alb-cre*; *Tpo*$^{fl/fl}$ mice formed fewer colonies in methylcellulose (**Figure 3.9i-j**). Spleen HSC frequency was normal in *Alb-cre; Tpo*$^{fl/fl}$ mice (**Figure 3.9h**), suggesting that there was no compensatory extramedullary hematopoiesis. Bone marrow cells from *Alb-cre*; *Tpo*$^{fl/fl}$ had severe defects in their ability to reconstitute irradiated recipients (**Figure 3.9k-l**). Overall, these data show that hepatic TPO is critical for the maintenance of bone marrow HSCs.

During development, HSCs transiently reside in the fetal liver (Mikkola and Orkin, 2006), where *Alb-cre* recombines (Weisend et al., 2009). Thus, it is possible that bone marrow HSCs in *Alb-cre; Tpo*$^{fl/fl}$ mice acquire a persistent defect during development. Nonetheless, we conditionally deleted *Tpo* from adult hepatocytes by administrating the hepatotropic Cre-bearing virus AAV8-TBG-cre. Consistent with a prior report (Yanger et al., 2013), we observed specific and efficient recombination in hepatocytes after a single intravenous administration of AAV8-TBG-cre to adult mice (**Figure 3.10a-d**).

We administered AAV8-TBG-cre virus once to 8-week old *Tpo*$^{fl/fl}$ and wild-type littermate control mice and analyzed them 4-8 weeks later. AAV8-TBG-cre-treated wild-type mice had identical phenotypes as buffer-treated *Tpo*$^{fl/fl}$ mice. They were pooled together as controls. There was no change in bone marrow and spleen cellularity (**Figure 3.10e**). However, *AAV8-cre; Tpo*$^{fl/fl}$ mice had reductions in bone marrow and spleen HSC cell frequencies (**Figure 3.10f-g**). The colony-forming capacity of bone marrow and spleen cells was also reduced (**Figure 3.10h-i**). Bone marrow cells from *AAV8-cre*; *Tpo*$^{fl/fl}$ mice 2 months after the virus treatment had a significant decrease in their ability to reconstitute irradiated recipients, whereas bone marrow cells from *AAV8-cre*; *Tpo*$^{fl/fl}$ mice 1 month after the virus treatment had an intermediate phenotype (**Figure 3.10j**). To quantify the frequency of functional HSCs, we performed limit dilution assays. In these assays, the frequency of long-term multilineage reconstituting cells in bone marrow cells from control and *AAV8-cre*; *Tpo*$^{fl/fl}$ were 1/87,660 and 1/498,020, respectively, corresponding to a 6-fold reduction (**Figure 3.10k**). There was no significant difference in Annexin V^{+} bone marrow HSCs from *AAV8-cre; Tpo*$^{fl/fl}$ mice compare with controls (**Figure 3.10l**) but HSCs from *AAV8-cre; Tpo*$^{fl/fl}$ mice cycled more (**Figure 3.10m**). These data indicate that adult HSCs lacking a hepatocyte-derived TPO signal are depleted through a self-renewal defect, not senescence or apoptosis.

Tpo transcription is upregulated in the bone marrow during hematopoietic stress (Sungaran et al., 1997), and mice deficient in TPO signaling show an impaired hematopoietic response to treatment with the chemotherapeutic agent 5-fluorouracil (5-FU) (Li and Slayton, 2013). We injected tamoxifen-treated *Tpo*$^{DsRed\text{-}CreER}$*; loxpZsGreen* mice with 5-FU but failed to detect ZsGreen expression in the bone marrow **(Figure 3.11**), suggesting that bone marrow does not significantly upregulate translation of TPO in response to hematopoietic challenge by 5-FU.

Further studies are required to determine the role of local and systemic TPO in other non-homeostatic conditions.

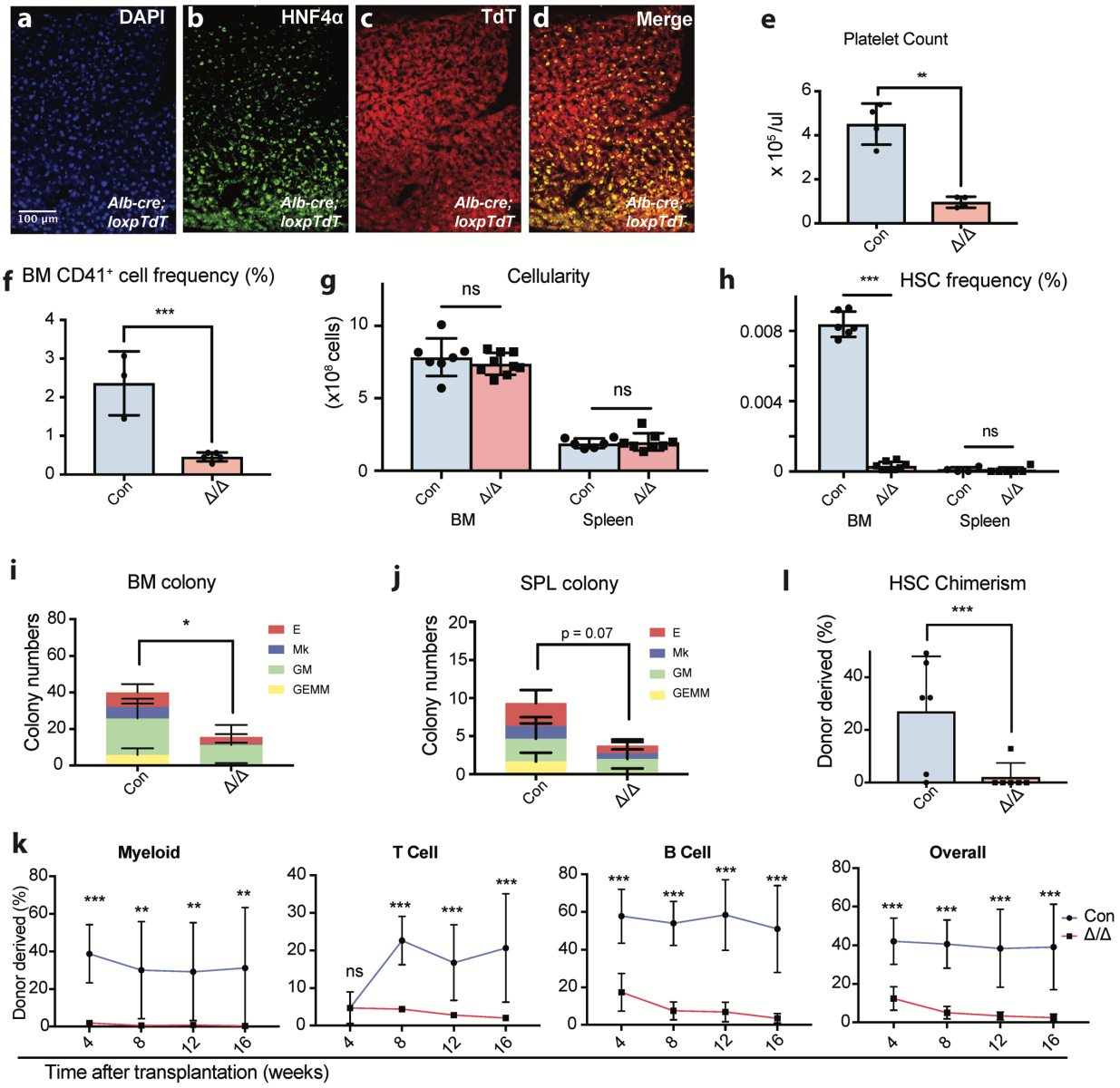

Figure 3.9 Hepatocyte-derived TPO is required for HSC maintenance

Figure 3.9 Hepatocyte-derived TPO is required for HSC maintenance

a-d. Confocal images of liver sections from *Alb-cre; loxpTdTomato* mice.

e. Platelet count was decreased in *Alb-cre; Tpo$^{fl/fl}$* mice (n = 4).

f. Bone marrow CD41^{+} cell frequency was decreased in *Alb-cre; Tpo$^{fl/fl}$* mice (n = 3-5).

g. Cellularity was normal in the bone marrow and spleens from *Alb-cre; Tpo$^{fl/fl}$* mice (n = 5-6).

h. HSCs were depleted in the bone marrow but not in spleens from *Alb-cre; Tpo$^{fl/fl}$* mice (n = 6-8).

i-j. Colony-forming cell numbers were decreased in the bone marrow and trended lower in spleens from *Alb-cre; Tpo$^{fl/fl}$* mice (n = 5-6).

k. 5 x 10^5 bone marrow cells from *Alb-cre; Tpo$^{fl/fl}$* mice gave lower levels of donor cell reconstitution (two experiments with a total of 8-9 recipient mice per genotype).

l. Recipient mice from (K) showed significant decrease in donor bone marrow HSC chimerism 16 weeks post-transplant (n = 6 mice per genotype).

Con: *Alb-cre; Tpo$^{+/+}$* or *Tpo$^{fl/fl}$* or *Tpo$^{fl/+}$*; Δ/ Δ: *Alb-cre; Tpo$^{fl/fl}$*. Data represent mean ± s.d. ns, not significant. * P<0.05, ** P<0.01, *** P<0.001.

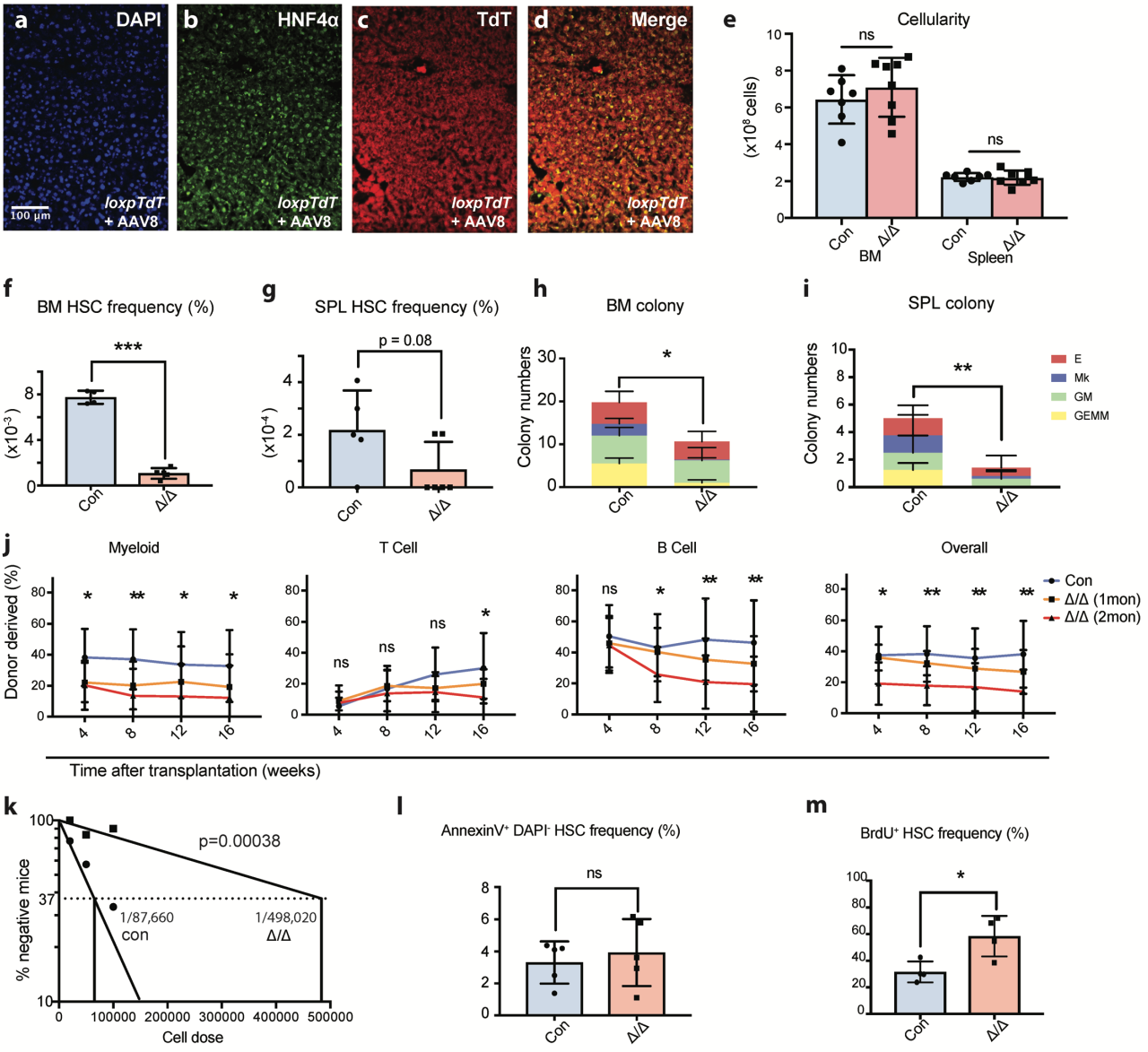

Figure 3.10 TPO from adult hepatocytes regulates bone marrow HSC maintenance and quiescence

Figure 3.10 TPO from adult hepatocytes regulates bone marrow HSC maintenance and quiescence.

a-d. Confocal images of liver sections from AAV8-TBG-cre-treated *loxpTdTomato* mice.

e. Bone marrow and spleen cellularity was normal in *Alb-cre; Tpo$^{fl/fl}$* mice (n = 7-8).

f. Bone marrow HSCs were depleted in AAV8-TBG-cre-treated *Tpo$^{fl/fl}$* mice (n = 4-5).

g. Spleen HSC frequency had a trend to decrease in AAV8-TBG-cre-treated *Tpo$^{fl/fl}$* mice.

h-i. Bone marrow and spleen colony-forming cell frequency was decreased in *AAV8-cre; Tpo$^{fl/fl}$* mice (n = 6-7).

j. 5 x 10^5 bone marrow cells from *AAV8-cre; Tpo$^{fl/fl}$* mice gave lower levels of donor cell reconstitution (2-3 experiments with a total of n=16 for controls, n=9 for 1 month after AAV8 treatment and n=14 for 2 months after AAV8 treatment).

k. Limit dilution assays showed that this was a 6-fold reduction of functional HSCs in the bone marrow from *AAV8-cre; Tpo$^{fl/fl}$* mice compared with controls (two independent experiments).

l. Annexin V^+ $DAPI^-$ bone marrow HSC frequency was not affected in *AAV8-cre; Tpo$^{fl/fl}$* mice (n = 5).

m. Bone marrow HSCs incorporated more BrdU in *AAV8-cre; Tpo$^{fl/fl}$* mice (n = 4).

Con: *Tpo$^{+/+}$* mice treated with AAV8-TBG-cre or *Tpo$^{fl/fl}$* mice treated with PBS; Δ/ Δ: *Tpo$^{fl/fl}$* mice treated with AAV8-TBG-cre. Data represent mean ± s.d. ns, not significant. * $P<0.05$, ** $P<0.01$, *** $P<0.001$.

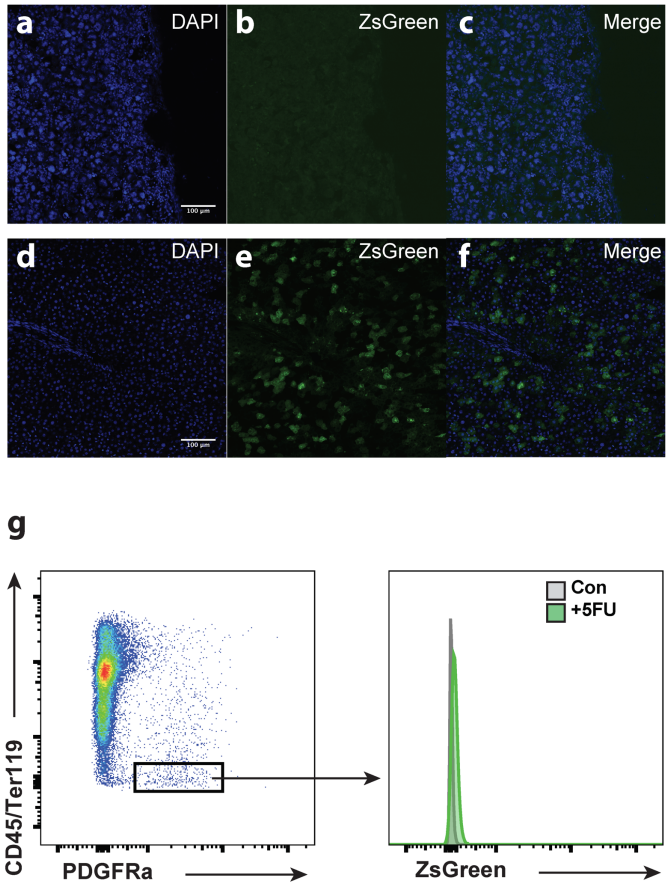

Figure 3.11 The bone marrow is not a major source of TPO in stress induced by 5-FU treatment.

a-c. Representative confocal images of a femur section from tamoxifen-treated *Tpo*$^{DsRed\text{-}CreER}$*; loxpZsGreen* mice dosed with 5-FU showing no ZsGreen expression in the bone marrow.

d-f. Representative confocal images of liver sections from tamoxifen-treated *Tpo*$^{DsRed\text{-}CreER}$*; loxpZsGreen* mice dosed with 5-FU showing robust expression of ZsGreen.

g. Representative flow cytometry plots showing no ZsGreen expression in bone marrow CD45/Ter119-PDGFRa+ mesenchymal stromal cells. Con, tamoxifen-treated loxpZsGReen mice administered with 5-FU. +5-FU, tamoxifen-treated *Tpo*$^{DsRed\text{-}CreER}$*; loxpZsGreen* mice dosed with 5-FU. All images representative of 3 biological replicates.

DISCUSSION

Our data demonstrate that bone marrow HSCs do not depend on previously identified local sources of TPO, but instead are maintained by hepatic TPO. To our knowledge, this is the first direct evidence of an endocrine-type regulation of HSC maintenance. Our results highlight the importance of systemic regulators in HSC biology, and raise questions about how these regulators communicate with HSCs in a coordinated manner. It is conceivable that hepatocytes sense certain physiological perimeters to appropriately maintain HSCs and hematopoiesis in the bone marrow. One possibility is that hepatocytes rely on detection of aging platelets via the Ashwell-Morell receptor (Grozovsky et al., 2015) as a proxy for HSC activity.

Our finding that hepatic TPO is critical for HSC maintenance is consistent with clinical observations on patients with liver diseases (Lv et al., 2014; Bihari et al., 2016). A recent clinical study showed an adverse correlation between liver cirrhosis and HSC number (Bihari et al., 2016). A separate study found that treatment of hepatitis B patients with entecavir simultaneously improved liver function and increased the number of circulating and peripheral HSCs by 2-4 fold (Lv et al., 2014). Consideration of the impact of liver defects on HSCs and hematopoiesis may lead to better management of these diseases.

Other than the liver and bone marrow stroma, several other organs have been reported to express *Tpo* transcripts (de Sauvage et al., 1994). It has been suggested that megakaryocytes are a source of TPO (Nakamura-Ishizu et al., 2014, 2015). However, we could not detect any *Tpo* expression in megakaryocytes by qRT-PCR or reporter mice (**Figure 3.1**). Despite the presence of *Tpo* transcripts in non-hepatic populations, HSC numbers in *Alb-cre; Tpo*$^{fl/fl}$ or *AAV8-cre; Tpo*$^{fl/fl}$ mice were depleted to levels comparable to whole body *Tpo* knockout mice (*Tpo*$^{-/-}$ or *Tpo*$^{gfp/gfp}$) (compare **Figure 3.4m**, **Figure 3.5f, Figure 3.9h**, and **Figure 3.10f**). Thus,

hepatocytes in the liver appear to be the major functional source of TPO for HSC maintenance. The role of the TPO expressed by other organs or cell types need further investigation.

Megakaryocytes are an important component of the bone marrow HSC niche (Bruns et al., 2014; Zhao et al., 2014). In *Alb-cre; Tpo*$^{fl/fl}$ or *AAV8-cre; Tpo*$^{fl/fl}$ mice, HSCs were depleted and megakaryocytes were also reduced (**Figure 3.9** and **Figure 3.10**) This raises the question of whether the HSC phenotype was mediated by a reduction of megakaryocytes. However, ablation of megakaryocytes leads to more HSCs and higher reconstitution activity (Bruns et al., 2014; Zhao et al., 2014), the opposite of what we observed when TPO was deleted from hepatocytes. Thus, it is likely that hepatic TPO directly regulates bone marrow HSCs.

Although we have determined that osteoblasts and mesenchymal stromal cells are not critical sources of TPO at steady state, these cells could be critical sources of TPO under other conditions. It has been shown that *Tpo* transcription is upregulated in the bone marrow during hematopoietic stress (Sungaran et al., 1997), and that TPO/cMPL signaling is crucial to bone marrow recovery from irradiation and 5-FU treatment (Li and Slayton, 2013; Olson et al., 2013). While we have shown that TPO is not robustly translated in the bone marrow following 5-FU administration (**Figure 3.11**), other studies will be required to determine the functional role of local and systemic TPO in non-homeostatic conditions.

EXPERIMENTAL METHODS

Mice

Lepr-cre (DeFalco et al., 2001), *LoxptdTomato* (Madisen et al., 2010), *LoxpZsGreen* (Madisen et al., 2010), and *EIIa-cre* (Lakso et al., 1996) mice were obtained from the Jackson Laboratory and maintained on C57BL/B6 background. *Col2.3-cre* mice were described previously (Liu et al., 2004). Targeting vectors for generating Tpo^{gfp}, $Tpo^{DsRed\text{-}creER}$ and Tpo^{fl} mice were constructed by recombineering (Liu et al., 2003). Linearized targeting vector was electroporated into KV1 ES cells (129B6 hybrid). Positive clones were identified by PCR and/or Southern blotting and then injected into B6 blastocysts. Chimeric mice were bred with B6 mice to obtain germline transmission. The *Frt* flanked Neo cassette was subsequently removed by mating with Flpe mice. These mice were backcrossed at least 5 times onto C57BL/6 background before analysis. All mice were housed in specific pathogen-free, Association for the Assessment and Accreditation of Laboratory Animal Care (AAALAC)- approved facilities at the Columbia University Medical Center. All protocols were approved by the Institute Animal Care and Use Committee of Columbia University.

Genotyping PCR

Primers for genotyping *Tpo-DsRed-CreER*: OLD815, 5'-CCACCACCATGCCTAACTCT-3'; OLD816, 5'-GTTCTCCTCCACGTCTCCAG-3'; and OLD817, 5'-TCGCTAGCTGCTCTGATGAA-3'.

Primers for genotyping *loxpTdTomato*: OLD558, 5'-AAGGGAGCTGCAGTGGAGTA-3' ; OLD559, 5'-CCGAAAATCTGTGGGAAGTC-3' ; OLD560, 5'-GGCATTAAAGCAGCGTATCC-3'; OLD561, 5'-CTGTTCCTGTACGGCATGG-3'.

Primers for genotyping *loxpZsGreen*: OLD GGCATTAAAGCAGCGTATCC and AACCAGAAGTGGCACCTGAC

Primers for genotyping Tpo^{fl}: OLD581, 5'-CATCTCGCTGCTCTTAGCAGGG-3' and OLD582, 5'-GAGCTGTTTGTGTTCCAACTGG-3'.

Primers for genotyping Tpo^{gfp}: OLD292, 5'-CGGACACGCTGAACTTGTGG-3'; OLD528 5'-ACTTATTCTCAGGTGGTGACTC-3' and OLD653 5'-AGGGAGCCACTTCAGTTAGAC-3'.

Primers for genotyping Tpo^{del}: OLD748, 5'-TTAGGGAGCAGGAGGGATCT-3' and OLD749 5'-CCCAGCTAACAACCAATGCT-3'.

Primers for genotyping *Lepr-cre*: OLD434 5'-CATTGTATGGGATCTGATCTGG-3' and OLD435 5'-GGCAAATTTTGGTGTACGGTC-3'.

Primers for genotyping *cre*: OLD338, 5'-GCATTTCTGGGGATTGCTTA-3' and OLD339, 5'-ATTCTCCCACCGTCAGTACG-3'.

Tamoxifen administration

Tamoxifen (Sigma) was dissolved in corn oil for a final concentration of 20mg/mL. Every other day for 10 days, 50uL of the solution was administered by oral gavage. Mice were analyzed 2-4 days after the final tamoxifen administration.

Viral infections

Replication-incompetent AAV8-TBG-cre was obtained from the Penn Vector Core. AAV8-TBG-cre carries Cre recombinase under the regulatory control of the hepatocyte-specific thyroid-binding globulin (TBG) promoter. Efficient recombination was achieved at a dose of 2.5×10^{11} viral particles diluted in sterile 1x PBS. AAV8-TBG-cre was administered to mice *via* retro-orbital venous sinus injection.

Long-term competitive reconstitution assay and limit dilution assay

Adult recipient mice were lethally irradiated by a Cesium 137 Irradiator (JL Shepherd and Associates) at 300 rad/min with two doses of 540 rad (total 1080 rad) delivered at least two hours apart. Cells were transplanted by retro-orbital venous sinus injection of anesthetized mice. 5×10^5 donor bone marrow cells were transplanted along with 5×10^5 competitor bone marrow cells unless otherwise indicated. Mice were maintained on antibiotic water (Baytril 0.17g/L) for 14 days then switched to regular water. Recipient mice were periodically bled to assess the level of donor-derived blood lineages, including myeloid, B, and T cells for at least 16 weeks. Blood was subjected to ammonium chloride potassium red cell lysis before antibody staining. Antibodies including anti-CD45.2 (104), anti-CD45.1 (A20), anti-CD3 (17A2), anti-B220 (6B2), anti-Gr-1 (8C5), and anti-Mac-1 (M1/70) were used to stain cells.

Flow cytometry

Bone marrow cells were isolated by flushing the long bones or by crushing the long bones, pelvis, and vertebrae with mortar and pestle in Ca^{2+} and Mg^{2+}free HBSS with 2% heat-inactivated bovine serum. Spleen cells were obtained by crushing the spleens between two glass

slides. The cells were passed through a 25G needle several times and filtered with a 70μm nylon mesh. The following antibodies were used to perform HSC staining: lineage markers (anti-CD2 (RM2-5), anti-CD3 (17A2), anti-CD5 (53-7.3), anti-CD8a (53-6.7), anti-B220 (6B2), anti-Gr-1 (8C5), anti-Ter119), anti-Sca-1 (E13-161.7), anti-c-kit (2B8), anti-CD48 (HM48-1), anti-CD150 (TC15-12F12.2). Additionally, the following antibodies were used to perform hematopoietic progenitor staining as previously described[6]: lineage markers (anti-CD2 (RM2-5), anti-CD3 (17A2), anti-CD5 (53-7.3), anti-CD8a (53-6.7), anti-B220 (6B2), anti-Gr-1 (8C5), anti-Ter119), anti-Sca-1 (E13-161.7), anti-c-kit (2B8), anti-CD34 (RAM34), anti-FLT3 (A2F10), anti-CD16/32 (93), anti-IL7Rα (A7R34).

For flow cytometric analysis of stromal cells, bone marrow plugs were flushed as described above, then digested with collagenase IV (200 U/mL) and DNase1 (200 U/mL) at 37°C for 20min. Samples were then stained with anti-CD140a (APA-5), anti-CD45 (30F-11), and anti-Ter119 antibodies and analyzed by flow cytometry.

Methylcellulose culture

10,000 bone marrow cells or 100,000 spleen cells were plated in 1.5mL of methylcellulose culture medium (StemCell Technology) and incubated at 37°C for 12-15 days. Colonies were counted on an Olympus CKX41 microscope (Olympus Life Science).

Bone and liver sectioning

Freshly disassociated long bones were fixed for 3h in a solution of 4% paraformaldehyde, 7% picric acid, and 10% sucrose (W/V). The bones were then embedded in 8% gelatin, immediately snap frozen in liquid N_2, and stored at -80°C. Bones were sectioned using a CryoJane system

(Instrumedics). For liver, cardiac perfusion with formalin was performed immediately after mouse sacrifice, and perfused liver tissue was dehydrated in a 30% sucrose solution overnight at 4°C. Liver tissue was then placed in PELCO Cryo-Embedding compound (Ted Pella, Inc.), frozen on dry ice, and stored at -80°C. Liver tissue was sectioned and directly transferred onto microscope slides. Both bone and liver sections were dried overnight at room temperature and stored at -80°C.

Immunostaining

Bone and liver sections were rehydrated in PBS for 5min before immunostaining. 5% goat serum and 0.02% Triton X-100 in PBS was used to block the sections. Primary antibodies were applied to the slides overnight at 4°C, followed by secondary antibody incubation for 2h at RT with repetitive washes in-between. Slides were mounted with ProLong Gold anti-fade reagent (LifeTech) and images were acquired on a Nikon Eclipse Ti microscope (Nikon Instruments). Rabbit-anti-HNF4α (Abcam), rabbit-anti-laminin (Sigma) and rat-anti-CD41 (eBioscience) were used as primary antibodies.

qRT-PCR

Cells were sorted directly into Trizol. Total RNA was extracted according to manufacture's instructions. Total RNA was subjected to reverse transcription using SuperScript III (Invitrogen). Quantitative real-time PCR was run using SYBR green on a CFX Connect (Biorad) or a Stepone Plus (Invitrogen) system. β-actin was used to normalize the RNA content of samples. Primers used were: Tpo: OLD390, CCTTTGTCTATCCCTGTTCTGC and OLD391,

ACTGCCCCTAGAATGTCCTGT. β-actin: OLD27, 5'-GCTCTTTTCCAGCCTTCCTT-3' and OLD28, 5'-CTTCTGCATCCTGTCAGCAA-3'.

Cell cycle analysis

For BrdU incorporation analysis, mice were given an intraperitoneal injection of 0.1mg BrdU in water per g of body weight. Then the mice were maintained on 0.5mg/ml BRDU water for 5 days before the analysis. The frequency of $BrdU^+$ cells was determined by flow cytometry using an APC BrdU Flow Kit (BD Biosciences).

ACKNOWLEDGEMENTS

This work was supported by the Rita Allen Foundation and the National Heart, Lung and Blood Institute (R01HL132074). M.D. was supported by the Columbia Medical Scientist Training Program and the NIH (1F30HL137323). We thank V. Lin at the Columbia University transgenic core for helping to generate Tpo^{gfp} , Tpo^{CreER} and Tpo^{fl} mice. We thank S. Ho at Columbia Center for Translational Immunology, A. Figueroa at Department of Microbiology and Immunology, and M. Kissner at the Columbia Stem Cell Initiative for flow cytometry. Images were collected in the Confocal and Specialized Microscopy Shared Resource of the Herbert Irving Comprehensive Cancer Center at Columbia University, supported by NIH grant #P30 CA013696 (National Cancer Institute).

Chapter 4

General Discussion

Hematopoietic stem cells provide a reservoir of regenerative potential that helps the body endure the insults of trauma, disease, and age. Maintenance of a robust HSC population is therefore essential for a long and healthy life. This maintenance depends not only on cell-intrinsic homeostatic processes, but on the complex milieu of extrinsic cues that reinforce the internal programs of HSCs. The most well characterized components of this external regulatory network are in bone marrow microenvironment, where local paracrine signaling from a variety of cell populations drives HSC retention, self-renewal, and quiescence.

Changes to this local microenvironment can have a host of cascading pathologic effects. In Chapter 2, we found that inappropriate expansion of mature myeloid cells converts bone marrow stromal cells from their normal niche identity into a fibrogenic cell fate through PDGFR signaling. The disruption of the bone marrow caused by the combined stromal transformation and mature hematopoietic cell expansion leads to HSC dysfunction. This triad of clonal expansion, stromal transformation, and hematopoietic failure is seen in many human diseases. While most available clinical therapeutics targeting driver mutations of clonal expansion, niche-targeting therapies that block pathways such as PDGFR may also have a place in treatment regimens. It is important to note that while PDGFR signaling is necessary for robust induction of bone marrow fibrosis, it is not sufficient to drive severe pathological change. Further work is needed to elucidate other pathways that contribute to bone marrow fibrosis. Additional studies

could utilize targeted therapies with low side-effect profiles, such as monoclonal antibodies, to prevent signal transduction of niche-altering cues. In total the types of investigations described could significantly advance our understanding and treatment of chronic hematologic disease.

Although the bone marrow remains the center of much scientific and clinical interest, the essential role of extramedullary factors such as hepatocyte-derived thrombopoietin is shown in Chapter 3. The complete depletion of the body's HSC reserve after loss of a single circulating endocrine factor demonstrates a remarkably integrated regulatory program that governs a tissue-specific adult stem cell population. However, very little is known about the feedback mechanisms or pathways that allow organ systems such as the liver and the blood to coordinate HSC regulation, or if analogous mechanisms may maintain other adult stem cell populations. With the recent development of powerful genomic and proteomic screening techniques, the field has an opportunity to begin careful investigation into these questions. Our interest should not only be directed at steady-state biology, but also how these inter-organ relationships change in response to physiological challenge. In the case of the hematopoietic system, better understanding how common therapeutic modalities like chemotherapy and radiation affect HSC regulation has major implications for developing clinical guidelines and treatments.

Together the studies described in previous chapters have helped expand our understanding of the homeostatic and pathological extrinsic regulators of HSCs, and set the stage for exciting new basic and translational research in hematopoietic biology.

REFERENCES

Abdel-Wahab, O.I., and Levine, R.L. (2009). Primary myelofibrosis: update on definition, pathogenesis, and treatment. Annu. Rev. Med. *60*, 233–245.

Abkowitz, J.L., Golinelli, D., Harrison, D.E., and Guttorp, P. (2000). In vivo kinetics of murine hemopoietic stem cells. Blood *96*, 3399–3405.

Acar, M., Kocherlakota, K.S., Murphy, M.M., Peyer, J.G., Oguro, H., Inra, C.N., Jaiyeola, C., Zhao, Z., Luby-Phelps, K., and Morrison, S.J. (2015). Deep imaging of bone marrow shows non-dividing stem cells are mainly perisinusoidal. Nature *526*, 126–130.

Alexander, W.S., Roberts, A.W., Nicola, N.A., Li, R., and Metcalf, D. (1996). Deficiencies in progenitor cells of multiple hematopoietic lineages and defective megakaryocytopoiesis in mice lacking the thrombopoietic receptor c-Mpl. Blood *87*, 2162–2170.

Arai, F., Hirao, A., Ohmura, M., Sato, H., Matsuoka, S., Takubo, K., Ito, K., Koh, G.Y., and Suda, T. (2004). Tie2/Angiopoietin-1 Signaling Regulates Hematopoietic Stem Cell Quiescence in the Bone Marrow Niche. Cell *118*, 149–161.

Araki, M., Yang, Y., Masubuchi, N., Hironaka, Y., Takei, H., Morishita, S., Mizukami, Y., Kan, S., Shirane, S., Edahiro, Y., et al. (2016). Activation of the thrombopoietin receptor by mutant calreticulin in CALR-mutant myeloproliferative neoplasms. Blood *127*, 1307–1316.

Arranz, L., Sánchez-Aguilera, A., Martín-Pérez, D., Isern, J., Langa, X., Tzankov, A., Lundberg, P., Muntión, S., Tzeng, Y.-S., Lai, D.-M., et al. (2014). Neuropathy of haematopoietic stem cell niche is essential for myeloproliferative neoplasms. Nature *512*, 78–81.

Baldridge, M.T., King, K.Y., Boles, N.C., Weksberg, D.C., and Goodell, M.A. (2010). Quiescent haematopoietic stem cells are activated by IFN-γ in response to chronic infection. Nature *465*, 793–797.

Ballmaier, M., Germeshausen, M., Krukemeier, S., and Welte, K. (2003). Thrombopoietin is essential for the maintenance of normal hematopoiesis in humans: development of aplastic anemia in patients with congenital amegakaryocytic thrombocytopenia. Ann. N. Y. Acad. Sci. *996*, 17–25.

Becker, A.J., McCULLOCH, E.A., and Till, J.E. (1963). Cytological demonstration of the clonal nature of spleen colonies derived from transplanted mouse marrow cells. Nature *197*, 452–454.

Bertrand, J.Y., Chi, N.C., Santoso, B., Teng, S., Stainier, D.Y.R., and Traver, D. (2010). Hematopoietic stem cells derive directly from aortic endothelium during development. Nature *464*, 108–111.

Bihari, C., Anand, L., Rooge, S., Kumar, D., Saxena, P., Shubham, S., Sukriti, null, Trehanpati, N., Kumar, G., Pamecha, V., et al. (2016). Bone marrow stem cells and their niche components are adversely affected in advanced cirrhosis of the liver. Hepatology.

Boisset, J.-C., van Cappellen, W., Andrieu-Soler, C., Galjart, N., Dzierzak, E., and Robin, C. (2010). In vivo imaging of haematopoietic cells emerging from the mouse aortic endothelium. Nature *464*, 116–120.

Bonner, J.C. (2004). Regulation of PDGF and its receptors in fibrotic diseases. Cytokine Growth Factor Rev. *15*, 255–273.

Bromberg, O., Frisch, B.J., Weber, J.M., Porter, R.L., Civitelli, R., and Calvi, L.M. (2012). Osteoblastic N-cadherin is not required for microenvironmental support and regulation of hematopoietic stem and progenitor cells. Blood *120*, 303–313.

Broudy, V.C. (1997). Stem Cell Factor and Hematopoiesis. Blood *90*, 1345–1364.

Bruns, I., Lucas, D., Pinho, S., Ahmed, J., Lambert, M.P., Kunisaki, Y., Scheiermann, C., Schiff, L., Poncz, M., Bergman, A., et al. (2014). Megakaryocytes regulate hematopoietic stem cell quiescence through CXCL4 secretion. Nat Med *20*, 1315–1320.

Burberry, A., Zeng, M.Y., Ding, L., Wicks, I., Inohara, N., Morrison, S.J., and Núñez, G. (2014). Infection Mobilizes Hematopoietic Stem Cells through Cooperative NOD-like Receptor and Toll-like Receptor Signaling. Cell Host Microbe *15*, 779–791.

Butler, J.M., Nolan, D.J., Vertes, E.L., Varnum-Finney, B., Kobayashi, H., Hooper, A.T., Seandel, M., Shido, K., White, I.A., Kobayashi, M., et al. (2010). Endothelial Cells Are Essential for the Self-Renewal and Repopulation of Notch-Dependent Hematopoietic Stem Cells. Cell Stem Cell *6*, 251–264.

Calvi, L.M., Adams, G.B., Weibrecht, K.W., Weber, J.M., Olson, D.P., Knight, M.C., Martin, R.P., Schipani, E., Divieti, P., Bringhurst, F.R., et al. (2003). Osteoblastic cells regulate the haematopoietic stem cell niche. Nature *425*, 841–846.

Calvi, L.M., Bromberg, O., Rhee, Y., Weber, J.M., Smith, J.N.P., Basil, M.J., Frisch, B.J., and Bellido, T. (2012). Osteoblastic expansion induced by parathyroid hormone receptor signaling in murine osteocytes is not sufficient to increase hematopoietic stem cells. Blood *119*, 2489–2499.

Casanova-Acebes, M., Pitaval, C., Weiss, L.A., Nombela-Arrieta, C., Chèvre, R., A-González, N., Kunisaki, Y., Zhang, D., van Rooijen, N., Silberstein, L.E., et al. (2013). Rhythmic Modulation of the Hematopoietic Niche through Neutrophil Clearance. Cell *153*, 1025–1035.

Chachoua, I., Pecquet, C., El-Khoury, M., Nivarthi, H., Albu, R.-I., Marty, C., Gryshkova, V., Defour, J.-P., Vertenoeil, G., Ngo, A., et al. (2016). Thrombopoietin receptor activation by myeloproliferative neoplasm associated calreticulin mutants. Blood *127*, 1325–1335.

Chan, C.K.F., Chen, C.-C., Luppen, C.A., Kraft, D.L., Kim, J.-B., DeBoer, A., Wei, K., and Weissman, I.L. (2009). Endochondral ossification is required for hematopoietic stem cell niche formation. Nature *457*, 490–494.

Chen, J.Y., Miyanishi, M., Wang, S.K., Yamazaki, S., Sinha, R., Kao, K.S., Seita, J., Sahoo, D., Nakauchi, H., and Weissman, I.L. (2016). Hoxb5 marks long-term haematopoietic stem cells and reveals a homogenous perivascular niche. Nature *530*, 223–227.

Chow, A., Lucas, D., Hidalgo, A., Méndez-Ferrer, S., Hashimoto, D., Scheiermann, C., Battista, M., Leboeuf, M., Prophete, C., Rooijen, N. van, et al. (2011). Bone marrow CD169+ macrophages promote the retention of hematopoietic stem and progenitor cells in the mesenchymal stem cell niche. J Exp Med *208*, 261–271.

Colmone, A., Amorim, M., Pontier, A.L., Wang, S., Jablonski, E., and Sipkins, D.A. (2008). Leukemic cells create bone marrow niches that disrupt the behavior of normal hematopoietic progenitor cells. Science *322*, 1861–1865.

Conboy, I.M., Conboy, M.J., Wagers, A.J., Girma, E.R., Weissman, I.L., and Rando, T.A. (2005). Rejuvenation of aged progenitor cells by exposure to a young systemic environment. Nature *433*, 760–764.

Dasouki, M.J., Rafi, S.K., Olm-Shipman, A.J., Wilson, N.R., Abhyankar, S., Ganter, B., Furness, L.M., Fang, J., Calado, R.T., and Saadi, I. (2013). Exome sequencing reveals a thrombopoietin ligand mutation in a Micronesian family with autosomal recessive aplastic anemia. Blood *122*, 3440–3449.

De Minicis, S., Seki, E., Uchinami, H., Kluwe, J., Zhang, Y., Brenner, D.A., and Schwabe, R.F. (2007). Gene expression profiles during hepatic stellate cell activation in culture and in vivo. Gastroenterology *132*, 1937–1946.

DeFalco, J., Tomishima, M., Liu, H., Zhao, C., Cai, X., Marth, J.D., Enquist, L., and Friedman, J.M. (2001). Virus-assisted mapping of neural inputs to a feeding center in the hypothalamus. Science *291*, 2608–2613.

Ding, L., and Morrison, S.J. (2013). Haematopoietic stem cells and early lymphoid progenitors occupy distinct bone marrow niches. Nature *495*, 231–235.

Ding, L., Saunders, T.L., Enikolopov, G., and Morrison, S.J. (2012). Endothelial and perivascular cells maintain haematopoietic stem cells. Nature *481*, 457–462.

Doan, P.L., Himburg, H.A., Helms, K., Russell, J.L., Fixsen, E., Quarmyne, M., Harris, J.R., Deoliviera, D., Sullivan, J.M., Chao, N.J., et al. (2013). Epidermal Growth Factor Regulates Hematopoietic Regeneration Following Radiation Injury. Nat Med *19*, 295–304.

Dominici, M., Rasini, V., Bussolari, R., Chen, X., Hofmann, T.J., Spano, C., Bernabei, D., Veronesi, E., Bertoni, F., Paolucci, P., et al. (2009). Restoration and reversible expansion of the osteoblastic hematopoietic stem cell niche after marrow radioablation. Blood *114*, 2333–2343.

Ergen, A.V., Boles, N.C., and Goodell, M.A. (2012). Rantes/Ccl5 influences hematopoietic stem cell subtypes and causes myeloid skewing. Blood *119*, 2500–2509.

Essers, M.A.G., Offner, S., Blanco-Bose, W.E., Waibler, Z., Kalinke, U., Duchosal, M.A., and Trumpp, A. (2009). IFNα activates dormant haematopoietic stem cells in vivo. Nature *458*, 904–908.

Ford, C.E., Hamerton, J.L., Barnes, D.W., and Loutit, J.F. (1956). Cytological identification of radiation-chimaeras. Nature *177*, 452–454.

Fujisaki, J., Wu, J., Carlson, A.L., Silberstein, L., Putheti, P., Larocca, R., Gao, W., Saito, T.I., Celso, C.L., Tsuyuzaki, H., et al. (2011). In vivo imaging of Treg cells providing immune privilege to the haematopoietic stem-cell niche. Nature *474*, 216–219.

Geiger, H., de Haan, G., and Florian, M.C. (2013). The ageing haematopoietic stem cell compartment. Nat. Rev. Immunol. *13*, 376–389.

Gersuk, G.M., Carmel, R., and Pattengale, P.K. (1989). Platelet-derived growth factor concentrations in platelet-poor plasma and urine from patients with myeloproliferative disorders. Blood *74*, 2330–2334.

Ghilardi, N., Wiestner, A., and Skoda, R.C. (1998). Thrombopoietin Production Is Inhibited by a Translational Mechanism. Blood *92*, 4023–4030.

Goncalves, K.A., Silberstein, L., Li, S., Severe, N., Hu, M.G., Yang, H., Scadden, D.T., and Hu, G.-F. (2016). Angiogenin Promotes Hematopoietic Regeneration by Dichotomously Regulating Quiescence of Stem and Progenitor Cells. Cell *166*, 894–906.

Greenbaum, A., Hsu, Y.-M.S., Day, R.B., Schuettpelz, L.G., Christopher, M.J., Borgerding, J.N., Nagasawa, T., and Link, D.C. (2013). CXCL12 in early mesenchymal progenitors is required for haematopoietic stem-cell maintenance. Nature *495*, 227–230.

Grover, A., Mancini, E., Moore, S., Mead, A.J., Atkinson, D., Rasmussen, K.D., O'Carroll, D., Jacobsen, S.E.W., and Nerlov, C. (2014). Erythropoietin guides multipotent hematopoietic progenitor cells toward an erythroid fate. J Exp Med *211*, 181–188.

Grozovsky, R., Begonja, A.J., Liu, K., Visner, G., Hartwig, J.H., Falet, H., and Hoffmeister, K.M. (2015). The Ashwell-Morell receptor regulates hepatic thrombopoietin production via JAK2-STAT3 signaling. Nat. Med. *21*, 47–54.

Gurney, A.L., Carver-Moore, K., de Sauvage, F.J., and Moore, M.W. (1994). Thrombocytopenia in c-mpl-deficient mice. Science *265*, 1445–1447.

Hasselbalch, H.C., Bjerrum, O.W., Jensen, B.A., Clausen, N.T., Hansen, P.B., Birgens, H., Therkildsen, M.H., and Ralfkiaer, E. (2003). Imatinib mesylate in idiopathic and postpolycythemic myelofibrosis. Am. J. Hematol. *74*, 238–242.

He, S., Nakada, D., and Morrison, S.J. (2009). Mechanisms of stem cell self-renewal. Annu. Rev. Cell Dev. Biol. *25*, 377–406.

Himburg, H.A., Muramoto, G.G., Daher, P., Meadows, S.K., Russell, J.L., Doan, P., Chi, J.-T., Salter, A.B., Lento, W.E., Reya, T., et al. (2010). Pleiotrophin regulates the expansion and regeneration of hematopoietic stem cells. Nat Med *16*, 475–482.

Himburg, H.A., Harris, J.R., Ito, T., Daher, P., Russell, J.L., Quarmyne, M., Doan, P.L., Helms, K., Nakamura, M., Fixsen, E., et al. (2012). Pleiotrophin Regulates the Retention and Self-Renewal of Hematopoietic Stem Cells in the Bone Marrow Vascular Niche. Cell Reports *2*, 964–975.

Hoggatt, J., Kfoury, Y., and Scadden, D.T. (2016). Hematopoietic Stem Cell Niche in Health and Disease. Annu Rev Pathol *11*, 555–581.

Hooper, A.T., Butler, J.M., Nolan, D.J., Kranz, A., Iida, K., Kobayashi, M., Kopp, H.-G., Shido, K., Petit, I., Yanger, K., et al. (2009). Engraftment and Reconstitution of Hematopoiesis Is Dependent on VEGFR2-Mediated Regeneration of Sinusoidal Endothelial Cells. Cell Stem Cell *4*, 263–274.

Huang, D.W., Sherman, B.T., and Lempicki, R.A. (2009a). Bioinformatics enrichment tools: paths toward the comprehensive functional analysis of large gene lists. Nucleic Acids Res *37*, 1–13.

Huang, D.W., Sherman, B.T., and Lempicki, R.A. (2009b). Systematic and integrative analysis of large gene lists using DAVID bioinformatics resources. Nat Protoc *4*, 44–57.

Hur, J., Choi, J.-I., Lee, H., Nham, P., Kim, T.-W., Chae, C.-W., Yun, J.-Y., Kang, J.-A., Kang, J., Lee, S.E., et al. (2016). CD82/KAI1 Maintains the Dormancy of Long-Term Hematopoietic Stem Cells through Interaction with DARC-Expressing Macrophages. Cell Stem Cell *18*, 508–521.

Inra, C.N., Zhou, B.O., Acar, M., Murphy, M.M., Richardson, J., Zhao, Z., and Morrison, S.J. (2015). A perisinusoidal niche for extramedullary haematopoiesis in the spleen. Nature *527*, 466–471.

Itkin, T., Gur-Cohen, S., Spencer, J.A., Schajnovitz, A., Ramasamy, S.K., Kusumbe, A.P., Ledergor, G., Jung, Y., Milo, I., Poulos, M.G., et al. (2016). Distinct bone marrow blood vessels differentially regulate haematopoiesis. Nature *532*, 323–328.

Iwayama, T., Steele, C., Yao, L., Dozmorov, M.G., Karamichos, D., Wren, J.D., and Olson, L.E. (2015). PDGFRα signaling drives adipose tissue fibrosis by targeting progenitor cell plasticity. Genes Dev *29*, 1106–1119.

Jacobson, R.J., Salo, A., and Fialkow, P.J. (1978). Agnogenic myeloid metaplasia: a clonal proliferation of hematopoietic stem cells with secondary myelofibrosis. Blood *51*, 189–194.

Jang, Y.-Y., and Sharkis, S.J. (2007). A low level of reactive oxygen species selects for primitive hematopoietic stem cells that may reside in the low-oxygenic niche. Blood *110*, 3056–3063.

Jones, R.J., Wagner, J.E., Celano, P., Zicha, M.S., and Sharkis, S.J. (1990). Separation of pluripotent haematopoietic stem cells from spleen colony-forming cells. Nature *347*, 188–189.

Jones, R.J., Collector, M.I., Barber, J.P., Vala, M.S., Fackler, M.J., May, W.S., Griffin, C.A., Hawkins, A.L., Zehnbauer, B.A., Hilton, J., et al. (1996). Characterization of mouse lymphohematopoietic stem cells lacking spleen colony-forming activity. Blood *88*, 487–491.

Katayama, Y., Battista, M., Kao, W.-M., Hidalgo, A., Peired, A.J., Thomas, S.A., and Frenette, P.S. (2006). Signals from the Sympathetic Nervous System Regulate Hematopoietic Stem Cell Egress from Bone Marrow. Cell *124*, 407–421.

Kaushansky, K., Lok, S., Holly, R.D., Broudy, V.C., Lin, N., Bailey, M.C., Forstrom, J.W., Buddle, M.M., Oort, P.J., and Hagen, F.S. (1994). Promotion of megakaryocyte progenitor expansion and differentiation by the c-Mpl ligand thrombopoietin. Nature *369*, 568–571.

Kiel, M.J., Yilmaz, Ö.H., Iwashita, T., Yilmaz, O.H., Terhorst, C., and Morrison, S.J. (2005). SLAM Family Receptors Distinguish Hematopoietic Stem and Progenitor Cells and Reveal Endothelial Niches for Stem Cells. Cell *121*, 1109–1121.

Kiel, M.J., Acar, M., Radice, G.L., and Morrison, S.J. (2009). Hematopoietic Stem Cells Do Not Depend on N-Cadherin to Regulate Their Maintenance. Cell Stem Cell *4*, 170–179.

Kim, Y.-W., Koo, B.-K., Jeong, H.-W., Yoon, M.-J., Song, R., Shin, J., Jeong, D.-C., Kim, S.-H., and Kong, Y.-Y. (2008). Defective Notch activation in microenvironment leads to myeloproliferative disease. Blood *112*, 4628–4638.

Kimura, S., Roberts, A.W., Metcalf, D., and Alexander, W.S. (1998). Hematopoietic stem cell deficiencies in mice lacking c-Mpl, the receptor for thrombopoietin. PNAS *95*, 1195–1200.

Kissa, K., and Herbomel, P. (2010). Blood stem cells emerge from aortic endothelium by a novel type of cell transition. Nature *464*, 112–115.

Klampfl, T., Gisslinger, H., Harutyunyan, A.S., Nivarthi, H., Rumi, E., Milosevic, J.D., Them, N.C.C., Berg, T., Gisslinger, B., Pietra, D., et al. (2013). Somatic mutations of calreticulin in myeloproliferative neoplasms. N. Engl. J. Med. *369*, 2379–2390.

Kobayashi, H., Butler, J.M., O'Donnell, R., Kobayashi, M., Ding, B.-S., Bonner, B., Chiu, V.K., Nolan, D.J., Shido, K., Benjamin, L., et al. (2010). Angiocrine factors from Akt-activated endothelial cells balance self-renewal and differentiation of haematopoietic stem cells. Nat Cell Biol *12*, 1046–1056.

Kode, A., Manavalan, J.S., Mosialou, I., Bhagat, G., Rathinam, C.V., Luo, N., Khiabanian, H., Lee, A., Vundavalli, M., Friedman, R., et al. (2014). Leukemogenesis Induced by an Activating β-catenin mutation in Osteoblasts. Nature *506*, 240–244.

Komada, Y., Yamane, T., Kadota, D., Isono, K., Takakura, N., Hayashi, S.-I., and Yamazaki, H. (2012). Origins and Properties of Dental, Thymic, and Bone Marrow Mesenchymal Cells and Their Stem Cells. PLoS One *7*.

Kramann, R., Schneider, R.K., DiRocco, D.P., Machado, F., Fleig, S., Bondzie, P.A., Henderson, J.M., Ebert, B.L., and Humphreys, B.D. (2015). Perivascular Gli1+ progenitors are key contributors to injury-induced organ fibrosis. Cell Stem Cell *16*, 51–66.

Kunisaki, Y., Bruns, I., Scheiermann, C., Ahmed, J., Pinho, S., Zhang, D., Mizoguchi, T., Wei, Q., Lucas, D., Ito, K., et al. (2013). Arteriolar niches maintain haematopoietic stem cell quiescence. Nature *502*, 637–643.

Kusumbe, A.P., Ramasamy, S.K., Itkin, T., Mäe, M.A., Langen, U.H., Betsholtz, C., Lapidot, T., and Adams, R.H. (2016). Age-dependent modulation of vascular niches for haematopoietic stem cells. Nature *532*, 380–384.

Lakso, M., Pichel, J.G., Gorman, J.R., Sauer, B., Okamoto, Y., Lee, E., Alt, F.W., and Westphal, H. (1996). Efficient in vivo manipulation of mouse genomic sequences at the zygote stage. Proc. Natl. Acad. Sci. U.S.A. *93*, 5860–5865.

Lassila, O., Eskola, J., Toivanen, P., Martin, C., and Dieterlen-Lievre, F. (1978). The origin of lymphoid stem cells studied in chick yold sac-embryo chimaeras. Nature *272*, 353–354.

Lataillade, J.-J., Pierre-Louis, O., Hasselbalch, H.C., Uzan, G., Jasmin, C., Martyré, M.-C., Le Bousse-Kerdilès, M.-C., and French INSERM and the European EUMNET Networks on Myelofibrosis (2008). Does primary myelofibrosis involve a defective stem cell niche? From concept to evidence. Blood *112*, 3026–3035.

Li, X., and Slayton, W.B. (2013). Molecular mechanisms of platelet and stem cell rebound after 5-fluorouracil treatment. Experimental Hematology *41*, 635-645.e3.

Liang, Y., Van Zant, G., and Szilvassy, S.J. (2005). Effects of aging on the homing and engraftment of murine hematopoietic stem and progenitor cells. Blood *106*, 1479–1487.

Lin, S.-L., Kisseleva, T., Brenner, D.A., and Duffield, J.S. (2008). Pericytes and Perivascular Fibroblasts Are the Primary Source of Collagen-Producing Cells in Obstructive Fibrosis of the Kidney. Am J Pathol *173*, 1617–1627.

Liu, F., Woitge, H.W., Braut, A., Kronenberg, M.S., Lichtler, A.C., Mina, M., and Kream, B.E. (2004). Expression and activity of osteoblast-targeted Cre recombinase transgenes in murine skeletal tissues. Int. J. Dev. Biol. *48*, 645–653.

Liu, P., Jenkins, N.A., and Copeland, N.G. (2003). A highly efficient recombineering-based method for generating conditional knockout mutations. Genome Res. *13*, 476–484.

Lo Celso, C., Fleming, H.E., Wu, J.W., Zhao, C.X., Miake-Lye, S., Fujisaki, J., Côté, D., Rowe, D.W., Lin, C.P., and Scadden, D.T. (2009). Live-animal tracking of individual haematopoietic stem/progenitor cells in their niche. Nature *457*, 92–96.

Lok, S., Kaushansky, K., Holly, R.D., Kuijper, J.L., Lofton-Day, C.E., Oort, P.J., Grant, F.J., Heipel, M.D., Burkhead, S.K., and Kramer, J.M. (1994). Cloning and expression of murine thrombopoietin cDNA and stimulation of platelet production in vivo. Nature *369*, 565–568.

Lord, B.I., Testa, N.G., and Hendry, J.H. (1975). The relative spatial distributions of CFUs and CFUc in the normal mouse femur. Blood *46*, 65–72.

Losick, V.P., Morris, L.X., Fox, D.T., and Spradling, A. (2011). Drosophila stem cell niches: a decade of discovery suggests a unified view of stem cell regulation. Dev. Cell *21*, 159–171.

Lucas, D., Battista, M., Shi, P.A., Isola, L., and Frenette, P.S. (2008). Mobilized Hematopoietic Stem Cell Yield Depends on Species-Specific Circadian Timing. Cell Stem Cell *3*, 364–366.

Lundberg, P., Takizawa, H., Kubovcakova, L., Guo, G., Hao-Shen, H., Dirnhofer, S., Orkin, S.H., Manz, M.G., and Skoda, R.C. (2014). Myeloproliferative neoplasms can be initiated from a single hematopoietic stem cell expressing JAK2-V617F. J Exp Med *211*, 2213–2230.

Lv, B., Zhao, H., Bai, X., Huang, S., Fan, Z., Lu, J., Tang, R., Yin, K., Gao, P., Liu, B., et al. (2014). Entecavir promotes $CD34^+$ stem cell proliferation in the peripheral blood and liver of chronic hepatitis B and liver cirrhosis patients. Discov Med *18*, 227–236.

Lydon, N.B., and Druker, B.J. (2004). Lessons learned from the development of imatinib. Leuk. Res. *28 Suppl 1*, S29-38.

Lymperi, S., Horwood, N., Marley, S., Gordon, M.Y., Cope, A.P., and Dazzi, F. (2008). Strontium can increase some osteoblasts without increasing hematopoietic stem cells. Blood *111*, 1173–1181.

Madisen, L., Zwingman, T.A., Sunkin, S.M., Oh, S.W., Zariwala, H.A., Gu, H., Ng, L.L., Palmiter, R.D., Hawrylycz, M.J., Jones, A.R., et al. (2010). A robust and high-throughput Cre reporting and characterization system for the whole mouse brain. Nat Neurosci *13*, 133–140.

Maillard, I., Koch, U., Dumortier, A., Shestova, O., Xu, L., Sai, H., Pross, S.E., Aster, J.C., Bhandoola, A., Radtke, F., et al. (2008). Canonical Notch Signaling Is Dispensable for the Maintenance of Adult Hematopoietic Stem Cells. Cell Stem Cell *2*, 356–366.

Mantel, C.R., O'Leary, H.A., Chitteti, B.R., Huang, X., Cooper, S., Hangoc, G., Brustovetsky, N., Srour, E.F., Lee, M.R., Messina-Graham, S., et al. (2015). Enhancing Hematopoietic Stem Cell Transplantation Efficacy by Mitigating Oxygen Shock. Cell *161*, 1553–1565.

Marty, C., Pecquet, C., Nivarthi, H., El-Khoury, M., Chachoua, I., Tulliez, M., Villeval, J.-L., Raslova, H., Kralovics, R., Constantinescu, S.N., et al. (2016). Calreticulin mutants in mice induce an MPL-dependent thrombocytosis with frequent progression to myelofibrosis. Blood *127*, 1317–1324.

McIntosh, B., and Kaushansky, K. (2008). TRANSCRIPTIONAL REGULATION OF BONE MARROW THROMBOPOIETIN BY PLATELET PROTEINS. Exp Hematol *36*, 799–806.

Mederacke, I., Hsu, C.C., Troeger, J.S., Huebener, P., Mu, X., Dapito, D.H., Pradere, J.-P., and Schwabe, R.F. (2013). Fate-tracing reveals hepatic stellate cells as dominant contributors to liver fibrosis independent of its etiology. Nat Commun *4*, 2823.

Medyouf, H., Mossner, M., Jann, J.-C., Nolte, F., Raffel, S., Herrmann, C., Lier, A., Eisen, C., Nowak, V., Zens, B., et al. (2014). Myelodysplastic cells in patients reprogram mesenchymal stromal cells to establish a transplantable stem cell niche disease unit. Cell Stem Cell *14*, 824–837.

Mendelson, A., and Frenette, P.S. (2014). Hematopoietic stem cell niche maintenance during homeostasis and regeneration. Nat Med *20*, 833–846.

Méndez-Ferrer, S., Lucas, D., Battista, M., and Frenette, P.S. (2008). Haematopoietic stem cell release is regulated by circadian oscillations. Nature *452*, 442–447.

Méndez-Ferrer, S., Michurina, T.V., Ferraro, F., Mazloom, A.R., MacArthur, B.D., Lira, S.A., Scadden, D.T., Ma'ayan, A., Enikolopov, G.N., and Frenette, P.S. (2010). Mesenchymal and haematopoietic stem cells form a unique bone marrow niche. Nature *466*, 829–834.

Miharada, K., Karlsson, G., Rehn, M., Rörby, E., Siva, K., Cammenga, J., and Karlsson, S. (2011). Cripto Regulates Hematopoietic Stem Cells as a Hypoxic-Niche-Related Factor through Cell Surface Receptor GRP78. Cell Stem Cell *9*, 330–344.

Mikkola, H.K.A., and Orkin, S.H. (2006). The journey of developing hematopoietic stem cells. Development *133*, 3733–3744.

Mootha, V.K., Lindgren, C.M., Eriksson, K.-F., Subramanian, A., Sihag, S., Lehar, J., Puigserver, P., Carlsson, E., Ridderstråle, M., Laurila, E., et al. (2003). PGC-1alpha-responsive genes involved in oxidative phosphorylation are coordinately downregulated in human diabetes. Nat. Genet. *34*, 267–273.

Morikawa, S., Mabuchi, Y., Kubota, Y., Nagai, Y., Niibe, K., Hiratsu, E., Suzuki, S., Miyauchi-Hara, C., Nagoshi, N., Sunabori, T., et al. (2009). Prospective identification, isolation, and systemic transplantation of multipotent mesenchymal stem cells in murine bone marrow. J Exp Med *206*, 2483–2496.

Morrison, S.J., and Scadden, D.T. (2014). The bone marrow niche for haematopoietic stem cells. Nature *505*, 327–334.

Nakada, D., Oguro, H., Levi, B.P., Ryan, N., Kitano, A., Saitoh, Y., Takeichi, M., Wendt, G.R., and Morrison, S.J. (2014). Estrogen increases haematopoietic stem cell self-renewal in females and during pregnancy. Nature *505*, 555–558.

Nakamura-Ishizu, A., Takubo, K., Fujioka, M., and Suda, T. (2014). Megakaryocytes are essential for HSC quiescence through the production of thrombopoietin. Biochemical and Biophysical Research Communications *454*, 353–357.

Nakamura-Ishizu, A., Takubo, K., Kobayashi, H., Suzuki-Inoue, K., and Suda, T. (2015). CLEC-2 in megakaryocytes is critical for maintenance of hematopoietic stem cells in the bone marrow. J Exp Med *212*, 2133–2146.

Nangalia, J., Massie, C.E., Baxter, E.J., Nice, F.L., Gundem, G., Wedge, D.C., Avezov, E., Li, J., Kollmann, K., Kent, D.G., et al. (2013). Somatic CALR Mutations in Myeloproliferative Neoplasms with Nonmutated JAK2. N Engl J Med *369*, 2391–2405.

Naveiras, O., Nardi, V., Wenzel, P.L., Hauschka, P.V., Fahey, F., and Daley, G.Q. (2009). Bone-marrow adipocytes as negative regulators of the haematopoietic microenvironment. Nature *460*, 259–263.

Nombela-Arrieta, C., Pivarnik, G., Winkel, B., Canty, K.J., Harley, B., Mahoney, J.E., Park, S.-Y., Lu, J., Protopopov, A., and Silberstein, L.E. (2013). Quantitative imaging of haematopoietic stem and progenitor cell localization and hypoxic status in the bone marrow microenvironment. Nat Cell Biol *15*, 533–543.

Oguro, H., Ding, L., and Morrison, S.J. (2013). SLAM Family Markers Resolve Functionally Distinct Subpopulations of Hematopoietic Stem Cells and Multipotent Progenitors. Cell Stem Cell *13*, 102–116.

Olson, L.E., and Soriano, P. (2009). Increased PDGFRα Activation Disrupts Connective Tissue Development and Drives Systemic Fibrosis. Dev Cell *16*, 303–313.

Olson, T.S., Caselli, A., Otsuru, S., Hofmann, T.J., Williams, R., Paolucci, P., Dominici, M., and Horwitz, E.M. (2013). Megakaryocytes promote murine osteoblastic HSC niche expansion and stem cell engraftment after radioablative conditioning. Blood *121*, 5238–5249.

Omatsu, Y., Sugiyama, T., Kohara, H., Kondoh, G., Fujii, N., Kohno, K., and Nagasawa, T. (2010). The essential functions of adipo-osteogenic progenitors as the hematopoietic stem and progenitor cell niche. Immunity *33*, 387–399.

Omatsu, Y., Seike, M., Sugiyama, T., Kume, T., and Nagasawa, T. (2014). Foxc1 is a critical regulator of haematopoietic stem/progenitor cell niche formation. Nature *508*, 536–540.

Osawa, M., Hanada, K., Hamada, H., and Nakauchi, H. (1996). Long-Term Lymphohematopoietic Reconstitution by a Single CD34-Low/Negative Hematopoietic Stem Cell. Science *273*, 242–245.

Papadantonakis, N., Matsuura, S., and Ravid, K. (2012). Megakaryocyte pathology and bone marrow fibrosis: the lysyl oxidase connection. Blood *120*, 1774–1781.

Parmar, K., Mauch, P., Vergilio, J.-A., Sackstein, R., and Down, J.D. (2007). Distribution of hematopoietic stem cells in the bone marrow according to regional hypoxia. PNAS *104*, 5431–5436.

Pinho, S., Lacombe, J., Hanoun, M., Mizoguchi, T., Bruns, I., Kunisaki, Y., and Frenette, P.S. (2013). PDGFRα and CD51 mark human Nestin+ sphere-forming mesenchymal stem cells capable of hematopoietic progenitor cell expansion. J Exp Med *210*, 1351–1367.

Postic, C., Shiota, M., Niswender, K.D., Jetton, T.L., Chen, Y., Moates, J.M., Shelton, K.D., Lindner, J., Cherrington, A.D., and Magnuson, M.A. (1999). Dual roles for glucokinase in

glucose homeostasis as determined by liver and pancreatic beta cell-specific gene knock-outs using Cre recombinase. J. Biol. Chem. *274*, 305–315.

Poulos, M.G., Guo, P., Kofler, N.M., Pinho, S., Gutkin, M.C., Tikhonova, A., Aifantis, I., Frenette, P.S., Kitajewski, J., Rafii, S., et al. (2013). Endothelial Jagged-1 is necessary for homeostatic and regenerative hematopoiesis. Cell Rep *4*, 1022–1034.

Qian, H., Buza-Vidas, N., Hyland, C.D., Jensen, C.T., Antonchuk, J., Månsson, R., Thoren, L.A., Ekblom, M., Alexander, W.S., and Jacobsen, S.E.W. (2007). Critical Role of Thrombopoietin in Maintaining Adult Quiescent Hematopoietic Stem Cells. Cell Stem Cell *1*, 671–684.

Qian, S., Fu, F., Li, W., Chen, Q., and Sauvage, F.J. de (1998). Primary Role of the Liver in Thrombopoietin Production Shown by Tissue-Specific Knockout. Blood *92*, 2189–2191.

Raaijmakers, M.H.G.P., Mukherjee, S., Guo, S., Zhang, S., Kobayashi, T., Schoonmaker, J.A., Ebert, B.L., Al-Shahrour, F., Hasserjian, R.P., Scadden, E.O., et al. (2010). Bone progenitor dysfunction induces myelodysplasia and secondary leukaemia. Nature *464*, 852–857.

Rampal, R., Al-Shahrour, F., Abdel-Wahab, O., Patel, J.P., Brunel, J.-P., Mermel, C.H., Bass, A.J., Pretz, J., Ahn, J., Hricik, T., et al. (2014). Integrated genomic analysis illustrates the central role of JAK-STAT pathway activation in myeloproliferative neoplasm pathogenesis. Blood *123*, e123–e133.

Rashidi, A., and DiPersio, J.F. (2016). Targeting the leukemia–stroma interaction in acute myeloid leukemia: rationale and latest evidence. Ther Adv Hematol *7*, 40–51.

Reilly, J.T., McMullin, M.F., Beer, P.A., Butt, N., Conneally, E., Duncombe, A., Green, A.R., Michaeel, N.G., Gilleece, M.H., Hall, G.W., et al. (2012). Guideline for the diagnosis and management of myelofibrosis. Br. J. Haematol. *158*, 453–471.

Riether, C., Schürch, C.M., and Ochsenbein, A.F. (2015). Regulation of hematopoietic and leukemic stem cells by the immune system. Cell Death Differ *22*, 187–198.

Roberts, E.W., Deonarine, A., Jones, J.O., Denton, A.E., Feig, C., Lyons, S.K., Espeli, M., Kraman, M., McKenna, B., Wells, R.J.B., et al. (2013). Depletion of stromal cells expressing fibroblast activation protein-α from skeletal muscle and bone marrow results in cachexia and anemia. J Exp Med *210*, 1137–1151.

Rupec, R.A., Jundt, F., Rebholz, B., Eckelt, B., Weindl, G., Herzinger, T., Flaig, M.J., Moosmann, S., Plewig, G., Dörken, B., et al. (2005). Stroma-mediated dysregulation of myelopoiesis in mice lacking I kappa B alpha. Immunity *22*, 479–491.

Sacchetti, B., Funari, A., Michienzi, S., Cesare, S.D., Piersanti, S., Saggio, I., Tagliafico, E., Ferrari, S., Robey, P.G., Riminucci, M., et al. (2008). Self-Renewing Osteoprogenitors in Bone Marrow Sinusoids Can Organize a Hematopoietic Microenvironment. Cell *133*, 928.

de Sauvage, F.J., Hass, P.E., Spencer, S.D., Malloy, B.E., Gurney, A.L., Spencer, S.A., Darbonne, W.C., Henzel, W.J., Wong, S.C., and Kuang, W.J. (1994). Stimulation of megakaryocytopoiesis and thrombopoiesis by the c-Mpl ligand. Nature *369*, 533–538.

Sawai, C.M., Babovic, S., Upadhaya, S., Knapp, D.J.H.F., Lavin, Y., Lau, C.M., Goloborodko, A., Feng, J., Fujisaki, J., Ding, L., et al. (2016). Hematopoietic stem cells are the major source of multilineage hematopoiesis in adult animals. Immunity *45*, 597–609.

Scadden, D.T. (2014). Nice neighborhood: emerging concepts of the stem cell niche. Cell *157*, 41–50.

Schepers, K., Pietras, E.M., Reynaud, D., Flach, J., Binnewies, M., Garg, T., Wagers, A.J., Hsiao, E.C., and Passegué, E. (2013). Myeloproliferative Neoplasia Remodels the Endosteal Bone Marrow Niche into a Self-Reinforcing Leukemic Niche. Cell Stem Cell *13*, 285–299.

Schepers, K., Campbell, T.B., and Passegué, E. (2015). Normal and Leukemic Stem Cell Niches: Insights and Therapeutic Opportunities. Cell Stem Cell *16*, 254–267.

Schofield, R. (1978). The relationship between the spleen colony-forming cell and the haemopoietic stem cell. Blood Cells *4*, 7–25.

Schürch, C.M., Riether, C., and Ochsenbein, A.F. (2014). Cytotoxic CD8+ T Cells Stimulate Hematopoietic Progenitors by Promoting Cytokine Release from Bone Marrow Mesenchymal Stromal Cells. Cell Stem Cell *14*, 460–472.

Seo, A., Ben-Harosh, M., Sirin, M., Stein, J., Dgany, O., Kaplelushnik, J., Hoenig, M., Pannicke, U., Lorenz, M., Schwarz, K., et al. (2017). Bone marrow failure unresponsive to bone marrow transplant is caused by mutations in thrombopoietin. Blood *130*, 875–880.

Sharov, A.A., Dudekula, D.B., and Ko, M.S.H. (2005). A web-based tool for principal component and significance analysis of microarray data. Bioinformatics *21*, 2548–2549.

Shim, J., Mukherjee, T., Mondal, B.C., Liu, T., Young, G.C., Wijewarnasuriya, D.P., and Banerjee, U. (2013). Olfactory control of blood progenitor maintenance. Cell *155*.

Shivdasani, R.A., Fujiwara, Y., McDevitt, M.A., and Orkin, S.H. (1997). A lineage-selective knockout establishes the critical role of transcription factor GATA-1 in megakaryocyte growth and platelet development. EMBO J *16*, 3965–3973.

Signer, R.A.J., and Morrison, S.J. (2013). Mechanisms that Regulate Stem Cell Aging and Life Span. Cell Stem Cell *12*, 152–165.

Silberstein, L., Goncalves, K.A., Kharchenko, P.V., Turcotte, R., Kfoury, Y., Mercier, F., Baryawno, N., Severe, N., Bachand, J., Spencer, J.A., et al. (2016). Proximity-Based Differential Single-Cell Analysis of the Niche to Identify Stem/Progenitor Cell Regulators. Cell Stem Cell.

Simsek, T., Kocabas, F., Zheng, J., DeBerardinis, R.J., Mahmoud, A.I., Olson, E.N., Schneider, J.W., Zhang, C.C., and Sadek, H.A. (2010). The Distinct Metabolic Profile of Hematopoietic Stem Cells Reflects Their Location in a Hypoxic Niche. Cell Stem Cell *7*, 380–390.

Sipkins, D.A., Wei, X., Wu, J.W., Runnels, J.M., Côté, D., Means, T.K., Luster, A.D., Scadden, D.T., and Lin, C.P. (2005). In vivo imaging of specialized bone marrow endothelial microdomains for tumour engraftment. Nature *435*, 969–973.

Smith-Berdan, S., Nguyen, A., Hassanein, D., Zimmer, M., Ugarte, F., Ciriza, J., Li, D., García-Ojeda, M.E., Hinck, L., and Forsberg, E.C. (2011). Robo4 Cooperates with Cxcr4 to Specify Hematopoietic Stem Cell Localization to Bone Marrow Niches. Cell Stem Cell *8*, 72–83.

Smith-Berdan, S., Nguyen, A., Hong, M.A., and Forsberg, E.C. (2015). ROBO4-Mediated Vascular Integrity Regulates the Directionality of Hematopoietic Stem Cell Trafficking. Stem Cell Reports *4*, 255–268.

Song, J., Kiel, M.J., Wang, Z., Wang, J., Taichman, R.S., Morrison, S.J., and Krebsbach, P.H. (2010). An in vivo model to study and manipulate the hematopoietic stem cell niche. Blood *115*, 2592–2600.

Spencer, J.A., Ferraro, F., Roussakis, E., Klein, A., Wu, J., Runnels, J.M., Zaher, W., Mortensen, L.J., Alt, C., Turcotte, R., et al. (2014). Direct measurement of local oxygen concentration in the bone marrow of live animals. Nature *508*, 269–273.

Spiegel, A., Shivtiel, S., Kalinkovich, A., Ludin, A., Netzer, N., Goichberg, P., Azaria, Y., Resnick, I., Hardan, I., Ben-Hur, H., et al. (2007). Catecholaminergic neurotransmitters regulate migration and repopulation of immature human CD34+ cells through Wnt signaling. Nat Immunol *8*, 1123–1131.

Subramanian, A., Tamayo, P., Mootha, V.K., Mukherjee, S., Ebert, B.L., Gillette, M.A., Paulovich, A., Pomeroy, S.L., Golub, T.R., Lander, E.S., et al. (2005). Gene set enrichment analysis: A knowledge-based approach for interpreting genome-wide expression profiles. Proc Natl Acad Sci U S A *102*, 15545–15550.

Sugimura, R., He, X.C., Venkatraman, A., Arai, F., Box, A., Semerad, C., Haug, J.S., Peng, L., Zhong, X., Suda, T., et al. (2012). Noncanonical Wnt Signaling Maintains Hematopoietic Stem Cells in the Niche. Cell *150*, 351–365.

Sugiyama, T., Kohara, H., Noda, M., and Nagasawa, T. (2006). Maintenance of the hematopoietic stem cell pool by CXCL12-CXCR4 chemokine signaling in bone marrow stromal cell niches. Immunity *25*, 977–988.

Sungaran, R., Markovic, B., and Chong, B.H. (1997). Localization and Regulation of Thrombopoietin mRNA Expression in Human Kidney, Liver, Bone Marrow, and Spleen Using In Situ Hybridization. Blood *89*, 101–107.

Taichman, R.S., and Emerson, S.G. (1994). Human osteoblasts support hematopoiesis through the production of granulocyte colony-stimulating factor. J Exp Med *179*, 1677–1682.

Takubo, K., Goda, N., Yamada, W., Iriuchishima, H., Ikeda, E., Kubota, Y., Shima, H., Johnson, R.S., Hirao, A., Suematsu, M., et al. (2010). Regulation of the HIF-1α Level Is Essential for Hematopoietic Stem Cells. Cell Stem Cell *7*, 391–402.

Tallquist, M.D., and Soriano, P. (2003). Cell autonomous requirement for PDGFRalpha in populations of cranial and cardiac neural crest cells. Development *130*, 507–518.

Tefferi, A. (2005). Pathogenesis of myelofibrosis with myeloid metaplasia. J. Clin. Oncol. *23*, 8520–8530.

Tefferi, A. (2016). Myeloproliferative neoplasms: A decade of discoveries and treatment advances. Am. J. Hematol. *91*, 50–58.

Tefferi, A., Mesa, R.A., Gray, L.A., Steensma, D.P., Camoriano, J.K., Elliott, M.A., Pardanani, A., Ansell, S.M., Call, T.G., Colon-Otero, G., et al. (2002). Phase 2 trial of imatinib mesylate in myelofibrosis with myeloid metaplasia. Blood *99*, 3854–3856.

Till, J.E., and McCulloch, E.A. (1961). A Direct Measurement of the Radiation Sensitivity of Normal Mouse Bone Marrow Cells. Radiation Research *14*, 213–222.

Tran, E., Chinnasamy, D., Yu, Z., Morgan, R.A., Lee, C.-C.R., Restifo, N.P., and Rosenberg, S.A. (2013). Immune targeting of fibroblast activation protein triggers recognition of multipotent bone marrow stromal cells and cachexia. J Exp Med *210*, 1125–1135.

Vannucchi, A.M., Bianchi, L., Cellai, C., Paoletti, F., Rana, R.A., Lorenzini, R., Migliaccio, G., and Migliaccio, A.R. (2002). Development of myelofibrosis in mice genetically impaired for GATA-1 expression (GATA-1(low) mice). Blood *100*, 1123–1132.

Villeda, S.A., Luo, J., Mosher, K.I., Zou, B., Britschgi, M., Bieri, G., Stan, T.M., Fainberg, N., Ding, Z., Eggel, A., et al. (2011). The aging systemic milieu negatively regulates neurogenesis and cognitive function. Nature *477*, 90–94.

Villeval, J.L., Cohen-Solal, K., Tulliez, M., Giraudier, S., Guichard, J., Burstein, S.A., Cramer, E.M., Vainchenker, W., and Wendling, F. (1997). High thrombopoietin production by hematopoietic cells induces a fatal myeloproliferative syndrome in mice. Blood *90*, 4369–4383.

Visnjic, D., Kalajzic, Z., Rowe, D.W., Katavic, V., Lorenzo, J., and Aguila, H.L. (2004). Hematopoiesis is severely altered in mice with an induced osteoblast deficiency. Blood *103*, 3258–3264.

Vukovic, M., Sepulveda, C., Subramani, C., Guitart, A.V., Mohr, J., Allen, L., Panagopoulou, T.I., Paris, J., Lawson, H., Villacreces, A., et al. (2016). Adult haematopoietic stem cells lacking Hif-1α self-renew normally. Blood blood-2015-10-677138.

Walkley, C.R., Olsen, G.H., Dworkin, S., Fabb, S.A., Swann, J., McArthur, G.A., Westmoreland, S.V., Chambon, P., Scadden, D.T., and Purton, L.E. (2007a). A Microenvironment-Induced Myeloproliferative Syndrome Caused by RARγ Deficiency. Cell *129*, 1097–1110.

Walkley, C.R., Shea, J.M., Sims, N.A., Purton, L.E., and Orkin, S.H. (2007b). pRb Extrinsically Regulates Hematopoietic Stem Cells via Myeloid Cell -Bone Marrow Microenvironment Interactions. Cell *129*, 1081–1095.

Wang, L., Benedito, R., Bixel, M.G., Zeuschner, D., Stehling, M., Sävendahl, L., Haigh, J.J., Snippert, H., Clevers, H., Breier, G., et al. (2013). Identification of a clonally expanding haematopoietic compartment in bone marrow. EMBO J *32*, 219–230.

Wang, L., Zhang, H., Rodriguez, S., Cao, L., Parish, J., Mumaw, C., Zollman, A., Kamocka, G., Mu, J., Chen, D.Z., et al. (2014). Notch-dependent repression of miR-155 in the bone marrow niche regulates hematopoiesis in an NF-κB dependent manner. Cell Stem Cell *15*, 51–65.

Weisend, C.M., Kundert, J.A., Suvorova, E.S., Prigge, J.R., and Schmidt, E.E. (2009). Cre activity in fetal albCre mouse hepatocytes: Utility for developmental studies. Genesis *47*, 789–792.

Weissman, I.L., and Shizuru, J.A. (2008). The origins of the identification and isolation of hematopoietic stem cells, and their capability to induce donor-specific transplantation tolerance and treat autoimmune diseases. Blood *112*, 3543–3553.

Wen, Q.J., Yang, Q., Goldenson, B., Malinge, S., Lasho, T., Schneider, R.K., Breyfogle, L.J., Schultz, R., Gilles, L., Koppikar, P., et al. (2015). Targeting megakaryocytic induced fibrosis by AURKA inhibition in the myeloproliferative neoplasms. Nat Med *21*, 1473–1480.

Winkler, I.G., Sims, N.A., Pettit, A.R., Barbier, V., Nowlan, B., Helwani, F., Poulton, I.J., Rooijen, N. van, Alexander, K.A., Raggatt, L.J., et al. (2010). Bone marrow macrophages maintain hematopoietic stem cell (HSC) niches and their depletion mobilizes HSCs. Blood *116*, 4815–4828.

Worthley, D.L., Churchill, M., Compton, J.T., Tailor, Y., Rao, M., Si, Y., Levin, D., Schwartz, M.G., Uygur, A., Hayakawa, Y., et al. (2015). Gremlin 1 Identifies a Skeletal Stem Cell with Bone, Cartilage, and Reticular Stromal Potential. Cell *160*, 269–284.

Xie, Y., Yin, T., Wiegraebe, W., He, X.C., Miller, D., Stark, D., Perko, K., Alexander, R., Schwartz, J., Grindley, J.C., et al. (2009). Detection of functional haematopoietic stem cell niche using real-time imaging. Nature *457*, 97–101.

Yamazaki, S., Ema, H., Karlsson, G., Yamaguchi, T., Miyoshi, H., Shioda, S., Taketo, M.M., Karlsson, S., Iwama, A., and Nakauchi, H. (2011). Nonmyelinating Schwann Cells Maintain Hematopoietic Stem Cell Hibernation in the Bone Marrow Niche. Cell *147*, 1146–1158.

Yan, X.Q., Lacey, D., Fletcher, F., Hartley, C., McElroy, P., Sun, Y., Xia, M., Mu, S., Saris, C., Hill, D., et al. (1995). Chronic exposure to retroviral vector encoded MGDF (mpl-ligand) induces lineage-specific growth and differentiation of megakaryocytes in mice. Blood *86*, 4025–4033.

Yanger, K., Zong, Y., Maggs, L.R., Shapira, S.N., Maddipati, R., Aiello, N.M., Thung, S.N., Wells, R.G., Greenbaum, L.E., and Stanger, B.Z. (2013). Robust cellular reprogramming occurs spontaneously during liver regeneration. Genes Dev. *27*, 719–724.

Yao, L., Yokota, T., Xia, L., Kincade, P.W., and McEver, R.P. (2005). Bone marrow dysfunction in mice lacking the cytokine receptor gp130 in endothelial cells. Blood *106*, 4093–4101.

Yata, Y., Scanga, A., Gillan, A., Yang, L., Reif, S., Breindl, M., Brenner, D.A., and Rippe, R.A. (2003). DNase I-hypersensitive sites enhance alpha1(I) collagen gene expression in hepatic stellate cells. Hepatology *37*, 267–276.

Yoshihara, H., Arai, F., Hosokawa, K., Hagiwara, T., Takubo, K., Nakamura, Y., Gomei, Y., Iwasaki, H., Matsuoka, S., Miyamoto, K., et al. (2007). Thrombopoietin/MPL Signaling Regulates Hematopoietic Stem Cell Quiescence and Interaction with the Osteoblastic Niche. Cell Stem Cell *1*, 685–697.

Yue, R., Zhou, B.O., Shimada, I.S., Zhao, Z., and Morrison, S.J. (2016). Leptin Receptor Promotes Adipogenesis and Reduces Osteogenesis by Regulating Mesenchymal Stromal Cells in Adult Bone Marrow. Cell Stem Cell *18*, 782–796.

Zhang, B., Ho, Y.W., Huang, Q., Maeda, T., Lin, A., Lee, S., Hair, A., Holyoake, T.L., Huettner, C., and Bhatia, R. (2012). Altered microenvironmental regulation of leukemic and normal stem cells in chronic myelogenous leukemia. Cancer Cell *21*, 577–592.

Zhang, J., Niu, C., Ye, L., Huang, H., He, X., Tong, W.-G., Ross, J., Haug, J., Johnson, T., Feng, J.Q., et al. (2003). Identification of the haematopoietic stem cell niche and control of the niche size. Nature *425*, 836–841.

Zhao, M., Perry, J.M., Marshall, H., Venkatraman, A., Qian, P., He, X.C., Ahamed, J., and Li, L. (2014). Megakaryocytes maintain homeostatic quiescence and promote post-injury regeneration of hematopoietic stem cells. Nat Med *20*, 1321–1326.

Zhou, B.O., Yue, R., Murphy, M.M., Peyer, J.G., and Morrison, S.J. (2014). Leptin-Receptor-Expressing Mesenchymal Stromal Cells Represent the Main Source of Bone Formed by Adult Bone Marrow. Cell Stem Cell *15*, 154–168.

Zhou, B.O., Ding, L., and Morrison, S.J. (2015). Hematopoietic stem and progenitor cells regulate the regeneration of their niche by secreting Angiopoietin-1. ELife *4*, e05521.

Zhu, J., Garrett, R., Jung, Y., Zhang, Y., Kim, N., Wang, J., Joe, G.J., Hexner, E., Choi, Y., Taichman, R.S., et al. (2007). Osteoblasts support B-lymphocyte commitment and differentiation from hematopoietic stem cells. Blood *109*, 3706–3712.